ME450 Team 24 - Open Source Assistive Device for Cylindrical Cell Spot Welding
Final Report

Team Members: Esben Nielsen, Benjamin Andelman, Matt Gibson, Vincent Bourgeois, and Ryan Applegate

Executive Summary

Spark Electric Racing, the sponsor of the project, is a student project team at the University of Michigan that designs, builds, and races electric motorcycles. For each new motorcycle, the team designs and manufactures a custom EV battery pack using lithium ion cylindrical cells, and has found the manual spot welding process to be inconsistent, slow, and unsafe. Industry solutions such as robotic arms require significant investment in terms of capital and time to maintain, making them impractical for a student project team. Thus, our team set out with the objective to develop a low-cost and accessible solution to aid in the spot welding of cylindrical cells.

Our team first started by interviewing members of Spark who had hand-on experience with the manual spot welding process to better understand the pain points. Using the information learned from the interviews, a set of user requirements was developed, being split into “needs” and “wants.” The “needs” required accuracy for the location and orientation of the welding probes, that the solution could withstand the force required to create a spot weld, and that the weld nuggets created by the solution could stand up to the loads experienced by the battery pack in its use case. These requirements were translated into engineering specifications, which included quantitative, measurable goals to drive the design going forward.

Our team decided that functional decomposition and the use of morphological charts would be the most efficient way to develop a solution to such a nuanced problem. The subsystem groups in the decomposition were determined by the user requirements. After the morphological charts were filled with ideas, our team worked to unanimously decide on a solution for each subsystem. The solution design then combined all of these subsystems into one consistent design. Engineering analysis was conducted to determine key aspects of the design, such as the length of the linkage arms and the bearing stackup of the rotating joints.

The final design utilizes a double four bar linkage arm to enforce the verticality of the welding probes, with a swivel connection at the base and end effector to allow for movement in all axes. The end effector uses an equalizer bar to enforce that both welding probes make full contact with the battery and current collector, as well as incorporates a load cell to give the user feedback on the force they apply. The design also utilizes custom circuits for measuring voltage, current, and load to ensure certain metrics are met prior to sending weld pulses, as well as to provide real-time weld quality feedback to the user.

Verification testing plans were developed that related directly to the requirements and specifications, especially for enforcing the orientation of the probes and the force application. The solution passed all verification tests for manufactured mechanical components, and supporting electronics were verified using LTspice and TINA-TI. The team was able to develop the solution for approximately $1030, which is less than the $2000 goal that was originally set.

With more time, the team would hope to refine the design of the end effector, as the physical design relies on precise machining to function correctly, which may not be available to our end users. The team would also like to troubleshoot abnormal circuitry behavior not predicted by SPICE simulations, and to transition to a custom PCB manufacturing process.

Table of Contents:

Executive Summary **2**
Table of Contents: **3**
1. Abstract **7**
2. Introduction **7**
2.1 Background 7
2.2 Benchmarking 8
2.3 Information Sources 10
2.4 Stakeholder Analysis 11
2.4.1 Stakeholder Interviews 12
3. Design Process Selection **13**
4. User Requirements and Engineering Specifications **14**
4.1 Requirements Determination 14
4.2 Determination of Mandatory Requirements and Specifications and Verification Methods 16
4.2.1 Weld Location Accuracy 16
4.2.2 Weld Probes Orientation 16
4.2.3 Weld Force Application 16
4.2.4 Weld Quality Verification 17
4.2.5 Spot-Welding Rate 17
4.2.6 Stability 18
4.2.7 Safety 18
4.2.8 Open-Source 18
4.2.9 Cost 18
4.3 Determination of Desired Requirements and Specifications and Verification Methods 19
4.3.1 System Dimensions 19
4.3.2 Weld Energy Consistency 19
4.3.3 Ease of Maintenance 19
4.3.4 Easy Setup and Use 20
5. Concept Generation and Selection **20**
5.1 Design Heuristics 21
5.2 Functional Decomposition 22
5.2.1 Expanding Beyond Automated Solutions 23
5.3 Automated and Human-Powered Morphological Charts 24
5.4 Automated and Human-Powered Concept Selection Process 25
5.5 Deciding on Alpha Concept 29
6. The Alpha Design **30**
6.1 Initial CAD Model 30
6.2 Subsystem Interaction 31
7. Problem Analysis and Iteration **33**

7.1 Initial Engineering Analysis for Controller Selection..... 33
7.2 Initial Engineering Analysis of Human-Powered Arm Length..... 34
7.3 Finalized Engineering Analysis of Arm Length..... 35
7.4 Joint Stackup Angular Deviation Analysis..... 36
7.5 Analysis of Radial and Thrust Loads at Base..... 38
7.6 Determination of Pneumatic Cylinder Dimensions..... 40
7.7 Analysis of Electrical Component Needs..... 41
7.7.1 Load Sensing Circuitry..... 42
7.7.2 Current Sensing Circuitry..... 42
7.7.3 Current Source Circuitry..... 43
7.7.4 Voltage Sensing Circuit..... 43
7.7.5 Power Supply..... 44
8. Build Design..... 45
8.1 CAD of Final Build Design..... 45
8.2 Subsystem Overview..... 45
8.3 Manufactured Components..... 47
8.3.1 Base Aluminum Extrusion..... 47
8.3.2 Base Plate..... 47
8.3.3 Base Pivot Post..... 48
8.3.4 Linkage Arm..... 48
8.3.5 Linkage Joiner..... 49
8.3.6 End Effector Joint Block..... 50
8.3.7 End Effector Pivot Connector..... 50
8.3.8 End Effector Side Wall..... 51
8.3.9 Load Cell Top Plate..... 52
8.3.10 Load Cell Holder..... 52
8.3.11 Piston Support - Fittings Side..... 53
8.3.12 Linear Shaft Guide..... 54
8.3.13 Straight Electrode Holder..... 54
8.3.14 Angled Electrode Holder..... 55
8.3.15 Load Sensing Circuitry..... 56
8.3.16 Current Sensing Circuitry..... 56
8.3.17 Current Source Circuitry..... 57
8.3.18 Voltage Sensing Circuitry..... 57
8.3.19 Power Supply Circuitry..... 58
8.4 Off-the-Shelf Mechanical Components..... 59
8.5 Off-the-Shelf Electrical Components..... 61
9. Final Design..... 63
9.1 Relation to Build Design..... 63
9.2 Final Design Functional Explanation..... 64
9.2.1 Degrees of Freedom..... 64

9.2.2 End Effector Functionality....66
9.2.3 Supporting Electronics....68
10. Verification and Validation....70
10.1 Verification Plans....70
10.1.1 Weld Location Accuracy Verification....70
10.1.2 Weld Probe Orientation Verification....71
10.1.3 Weld Force Application Verification....71
10.1.4 Weld Quality Verification....72
10.1.5 Spot Welding Rate Verification....72
10.1.6 Stability Verification....73
10.1.7 Weld Energy Consistency Verification....73
10.1.8 Ease of Maintenance Verification....73
10.1.9 Easy Setup and Use Verification....74
10.1.10 Circuitry Verification....74
10.2 Non-Physically Testable Verifications....74
10.3 Verification Results....75
10.3.1 Weld Location Accuracy Verification Result....75
10.3.2 Weld Probe Orientation Verification Result....75
10.3.3 Weld Force Application Verification Result....77
10.3.4 Weld Quality Verification Result....77
10.3.5 Spot Welding Rate Verification Result....78
10.3.6 Stability Verification Result....79
10.3.7 Weld Energy Consistency Verification Result....79
10.3.8 Ease of Maintenance Verification Result....79
10.3.9 Easy Setup and Use Verification Result....79
10.3.10 Circuitry Verification Results....79
10.4 Validation Plan....83
11. Discussion....83
11.1 Problem Definition....83
11.2 Design Critique....84
11.3 Risk....84
11.3.1 Risk mitigation....84
11.3.1 Risk to end user....84
12. Reflection....84
12.1 Social Context....84
12.1.1 Public health, safety, and welfare....84
12.1.2 Global context and benefit in a global marketplace....85
12.1.3 Social impacts associated with manufacture, use, and disposal....85
12.1.4 Economic impacts associated with manufacture, use, and disposal....85
12.1.5 Tools used to characterize societal impacts....85
12.2 Culture, Privilege, and Identity....85

12.2.1 Differences between team members..... 85
12.2.2 Differences with the sponsor.....86
12.3 Inclusion and Equity.....86
12.4 Ethics..... 87
13. Recommendations.....88
14. Conclusion..... 88
15. Acknowledgements..... 89
16. References..... 90
17. Bios..... 93
APPENDIX A..... 95
A.1 Concepts Generated - Esben Nielsen..... 95
A.1.1 Initial Ideas - Text Descriptions.....95
A.1.2 Expanded Ideas Using Design Heuristics..... 95
A.1.3 Expanded Ideas Utilizing Functional Decomposition.....98
A.2 Concepts Generated - Benjamin Andelman.....100
A.3 Concepts Generated - Vincent Bourgeois.....102
Initial Ideas.....102
Improved Ideas using Morph Chart and Design Heuristics.....102
Design Heuristics.....103
A.4 Concepts Generated - Ryan Applegate..... 103
Initial Ideas.....103
Additional Designs Generated Using SCAMPER Technique.....104
A.5 - Concepts Generated - Matthew Gibson.....104
A.6 Engineering Analysis Calculations..... 106
A.6.1 Joint Stackup Angular Deviation (continued from section 7.4).....106
A.6.2 Numerical Calculations for Bearing Selection..... 107
A.6.3 Full Dataset from Empirical Applied Force Testing.....108
A.6.4 Sensitivity Analysis of Piston Loading..... 108
A.8 Verification Plans.....108
A.8.1 Weld Location Accuracy Verification..... 108
A.8.2 Weld Probe Orientation Verification.....109
A.8.3 Weld Force Application Verification..... 109
A.8.4 Weld Quality Verification.....109
A.8.5 Spot Welding Rate Verification..... 109
A.8.6 Stability Verification..... 109
A.8.7 Weld Energy Consistency Verification..... 110
A.8.8 Ease of Maintenance Verification..... 110
A.8.9 Easy Setup and Use Verification..... 110
A.8.10 Circuitry Verification..... 110
Appendix A.9 Bill of Materials and Manufacturing Plan..... 112
A.9.1 Bill of Materials - Purchased Items..... 112

A.9.2 Bill of Materials - Manufactured Items..... 113
A.9.3 Bill of Materials - Electrical Items..... 114
A.9.4 Manufacturing Plans..... 116
A.9.5 Assembly Plans..... 124

1. Abstract

The development of prototype electric vehicles requires the construction of custom battery pack geometries. For student teams, cylindrical cells often are the preferred option over pouch cells, enabling complex geometrical pack shapes. Spot welding the cells manually to the current collectors, as is commonly done by student teams on a tight budget, is an inefficient process that produces inconsistent welds and poses a risk of puncturing the cells. To address these challenges, an improved spot welding system will be designed to increase efficiency, improve weld consistency, and reduce the risk of cell damage.

2. Introduction

SPARK Electric Racing is a student project team at the University of Michigan that has been designing, building, and racing prototype electric motorcycles for nearly 10 years. Their newest bike, Zephyrus, featured a 1128-cell pack reaching nearly 600V and with the capability of nearly 400A of peak current. These cells were spot-welded by hand over 4000 times (2 spot-welds per terminal per cell), leading to major concerns about the team's ability to produce consistent, high-quality welds. As a result, SPARK has tasked our team with identifying a solution to address the tedious and unreliable process of spot welding cylindrical lithium-ion cells used in their batteries. Cameron Trumpy, the project sponsor and current technical director of SPARK Electric Racing, has extensive hands-on experience with manual spot welding and the challenges it poses to the team [15]. The process is time consuming, inconsistent, and poses a risk of damaging the lithium-ion cells, compromising both safety and reliability.

The objective of this project is to design and fabricate an affordable solution that will increase welding efficiency, create higher quality and more consistent welds, and reduce the risk of puncturing the cylindrical cells. This solution will be released into the public domain, making it accessible to student teams, start-ups, research groups, and any others who would benefit from this affordable alternative to manual spot welding.

The primary deliverable of this project will be the design and manufacturing of a single working welding unit delivered to SPARK Electric Racing by the end of the semester. Additional deliverables will include engineering drawings, assembly drawings, manufacturing plans, and a full BOM. This will ensure that our solution will be truly accessible and easily followed for other project teams to create themselves. We will also include a Standard Operating Procedure (SOP) addressing operation, maintenance, calibration and safety procedures. A successful project outcome will be defined by the implementation of a solution that improves the efficiency, weld quality, and safety of the current manual process while remaining affordable and open-source.

2.1 Background

Previous work by SPARK Electric Racing has relied entirely on manual welding, with no prior development of automated solutions. The process of manual spot welding consists of

manipulating two conducting probes and making contact through a current collector (often referred to as “bus bar”) to the cell surface. At the direction of a foot pedal, a low voltage high current pulse is sent that fuses the current collector to the cell. This process is time intensive, unreliable (often requiring the disposal of cells due to failed welds), and unsafe, as cells may be punctured, creating risk of runaway lithium fires. Additionally, if one of the welds in a parallel group fails or produces sparks, often the entire group must be scrapped, as terminals of other cells have already been scarred by welds, increasing the risk of puncture if they are welded again. Therefore, inconsistencies in weld application parameters has the potential to produce large amounts of lithium ion cell waste, which is notoriously difficult and dangerous to dispose of [12][13][14][15]. From our stakeholder interviews, we honed in on the true difficulties with manual spot-welding, identifying three main weld parameters where variability introduced by manual manipulation could cause the most damage: weld force, electrode orientation, and distance between electrodes. Because resistance welding uses the resistance between two electrodes to generate the heat required to fuse the current collector to the cell terminal, any changes to that resistance from weld to weld introduces variability in the weld quality. From these findings, we set out to research previous attempts to solve this problem and generate our own concepts for an alpha solution.

2.2 Benchmarking

Currently there are several capable industry solutions available that would address these issues, however they are overly complex and expensive. The first solution, shown in **Figure 2.2.1,** is a FANUC high degree of freedom robot arm that can be fitted with a spot welding end effector to perform complex 3D welds for nearly any application [4].



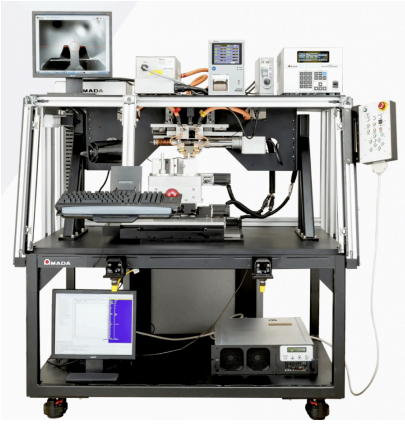
FANUC R1000iA/80H

- 5 DOF Robot Arm
- 80 kg Payload
- 2230 mm Reach
- Cost: Approximately $40,000

Figure 2.2.1. FANUC R1000iA/80H Photograph and Specifications

This solution is not suitable for our needs as it is excessively expensive and more capable than required for the simple geometries employed by student teams.

Another available solution, shown in **Figure 2.2.2** is a gantry system from AMADA that has 3 degrees of freedom. It functions like a 3D printer and would be applicable for our 2D welding needs [5].



AMADA Resistance Welding System

- 3 DOF Gantry
- Extensive Sensor Suite
- Expected to be expensive, requires quote request

Figure 2.2.2. AMADA Automated Resistance Welder Picture and Specifications

However this specific system from AMADA contains an overly complex amount of sensors and unnecessary features for our application.

A second offering from AMADA, shown in **Figure 2.2.3** is a laser welding system that foregoes resistance welding and uses fiber lasers to produce welds. These welds are incredibly precise, fast, and have a small heat affected area [6].



AMADA Jupiter Laser Welding System

- Automated Laser Welding
- 500 W Fiber Laser
- Integrated Combustion Suppression
- Expected to be expensive, requires quote request

Figure 2.2.3. AMADA Jupiter Automated Laser Welder Picture and Specifications

However this system has exorbitant cost (tens to hundreds of thousands of dollars, making it wildly out of reach for most non-commercial users. Since all of these solutions are expensive and

overly complex for project teams and start-ups, therefore we plan to bridge the gap with a low-cost, 2D solution that will address the challenges of manual spot welding effectively.

2.3 Information Sources

In regard to spot welding quality requirements and recommended practices, the following two standards are relevant: **ISO 14554-1** and **AWS C1.1M/C1.1**. ISO 14554-1 provides more general guidelines for what we should take into consideration to ensure weld quality, a current problem we are facing with manual welding [7]. These include breaking down the equipment chosen, electrode design, parent metals, dimensions of the component, etc, and having a true understanding of how each will affect the quality. It also suggests having a set process for inspection and testing, including having a designated resistance weld setter, and welding supervisor to mitigate variability during our testing phase. AWS C1.1M/C1.1 offers recommended practices for resistance welding regarding process parameters of different materials and safe operating procedures [8]. These guidelines include spot-welding parameter tables for various materials and their corresponding welding schedules, recommended electrode material/design, net electrode force considerations, hold times, and current requirements. This will help guide our testing process of identifying the force and hold time required to create an optimal spot weld.

In addition to standards governing our welds, user safety is also a critical requirement. The **ISO 12100** standard outlines a framework for identifying hazards, assessing risks, and implementing protective measures through design [9]. This will allow us to ensure we emphasize the importance of guarding against electrical hazards in our design, adding emergency stops, and designing an intuitive interface to ensure ease of use. These all reduce user risks/errors and make the system safer for long term use by project teams and start-ups.

Of great use to us was a white paper on the fundamentals of resistance welding, written by one of our potential competitors, AMADA WeldTech [10]. In this incredible resource, they launch into the specifics of how to optimize welding parameters to achieve the best spot-welds, covering multiple different types of resistance welds. We chose to pursue fusion bonds based on our usage of 21700 cells with nickel-plated steel terminals in combination with our SigmaClad current collecting material, which contains nickel-plated copper and stainless steel layers. Fusion bonds work best with similar materials where the melting point can be reached with a high weld energy over a short period of time [10]. This aligns well with our plan to utilize copper (conductive) electrodes with nickel-plated (resistive) cell terminals and current collecting material. In this white paper, they also discuss a method known as projection welding, where one of the weld surfaces is extruded in a third direction to focus the weld current into a single location [10]. This is a method that SPARK and Michigan Electric Boat have experimented with in the past, with varying degrees of success [15][16].

2.4 Stakeholder Analysis

The primary stakeholders, seen in **Figure 2.4.1**, for this design project include SPARK Electric Racing and Michigan Electric Boat, as these teams both currently rely on manual spot welding for their batteries. These teams will be positively impacted by our solution as it will improve efficiency, reduce safety risks, and provide consistent weld quality for their welding applications. More specifically, members directly involved with the battery, as well as any students from other project teams who may need to use the system, will experience these benefits firsthand. Secondary stakeholders include other project teams at universities across the globe that could benefit from our solution. For example, the BOLT electric motorcycle racing team from Virginia Tech [19] and the Electric Vehicle Team from the Rochester Institute of Technology [20] are comparable student-run teams that could be facing similar challenges in the construction of their own high-voltage battery packs. Tertiary stakeholders are primarily entities with existing spot welding automation technologies. They have a stake in this project as competitors in the small scale production space, in which our solution would offer an affordable alternative.

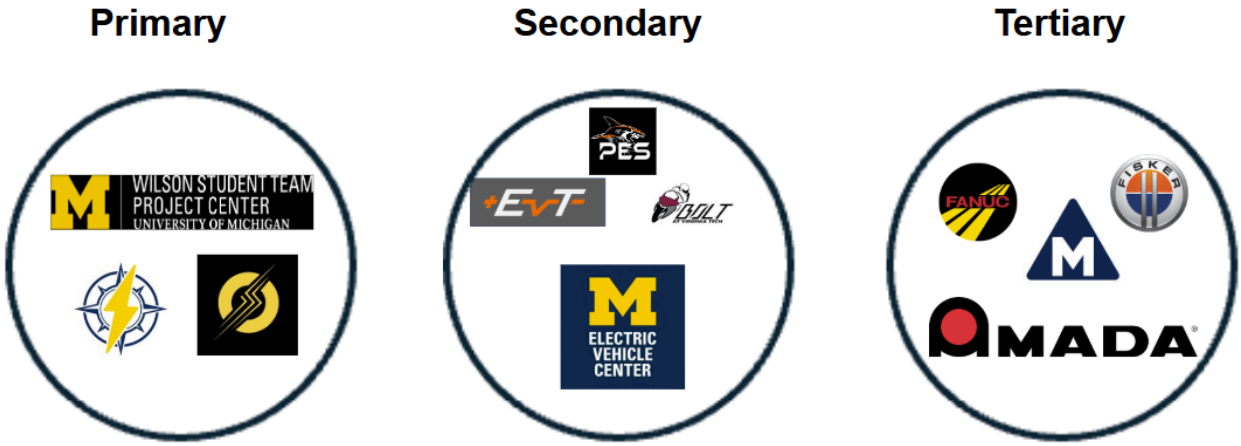


Figure 2.4.1. Stakeholder Map Sorted By Level of Influence.

Developing a solution to our problem will benefit many student teams by making it accessible to produce custom cylindrical cells. However, this does pose a slight ethical concern, as the solution will enable inexperienced teams to make dangerous batteries. A team with minimal lithium-ion battery design experience may not know how to properly handle the cells, especially if they are punctured or damaged, and pose a risk to themselves and others in their community. Our team has considered the implications of this, and understand that it is a responsibility of the team to develop appropriate SOPs and safety warnings as part of the open-source material. There is an additional ethical concern that even if another team can weld cells successfully, the battery they create could be dangerous. Our team has classified the design of the battery modules as out of scope, so while we do have to consider the ethical implications of sharing the solution, it is beyond the scope of the project on what happens after our project is open-sourced. These safety concerns can also be viewed in a positive light. With proper usage of the cell welding solution, we can prevent the hazardous use of manual spot welding. Current processes have inconsistent

results with failures ranging from improper connections to punctured cells. This can be especially impactful as welds cannot be repaired and a single fault reduces an entire parallel cell group to waste. Improving this process can reduce the risk associated with manual welding and alleviate the disposal of healthy cells when mistakes occur. This has a positive social impact, as rare earth metals used in lithium-ion battery cells are in great demand with limited supply. The efficient use of materials is both important for monetary reasons and for the larger economy. It is also of great social importance that we reduce the reckless use and therefore disposal of lithium batteries. Improperly disposed lithium-ion cells are known to start landfill fires and release toxic fumes while doing so, damaging the surrounding environment and potentially injuring landfill workers.

2.4.1 Stakeholder Interviews

When conducting stakeholder interviews, we placed emphasis on letting people explain their personal experiences rather than placing emphasis on closed questions. Our first interviews were conducted with SPARK battery team members Adam Heiler, Morgan Duvel, and Giovanna Celi [12][13][14]. Our initial inquiry was “Describe your experience with spot welding cells.” With this line of questioning, the difficulties they mentioned were those that bothered them the most, removing the possibility of our preconceived ideas prompting their responses. From this point, we expanded on the problems they mentioned in order to gather information on how we may alleviate it. Interviews were then conducted with SPARK Technical Director Cameron Trumpy and University of Michigan Battery Lab Welding Engineer Daniel Kedroske [15][17]. Our findings largely focused on frustration of failed welds as well as the overall time impact of the process, with dozens of hours spent optimizing process parameters and performing welds. As mentioned above, in this stage of the design process, we also started to discover that the time taken to apply a spot-weld wasn’t necessarily the largest obstacle to achieving a highly-efficient process with minimal downtime. Instead, it was the time taken to place the electrode probes, align them vertically, and apply an ambiguously-determined level of force to the electrodes before each weld could be performed. The last parameter was especially frustrating for our interviewees. During the long months spent welding cells for the SPARK motorcycle battery, multiple different members rotated welding responsibilities, with each member possessing a different idea of what the appropriate level of force was to apply to a weld. When switching between members, the new welder might have to practice a few times on dummy cells to re-determine what that appropriate level of force was, creating more waste and the potential for cell punctures. While the other challenges of electrode placement and orientation were less noticeably frustrating, they still introduced variability and were important to keep consistent, according to our interviewees.

Of particular note was our interview with former Michigan Electric Boat Electrical Director Andrew Dailey, whose team attempted to build an automated, CNC-controlled spot-welder to increase their weld rate for their 814V, 69 kWh battery, featuring over 3000 cells arranged in 220

14-cell parallel groups wired in series. They completed construction of a bedslinger-type design with a dual-axis toolhead, but ran into issues providing *enough* force to the weld surface to ensure good weld quality [17]. This finding became very useful later on during our concept exploration and selection processes.

3. Design Process Selection

Our team has been primarily following the ME450 design process outlined in the learning block. This framework is linear and stage-based with feedback loops connecting the problem definition and solution, as well as realization and need identification phases [1]. This will be the most useful framework for our project because it emphasizes the early stages of problem definition and concept generation [1]. As present team members of SPARK, we have seen firsthand how much time was spent manufacturing the battery, and have heard about the frustrations experienced by the battery team as they punctured cells and were even forced to scrap an entire module after failing to produce good welds multiple times. This led to our decision to pursue a problem-oriented design process, increasing our focus on assigning very specific root causes to our design problem during problem definition and creating very explicit targets for our concept generation process to address. Given our limited timeline, we will not be able to prototype a wide range of designs, therefore placing more emphasis on these two phases will allow us to systematically choose a strong and feasible solution to manufacture.

We considered using an alternative design process model such as the Dym and Little model. This framework has 5-stages focusing on the design aspect specifically [2]. We decided the ME450 framework was a simpler approach that would benefit us more due to its built-in feedback loops that connect problem definition and solution development. These iterations are essential before we begin prototyping/manufacturing our design, and the feedback loops will allow us to circle back if any problems arise.

Our approach differs slightly from the standard ME450 framework due to our exposure to both the need identification and realization phases [1]. Being members of the project team we were able to see the need identification in real time that led to this project being generated by our sponsor before the semester started. Additionally, because our solution will be implemented into our project team's workspace, we will be able to stay engaged in the realization phase after the semester has concluded. This will allow us to gather user feedback and provide us with insights into how well our design truly does at achieving the goals outlined in the introduction. The team can then address any improvements for future designs if needed. Our specified framework is laid out below in **Figure 3.1**, showing the detail behind our problem definition and concept generation processes. We relied heavily on our initial stakeholder interviews and market research to develop our list of requirements and specifications, which we then fed into the concept selection process to determine which generated concepts we should pursue. We also included the standard feedback loop from initial solution testing into the solution improvement process to

incorporate student team feedback. Additionally, we have extensive processes in place for solution improvement after dissemination (open-sourcing), since we will be directly exposed to the impacts our solution will have on the SPARK and Michigan Electric Boat battery teams as they prepare to design and construct their next battery prototypes.

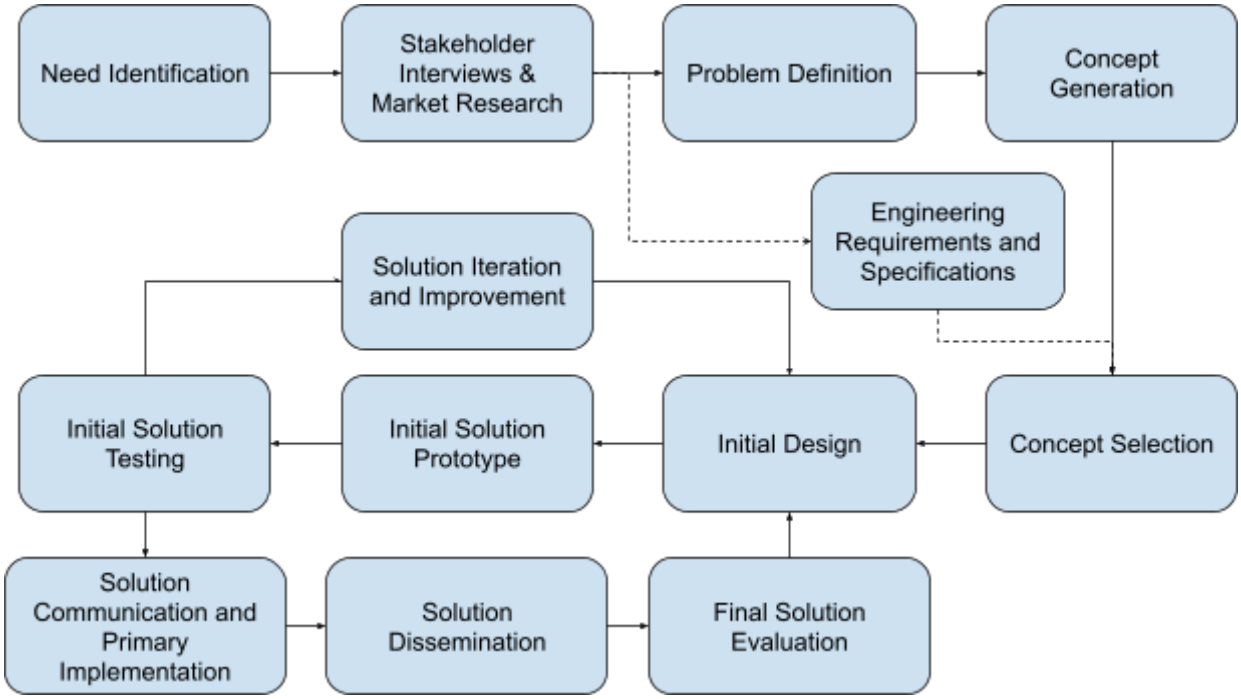


Figure 3.1: Design process framework emphasizing thorough problem definition, concept generation and evaluation, and our continued involvement with the final delivered solution after testing and dissemination.

4. User Requirements and Engineering Specifications

4.1 Requirements Determination

Determination of the engineering requirements and specifications was done using the extensive information we collected from our interviewees about the weld parameters that were most important for achieving high-quality, strong welds. As noted above in the Stakeholder Interviews section, these parameters included electrode location, electrode orientation/angle, and applied force, and are reflected below with individual requirements dedicated to each. In **Table 4.1.1 and 4.1.2**, we split the requirements and specifications into categories of those that are required to be met and those that are highly desired but ultimately optional.

Table 4.1.1. Updated Mandatory Requirements and Specifications

Requirement	Associated Specification(s)

Weld Location Accuracy	Solution must be able to move to 100 randomly generated target positions in a 2D plane which is overlaid on the surface of the battery cell terminals within a **0.5-millimeter radius of tolerance**.
Weld Probes Orientation	Solution must position both weld probes such that they are pointed normal to the plane of the cell terminal, within a **2-degree cone of tolerance**.
Weld Force Application	Solution must allow the user to apply at least **44 Newtons** of force in the Z-axis direction for each spot-weld probe.
Weld Quality Verification	A force of **22.2 N (5 lbf)** applied normal to the current collector to induce tension and applied in shear to a singular spot-weld must not damage the weld in any manner.
Spot-Welding Rate	Solution must allow the user to perform at least 6 spot-welds per minute within the accuracy, orientation, pressure application, force consistency, and quality verification standards listed above.
Stability	Solution must be able to accommodate at least **2 cm** of elevation difference between diagonally-opposed corners of the operational area while maintaining the plane of the surfaces of the cell terminals within an angle of incline/decline of no more than **2 degrees**.
Safety	Machine must allow for ease of plugging in to ensure quick disconnect of all power into the device.
Open-source	**100% of all materials** necessary for the manufacturing, assembly, and operation of the machine must be released into the public domain.
Cost	Costs to manufacture and assemble a working machine **must not exceed 2000 USD.**

Table 4.1.2: Updated Desired Requirements and Specifications

Requirement	Associated Specification(s)
System Dimensions	Operational welding area should extend at least **32 inches** in both the X and Y directions.
Weld Energy Consistency	The pre- and post-weld resistance and the energy expended per weld of 12

	consecutive welds produced by the solution must all fall within 95% confidence intervals for each metric, where the intervals are obtained from a sample of 30 successful welds produced using the standard manual method.
Ease of Maintenance	Disassembly of all moving parts on the tool head should require no more than two distinct tools and should be able to be completed in **≤ 10 minutes**.
Easy Setup and Use	Time required to place a battery module into the operation area and place current collectors in correct positions **should not exceed 60 seconds for initial placement of cells and 10 additional seconds per current collector.**

4.2 Determination of Mandatory Requirements and Specifications and Verification Methods

4.2.1 Weld Location Accuracy

Due to the small window size of the half-moon design used in SPARK's current collector design [15] and the approximately 10 mm diameter of the smallest 21700 cell terminal, location accuracy of the electrode placement mechanism of our final design will be paramount to ensuring that the current collector is joined to the correct part of the cell. Any contact with both terminals at once could cause an internal short and spell disaster for the battery. This requirement is therefore our primary mandatory requirement, and will be verified via trial using 100 randomly-generated target positions in the 2D plane, requiring the solution to allow electrodes to be moved to the target location within 0.5-millimeter accuracy. Target positions will be marked, and radial distance to the target position will be measured with calipers.

4.2.2 Weld Probes Orientation

SPARK's current collectors utilized dimpled designs to create two points with very small contact area between the collectors and cell terminals [15]. To achieve minimum resistance, the pointed electrodes needed to be oriented nearly perfectly vertically, such that the electrode tip rested in the dimple. Therefore, we included electrode orientation as a mandatory requirement. We plan to incorporate an accelerometer in the toolhead of our solution, aligned with the electrodes, to measure the angle of the electrodes with respect to the XY plane, using that feedback to determine if the electrode orientation is within the ±2-degree bounds and only enabling the welder when that condition is met.

4.2.3 Weld Force Application

As mentioned above in the summary of our stakeholder interviews, applied force was of profound importance for the quality of the welds. Variability in the applied force could drastically increase or decrease the weld resistance, dramatically changing the heat output of the

spot-weld and potentially puncturing the cell. It is therefore included as our third major mandatory requirement, and will be closely verified using a highly-accurate force measurement method (yet to be finalized) located in the toolhead and linked to each electrode. This metric, like the orientation requirement, will be measured in real-time and will be required to be greater than 44 Newtons per electrode for the welder to be enabled.

4.2.4 Weld Quality Verification

One of the major concerns expressed by our interviewees about post-weld performance was the possibility of weld nuggets being dislodged from their positions between the cell terminals and the current collectors, severing any conductive connection of the cell to the pack. This would represent a critical fault in any battery pack that does not include generous safety margins in its current limits, as the disconnection of one cell from a parallel group instantly transfers the battery's current draw through a smaller number of cells than originally designed for, presenting an imminent risk of thermal runaway and a subsequent lithium-ion battery fire. We plan to verify the quality of our welds by using the Michigan EV Center's weld puller, which can apply tensile and shear loads to spot-welded current collectors to validate that the welds can withstand such a force [17]. Since SPARK's current collector design places collectors on both sides of the cells, handling of the battery pack after spot-welding could introduce relatively small forces on the spot-weld nuggets that might dislodge the weld before they are protected by being tightly assembled into the combined pack.

4.2.5 Spot-Welding Rate

The time required to spot weld is small in the context of a single cell, but many student project vehicles utilize a battery consisting of hundreds or thousands of cells, so time of battery construction becomes significant. Improvements on the border of seconds to complete a single spot weld would have big impacts for the context of an entire battery. It is mandatory then, that the solution improves the rate of welding over the conventional welding technique. From stakeholder interviews with SPARK members with hands-on battery welding experience, it took about 20 seconds to complete a spot weld using the conventional method [12][13][14][15]. Thus, by completing 6 spot welds per minute, the user would be able to double their rate of spot welding, which still allows time for decisive positioning and confirmation before executing the weld. This specification can be verified by setting up a current collector on a group of dummy cells (cells that have the anode and cathode but no lithium inside), and seeing how long it takes a team member to complete 6 spot welds. The team members will not see the time so they are encouraged to focus on making welds that are full contact and consistent with other specifications. These welds will be pull-tested in the EV center, and the critical metrics of pre-weld resistance, post-weld resistance, and expended energy will be measured at weld-time and compared to their respective confidence intervals, specified below in 4.3.2, or to recommended values sourced from our references.

4.2.6 Stability

This requirement was generated based on some concerns raised by interviewees about the possibility of current collectors moving into undesirable positions as a result of any sort of vibrations from a moving toolhead, motors, or friction in joints. We have already established that the location accuracy of the toolhead is very important, but the success of the weld depends on the current collecting material being in the right position as well. We have therefore introduced a mandatory requirement that our solution must allow for at least 2 cm of elevation difference (~0.75 inches) between diagonally opposed corners of the operational area without introducing a degree of inclination of the plane of the cell terminals greater than 2 degrees. This requirement will be verified by placing a 2 cm tall spacer in one corner of the operational area, and using an electronic level to measure the maximum degree of inclination anywhere on the surface of a test battery module placed in the operational area.

4.2.7 Safety

When working with lithium-ion batteries, and especially when spot-welding them, there is always a high risk for cell puncture or other adverse events that could result in a fire. Additionally, lithium-ion cells are extremely sensitive to external heat sources, which could cause thermal runaway. Therefore, we instituted a mandatory requirement for our solution to include multiple emergency stop buttons, one to cut off all electrical power to the machine in the case of an electrical fire or malfunction, and one to cut off electrical power to solely the spot-welder. These features will be verified by testing the ability of the buttons to cut off the power to their designated targets, which must be done successfully 12 consecutive times.

4.2.8 Open-Source

Open-sourcing our solution will be the last step of our design process. Our project sponsor emphasized the ability for other teams at the University of Michigan to freely utilize or construct a version of our solution, so we will be releasing all materials necessary for the fabrication, programming, and assembly of our solution into the public domain. This requirement will be verified by said release of materials onto a webpage of the publicly published SPARK Electric Racing website.

4.2.9 Cost

Electric motorcycle racing is a new space for collegiate teams, especially compared to groups like SAE Baja and SAE Formula. This leaves many teams to have a tight budget, as sponsorships can be hard to come by as teams grow their visibility. Given this, it is important that our solution is cost-effective, so that any student project team can build and utilize our solution. The threshold of $2000 was chosen as it is a realistic amount for a student team to receive as a grant from their university, so teams with low capital could ask their university for funding specifically to build our solution. This specification will be verified by summing the cost of all purchased

components and raw material, with labor assumed to be free, and measuring that quantity against the $2000 threshold.

4.3 Determination of Desired Requirements and Specifications and Verification Methods

4.3.1 System Dimensions

As discussed in earlier sections of the report, the team is hopeful that this solution will be utilized by teams beyond SPARK Electric Racing. Through an interview, we determined that the largest scale battery our solution would need to accommodate is the UMich Electric Boat Battery, at 40” x 40” [16]. This specification can be tested on the hardware by tracing a 40” x 40” area and extending the probe of the spot welder to ensure that it reaches everywhere inside of the traced area.

4.3.2 Weld Energy Consistency

One of our desires with this project was to incorporate additional sensing capabilities into the spot-welder toolhead to measure the total energy expended per weld, as well as the pre- and post-weld resistance between the electrode tips. These metrics, combined with the spot-welder’s voltage and pulse time setting, creates a great picture of how much instantaneous heat is generated by the weld, and therefore how much damage is possible to the cell terminal. An ideal resistance weld is able to produce high currents with relatively low voltages, resulting in a strong bond between the welding materials and relatively low heat, mitigating the risk of cell terminal puncture. These three metrics will be generated for a series of 12 consecutive welds performed by our solution and compared against a 95% confidence interval generated for each metric from a sample of 30 manually-performed welds that were rated as “successful” by experienced SPARK battery team members.

4.3.3 Ease of Maintenance

The ease of maintenance is an essential part of ensuring that our solution will achieve its projected lifetime. However, maintenance is inherently part of owning a machine, and thus end users will be expecting to invest time and effort into maintenance, making ease of maintenance a desire. Project teams typically have many tools in use at once, so reducing the number of tools necessary is critical to ensure that maintenance is easy to do. During welding, the probes can wear down and lose material, so most of the maintenance goes into replacement of the probes [8] [15]. Given that the size scale of all fasteners on the tool head will be the same, ensuring that only two tools are necessary to swap the probes is a realistic specification to design for. This specification can be verified by giving a team member or other individual two tools and seeing if they can successfully replace both probes on the welding head in less than 10 minutes.

4.3.4 Easy Setup and Use

Similarly to the ease of maintenance, the team expects that end users will be willing to invest time into setting up the solution, especially given the time savings it will bring as discussed in 4.2.6. The target of 60 seconds to place in a battery was determined based on the speed at which a group of batteries can safely be moved, as safety is always a key consideration in the development of this solution. Similarly, the additional 10 seconds per current collector is also considering the safety of the user correctly loading in the new current collector so as to have proper alignment and not have issues due to haste. The numeric specifications can be verified by timing a member of the team as they attempt to load in a battery module, and load in additional current collectors.

5. Concept Generation and Selection

In our exploration of the design space, the team first discussed which concept generation methods worked well for them in past engineering projects, as well as what they found helpful from the ME450 Concept Generation Learning Block [18]. With these ideas, we formed a concept generation pathway, seen in **Figure 5.1**. To begin, we agreed that design heuristics were a strong starting point as it offered the ability to create novel ideas across a widespread range of functions and formats. Each team member individually created ten unique ideas to be brought forward to the group, seen in **Figure 5.1.1**. Our second step was to perform a functional decomposition [18] indicated by our stakeholder interviews, requirements, and specifications, as shown in **Table 5.2.1**. We then categorized the ideas created from the design heuristics [18] into the core functions. This is shown in **Figure 5.2.2**. From this we identified two overarching categories of our design, automated vs human-powered movement mechanisms. We conferred as a team and agreed that this distinction required two independent design pathways to be explored in tandem, where more specific functions were chosen for each method. Step three consisted of creating morphological charts [18], seen in **Table 5.3.1** and **Table 5.3.2**. Through round-table discussions, we performed common-sense checks to shrink the design pool. With a reduced concept pool, we created pros and cons for each proposed solution, seen in **Table 5.4.1** and **Table 5.4.2**, and selected one solution from each subgroup to form an overarching design, seen in **Table 5.4.3** and **Table 5.4.4**. Finally, shown in **Table 5.5.1**, we compared the results of the automated solution versus the human-powered solution and used a pugh chart to systematically choose our alpha concept.

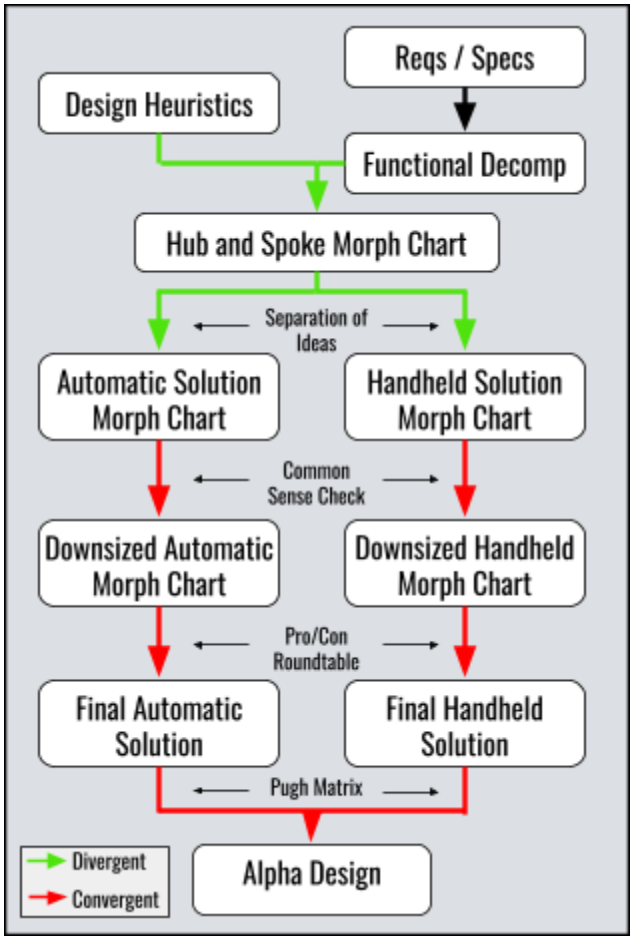
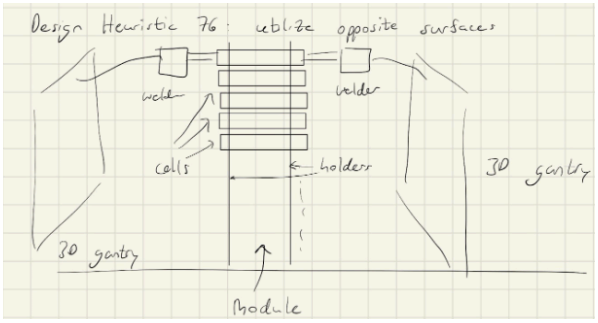


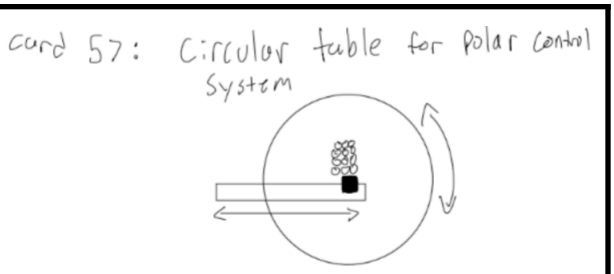
Figure 5.1. Concept Generation and Selection Pathway. The methods are categorized as either convergent or divergent, designating whether it adds or subtracts from the total number of considered concepts [18].

5.1 Design Heuristics

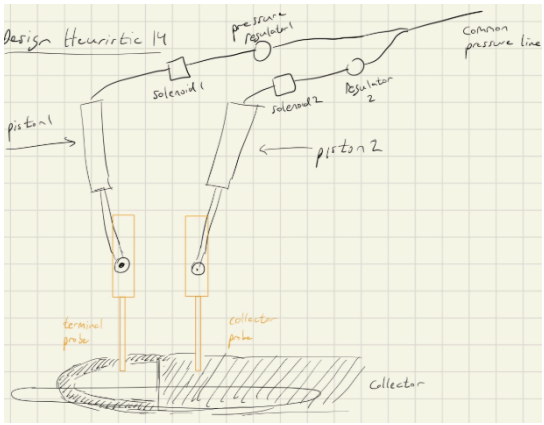
To begin our concept exploration, we employed the use of design heuristics cards [18]. The cards prompt users to widen preconceived notions of solutions with vague statements such as “twist” and “change direction of access.” When applied to a given idea, it sprouts new thoughts that extend farther into the greater design space. Our team employed design heuristics on an individual basis. Each member independently created ten new ideas, some of which are shown in **Figure 5.1.1.** Additional examples of our initial concept sketches are shown in Appendix A.1-A.5.



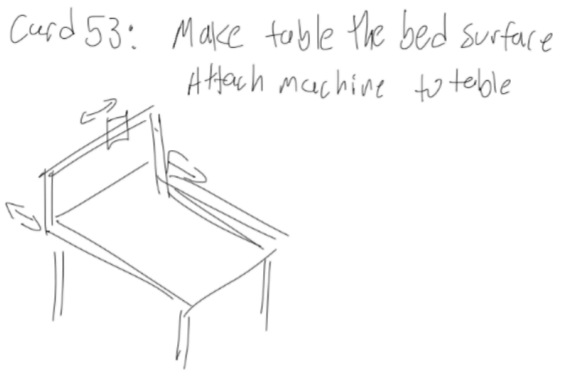
"*#76: Utilize Opposite Surface*"



"*#57: Rotate*"



"*#14: Attach Independent Functional Components*"



"*#53: Reduce Material*"

Figure 5.1.1. Examples of Design Heuristics. These sketches illustrate the widespread exploration of the design space with a wide range of unique ideas. The card used for each concept is listed below each sketch

The team then met and presented our ideas to the group, performing a round-table discussion on common themes and consolidating certain ideas into larger solutions.

5.2 Functional Decomposition

The second step taken by the team was to write down the core functions of the system as. These "axioms" of our design, shown in **Table 5.2.1.**

Table 5.2.1. The core functions of an assisted battery spot welder.

Weld Force	XY Movement Geometry	Structure	Weld Verification
User Interface	XY Movement Actuation	Weld Contact Material	Bed Surface

The ideas presented from the design heuristics round-table were then sorted into the functional decomposition categories using a “hub and spoke” model shown in **Figure 5.2.2**.

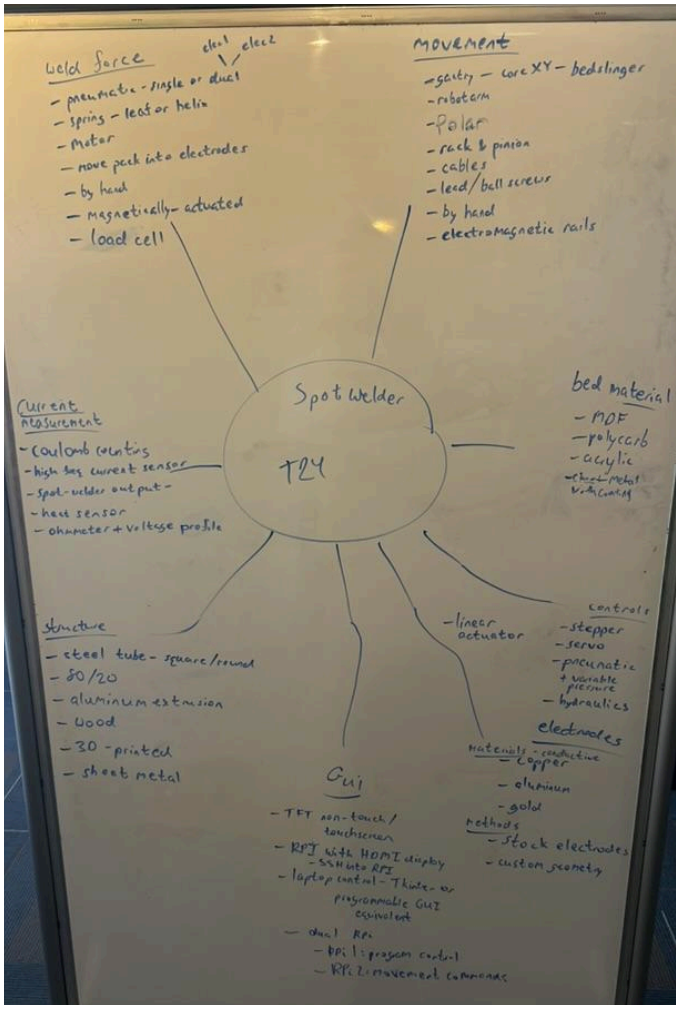


Figure 5.2.2. Hub and Spoke Illustration of Core Functions. Each sub-group shows initial brainstorming drawn from design heuristics

5.2.1 Expanding Beyond Automated Solutions

The team noticed that the concept generation process had been hindered by an assumption carried with them from the project title name that was originally given. The original title “Automated Battery Spot Welder” suggested that the solution should be made to be automatic, but further decomposition of the problem revealed that a successful solution did not necessarily have to be automatic. Through discussions with our sponsor, we determined the automation element was assumed to speed up the process of battery welding. However, the speed of welding is included in the requirements and specifications **Table 4.1.1**. The group thus determined that developing a non-automated solution was appropriate, so long as it satisfied the same requirements and specifications that were set originally for the automated solution. Concept

generation was then reopened to all ideas, and new relevant ideas to a human-powered solution were added to the pool of concepts.

5.3 Automated and Human-Powered Morphological Charts

Before continuing onto concept selection efforts, the team identified that the concept generation pool would best be sorted into two groups, a fully automated solution and a human-powered solution. The fully automated and human-powered solution concepts are represented below in **Table 5.3.1** and **Table 5.3.2.**

Table 5.3.1. The morphological chart showing the appropriate subsystems and various generated solutions for the fully automated solution bucket.

Functional Subsystem	Concept 1	Concept 2	Concept 3	Concept 4	Concept 5	Concept 6	Concept 7
Z-axis Actuation	Pneumatics - single or double	Spring - leaf or helix	Motor	Move pack itself into electrodes	Magnetically actuated		
X-Y Movement	Core XY	Bedslinger	Polar	Rack & pinion	Cables/belts	Lead screw/Ball screw	Electromagnetic Rails
Motion Actuator	Stepper motor	Servo motor	Pneumatic cylinders	hydraulic cylinders			
Structure	Steel tubing	80/20 Al extrusion	Wood	3D-print	Sheet Metal		
Bed Material	MDF	Polycarb	Acrylic	Acrylic coated sheet metal			
Electrodes	Copper	Aluminum	Gold				
Weld Verification	Vision System	Current Sensor	Coulomb Counting	Spot-welder display output	Heat Sensor	Ohmmeter + Weld Schedule	
GUI	Non-touch display	Touch display	Laptop Tkinter GUI				
System Control Processor	RPi	Laptop control	Teensy 4.1				
GUI Processor	shared RPi with system control	individual RPi for display					

Table 5.3.2. The morphological chart showing the appropriate subsystems and various generated solutions for the human-powered solution bucket.

Functional Subsystem	Concept 1	Concept 2	Concept 3	Concept 4
Z-axis Actuation	Human applied force	Active pneumatics		
Angle Enforcement	Accelerometer	Dual four-bar anti-grav boom-arm	Visual level	Wide-based applicator
Realtime Weld Verification	Vision System	Current Sensor	Coulomb Counting	Spot-welder display output
Force Enforcement	Spring	Load cell	Air spring/ pneumatic	
Table / Structure for holding module	Threaded feet on steel frame	Require a level table in SOP	Soft base to absorb surface roughness, stiff upper surface	
Electrode Clamping	Set screws	Direct bolted mounting	Insulated clamps	Designed quick-release connection
Ergonomics	Contoured rubber grips	Handle		
End Effector Structure	3D-printed	Machined metal	Sheet metal	
Electrode Material	Copper	Aluminum	Gold	
User Interface	Indicator lights	Mini display	Haptic feedback	Auditory feedback
Microcontroller	Teensy 4.1	Raspberry Pi	Arduino Nano	ESP32-S3

5.4 Automated and Human-Powered Concept Selection Process

The concept selection process was broken down into the two categories mentioned in section 5.2.1, an automated solution and human-powered solution. The team took the morphological chart of each and did an initial reduction of ideas that didn't align well with the problem, based on a mix of prior familiarity with the problem and information from stakeholder interviews [12,13,14,15]. After doing so, the team utilized a round-table discussion, discussing in depth the pros and cons of each solution. A unanimous agreement on each would need to be made to move forward with the idea. This led to the final concept generations for both the automated and human-powered solutions. **Table 5.4.1** shows the morphological chart of the automated solution and the pros and cons to each solution for the metrics. **Table 5.4.2** (p 21) shows the same for the human-powered solution.

Table 5.4.1. Morphological Chart with Pros and Cons for Each Automated Solution

Functional Subsystem	Concept 1	Concept 2	Concept 3
Z-axis Actuation	**Pneumatics - double piston**	**Spring - helix**	**Motor w/ load cell**
Pros	Provides both a soft and hard cutoff region	Does not require mechatronic integration	Gives consistent force and is fully automated
Cons	Requires precision machining and seals	Susceptible to slop in assembly and pushing past limit	Requires mechatronic integration and tuning
Motion Actuator	**Stepper motor**	**Servo motor**	
Pros	High Accuracy	High performing in all metrics	
Cons	Mediocre speed and acceleration	Expensive and complex control system	
Structure	**Steel tubing**	**80/20 Al extrusion**	
Pros	Very strong and relatively cheap	Lighter and modular	
Cons	Heavy and requires speciality machining for joints	More expensive, must procure	
Bed Material	**MDF**	**Polycarb**	**Acrylic**
Pros	Cheap and easy to manufacture	Strong, easy to manufacture	Less expensive, easy to manufacture
Cons	May get worn down over use from battery sliding	Expensive, sponsor has to procure	Less strong than polycarb
Weld Verification	**Current Sensor**	**Ohmmeter**	
Pros	Team accurately implements the measurement	Easy indicator of failure	
Cons	Complex and expensive to implement	Requires numerous electrical components	
GUI	Non-touch display	Touch display	Laptop Tkinter GUI
System Control Processor	RPi	Laptop control	Teensy 4.1
GUI Processor	shared RPi with system control	individual RPi for display	

Table 5.4.2. Morphological Chart with Pros and Cons for Each Human-Powered Solution

Functional Subsystem	Concept 1	Concept 2	Concept 3
Realtime Weld Verification	**Current Viewing Resistor**	**Ohmmeter post-weld**	
Pros	Allows for real time feedback	OEM solution, more robust	
Cons	Requires complex implementation and tuning	No way to receive feedback during weld	
Force Enforcement	**Pneumatic cylinder**	**Spring**	**Load Cell**
Pros	Provides both a soft and hard cutoff region	Simple force to distance relation	Gives consistent force feedback to user
Cons	Requires precision machining and seals	Susceptible to slop in assembly and pushing past limit	Requires electrical integration and tuning
Table	**Require level table**	**Threaded feet on steel frame**	
Pros	No additional cost or complexity	Adaptable to any conditions, absorbs vibration	
Cons	Does not work for users with bad table	Added cost and machining complexity	
Electrode Clamping	**Set-screws**	**Direct bolted mounting**	**Insulated clamps**
Pros	Simple, proven strength	Allows maintaining full contact with electrodes	Isolated welding current path
Cons	Impose load and can deform electrode	Require strong threaded reviewing areas	Takes up more space, not as secure
User Interface	**Haptic feedback**	**Auditory feedback**	**Indicator lights**
Pros	Hard for the user to ignore, intuitive	Grabs user's attention	Simple to implement and low power need
Cons	Haptic module is larger than other methods	Will not be effective for users with hearing disability	User may forget to look at the light
Micro Controller	**Teensy 4.1 + external ADC**	**ESP32-S3**	

Table 5.4.1 and 5.4.2 were the result of realistic constraints (sourcing, price, integration, etc.) applied to our initial concept generations. The pros and cons of each category were laid out below each solution in order to ensure we fully understand each option presented to us. With these pros and cons we discussed each as a team and agreed upon which ones to move forward with during a round-table discussion. We unanimously agreed on what would be best for the automated and human-powered design, and those choices are shown below in **Table 5.4.3** and **Table 5.4.4**, respectively (p 23).

Table 5.4.3. Chosen solutions for Automated Design

AUTOMATED FINAL	Chosen Solution
Z-axis Actuation	Pneumatics - Double Piston
Movement	Lead Screw
Motion Actuator	Stepper motor
Structure	80/20 Al Extrusion
Bed Material	MDF
Electrodes	Copper
Weld Verification	Current Sensor
GUI	Non-touch display
System Control Processor	Teensy 4.1
GUI Processor	Shared RPi with System Control

Table 5.4.4. Chosen Solutions for Human-Powered Design

Human-Powered Final	Chosen Solution
Z-axis Actuation	Human Applied force with passive pneumatics
Angle Enforcement	Dual freely-pinned four-bar boom-arm
Force Enforcement	Passive pneumatic pressure measurement
Table	SOP requires level working surface
Electrode Clamping	Direct bolted mounting
Ergonomics	Contoured rubber grips
Electrode Material	Copper
Realtime Weld Verification	Current Viewing Resistor and voltage probes + resistance measurement post-weld
User Interface	Haptic/auditory feedback + LED status lights
Micro Controller	Teensy 4.1 + external ADC

The solutions for each category were decided upon based on how well they would be able to accomplish the requirements and specifications we established. The solutions laid out in this table successfully allow for improved weld location accuracy, locked orientation of the welder, a consistent and controlled welding force, as well as stability. It will also increase spot welding efficiency and provide a way to verify our weld quality.

5.5 Deciding on Alpha Concept

After carefully evaluating both solutions laid out above, it is evident that both of these solutions would meet all of the requirements and specifications for our design problem. Because of this, we believe that the best way to proceed with our decision making is to consider the context of the position we are in and the timeline we must follow. The result of this decision process is shown below in **Table 5.5.1**.

Table 5.5.1. General Comparison of the two solutions

Metric	**Automated**	**Human-Powered**
Ease of Manufacturing	Difficult	Moderate
Weld Quality	Meets Requirements	Meets Requirements
Ease of Maintenance	Difficult	Easy
Ease of Use	Difficult,	Easy, Very Intuitive
Welds per Minute	High	Moderate
Cost	~$1200	~$600

This chart favors the human-powered design in regard to ease of manufacturing, ease of maintenance, and ease of use. Both are affordable and improve the welds per minute requirement, but the human-powered solution stands out in overall convenience of use while also achieving all of the requirements that the automated solution does. However we also wanted a more systematic approach to making our final decision for the alpha concept which is seen in the Pugh Chart below, with the automated solution acting as the baseline.

Table 5.5.2. Pugh Chart of automated vs human-powered

METRIC	Weight (1-5)	Baseline (Automated Solution)	Human-Powered Solution	Comparison	Notes
Z-axis Actuation	5	Pneumatics - Double Piston	Human Applied force with passive pneumatics	5	Easier to control
Movement	5	Lead Screw	Dual freely-pinned four-bar boom-arm	5	Easier to control
Motion Actuator	5	Stepper motor	Human Arm	5	Easier to control
Angle Enforcement	5	Gantry System	Dual freely-pinned four-bar boom-arm	0	Both keep angle fixed equally
Structure	3	Level Steel Tubing	SOP requires level working surface	3	Don't have to deal with table design
Bed Material	1	MDF	SOP requires user provide their own bed	1	Don't have to provide bed design
Electrodes	1	Copper	Copper	0	Same material
Electrode Clamping	1	Direct bolted mounting	Direct bolted mounting	0	Same process
Weld Verification	5	Current Viewing Resistor and voltage probes + resistance measurement post-weld	Current Viewing Resistor and voltage probes + resistance measurement post-weld	0	Same process
GUI	3	Non-touch display	Haptic/auditory feedback + LED status lights	3	Keeps user attention on task at hand
System Control Processor	2	Teensy 4.1	Teensy 4.1 + external ADC	0	Same controller
End Effector Structure	2	3D-Printed	3D-Printed	0	Same material

This Pugh Chart takes us through the metrics we had for our final design for both the automated and human-powered solution and compares them using a weighted scale from 1-5 with 5 being crucial. The total weighting score equals 38, and the human-powered design took the majority of the points at 22, making it the systematic winner here. This leads us to the initial alpha concept design and analysis that is discussed in section 7 of this report.

6. The Alpha Design

Our alpha design is the human-powered solution in **Table 5.6.2** that we determined systematically from section 5 of this report. This selected concept has the capability to successfully meet all of our requirements and specifications in both our needs and wants. It is especially enticing given the simplicity and low cost, which lend themselves well to the open-sourced nature of the project.

6.1 Initial CAD Model

The team developed a preliminary CAD model to understand the scale of the lengths needed to reach the welding area as laid out in the requirements. Components were modeled and given simple joints, as seen in **Figure 6.1.1**.



Figure 6.1.1. Initial CAD model of dual four-bar boom-arm with end effector

Within this CAD model, each of the subsystems stem from **Table 6.2**, and these subsystems are critical for ensuring that our requirements are being met both directly and indirectly. The pivot point location is seen on the left side of the model, free to rotate as desired. The two four-bar boom-arms (dark grey) are connected with a joint stack (light blue) located in the middle of the model, and the end effector (orange) is seen on the right side. The joints will be developed beyond simple pins to include bushings, bearings, and washers. The end effector design seen here simply serves to show the location of the handle (black) and passive pneumatic cylinders (green).

6.2 Subsystem Interaction

The relationship between each subsystem and the requirements and specifications are seen below in **Figure 6.2.1**. In this figure, the end effector and dual boom-arm are considered the primary subsystems and within them the components from **Table 6.2** and their interactions with each other are demonstrated. Additionally, the relationship between the end effector/boom-arm and their impact on the requirements and specifications are shown.

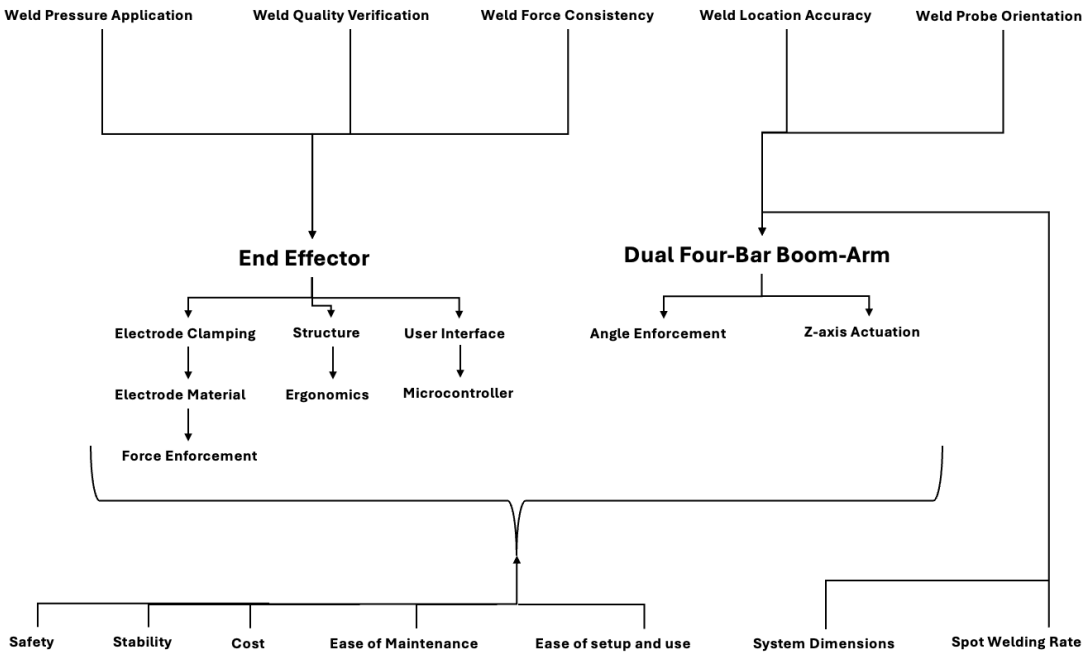


Figure 6.2.1. Layout drawing of relationship between subsystems and requirements

Our angle enforcement subsystem is a human-powered dual four-bar boom-arm that helps achieve the weld location accuracy, weld probe orientation, and spot-welding rate requirements. Being human-powered, the location accuracy and rate are up to the operator, but with this system being on a giant boom-arm, the motion is guided and two dimensional, making it much easier to achieve accuracy and increased rate of welding. The angle enforcement is directly achieved here and the four-bar design will enforce our end effector to be held at 90 degrees and any manufacturing tolerances will keep this angle within our 2-degree cone of tolerance. Our Z-axis actuation and force enforcement subsystems address our requirements of weld pressure application and weld force consistency. The passive pneumatic cylinders in the Z-axis will provide us with a direct value as to how much force is being applied to the battery cell from the human actuation. The optimal value required to make the welds will be determined based upon our empirical testing at different forces. Once this optimal force is determined, the pneumatics will help us keep this force consistent throughout all welds. Regarding the weld quality verification, our subsystems of electrode clamping, electrode material, and our realtime weld verification will all be working together. The realtime weld verification will allow for us to get a direct value on the amount of current passed through the electrodes and from there will indicate whether or not it was truly a good weld. The electrode clamping distance and material also play a role in the quality of the weld produced. Regarding the safety of this design, our user interface and microcontroller will allow for haptic feedback to the user indicating when the ideal force is reached, preventing any possibilities of puncturing the cell. This design and all of the subsystems

also allow for additional requirements and specifications to be achieved such as system dimensions, ease of maintenance, ease of setup and use, cost, and safety.

7. Problem Analysis and Iteration

7.1 Initial Engineering Analysis for Controller Selection

To enable our desired weld verification measurements of total energy input and weld resistance, we need to choose a controller capable of measuring data in a precise and accurate manner. In order to find the energy expenditure, we plan to install a current viewing resistor (CVR) in series with the welding pulse. These resistors are capable of handling pulses in the millisecond range and with several kila-amps of current. With the precise resistance value of the CVR, we can measure the voltage differential over the CVR to determine the current flowing through the system. Another voltage differential reading will be taken across the welding probes. By multiplying the current by the voltage across the probes, we can determine the instantaneous power delivered to the weld. We can then integrate this time dependent signal to find the total energy expenditure. With these sensors in mind, we need to outfit a controller that is capable of reading these signals both simultaneously and accurately.

First, we eliminated all controllers running an operating system, as they are not time-deterministic. This term refers to the precision of when a processing event occurs. Operating systems like Linux have event schedulers, which can introduce delays in CPU actions in the realm of milliseconds. Considering that our welding pulse is ~10 ms, and that both voltage and current need to be read in phase for accurate power determination, we believe choosing a microcontroller instead is the best path, as microcontrollers have time-deterministic behavior in the microsecond range.

Second, we performed napkin math to find the specifications needed for an analog-to-digital converter (ADC) capable of reading these signals. As we will be integrating the curves of current and voltage, we desire our ADC to have a high enough sampling rate to properly capture the curve. For a ~10ms pulse, we want at least 1000 samples to create a smooth curve. By using **Eqn 7.1.1**, we can determine the sampling rate needs to be 100 KS/s.

$$Sampling\ Rate\ =\ \frac{1000\ samples}{10\ ms} \tag{7.1.1}$$

Third, we took this value and multiplied it by the number of channels, the sampling time, and the cost of storage at 12 bit in **Eqn 7.1.2** to find the total RAM storage needs to be 300 KB

$$RAM\ =\ 100\ KS/s\ *\ 1\ second\ *\ 2\ channels\ *\ \frac{12\ bits}{sample}\ *\ \frac{1\ byte}{8\ bits} \tag{7.1.2}$$

As this is only part of the necessary use of RAM, we desire the total RAM to be in the realm of 1MB. When comparing a shortlist of commonly available microcontrollers in **Table 7.1.1**, we can see that the Teensy 4.1 controller meets our requirements of both sampling rate and RAM capacity.

Table 7.1.1. Comparison of Microcontroller ADC Specifications, RAM Capacity, and Cost.

Micro Controller	ADC Specs	RAM Space	Cost
Teensy 4.1	1 MS/s 12 bit x2	1 MB	~$40
Teensy 3.1	1 MS/s 10 bit x2	64 KB	~$20
ESP-32 S3	83 KS/s 12 bit x2	512 KB	~$7
Arduino Uno	9.6 KS/s 10 bit x1	2 KB	~$20
Arduino Due	1 MS/s 12 bit x1	96 KB	~$45

One aspect to note is that we did not perform resolution calculations for the ADC's as the resistance of the CVR can be chosen such that the full range of ADC reading can be utilized.

7.2 Initial Engineering Analysis of Human-Powered Arm Length

Part of our initial engineering analysis was determining how large this human-powered design would have to be in order to successfully meet the Michigan Electric Boat battery pack size requirement. We set the requirement for the operating field to be 40"x40" and from there the maximum radius that needs to be reached by our arm is 56.57". We also must ensure that the arm is not fully extended at this maximum radius, therefore a maximum angle of 150 degrees was enforced for the arm. With these parameters enforced, the law of cosines was utilized to determine the length of each arm. The calculations and sketch of the arm are shown below in **Figure 7.2.1**.

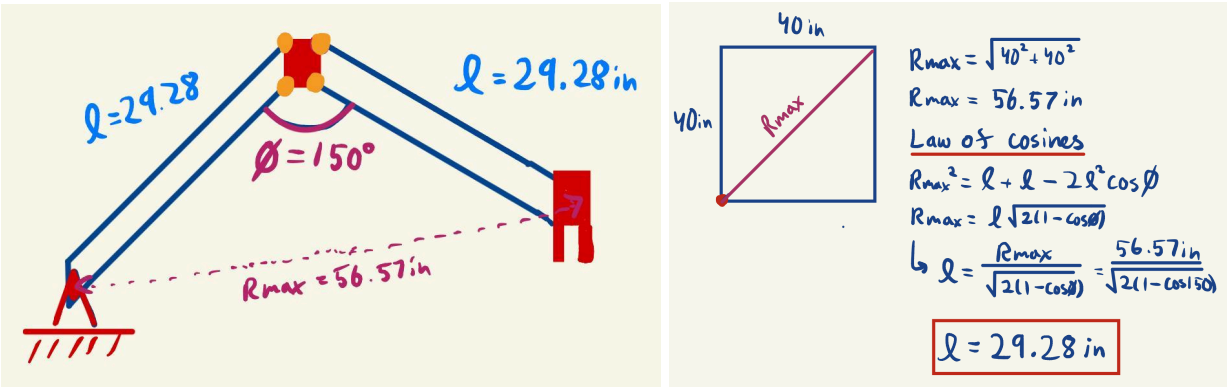


Figure 7.2.1. Arm length calculations based on required playing field dimensions.

The goal of this calculation was to provide us with a rough estimate of the scale of this human-powered welder, and we now know each arm will roughly be around 30”. This will meet our requirements for the playing field, however we must ensure that when it is manufactured that it is able to be operated with ease despite its size. Another aspect we must consider is where exactly to place the pivot point/base of the arm. That will depend more on how we design the joint between the two arms and what the maximum flexion will be there. That will allow us to understand how close to the origin of the 40”x40” playing field we can get and how far back diagonally from the origin we need to place the pivot point. With this change being put into place, the maximum radius will therefore be increased and naturally the length of the arms will need to be increased. This can be found with some simple changes to the calculations in **Figure 7.2.1**.

7.3 Finalized Engineering Analysis of Arm Length

Our budget of $2000, according to our Cost requirement (Section 4.2.9) presents a challenge when it comes to selecting the welding cable that we need to use to transmit the high-current, low-voltage pulse from the spot-welder to the end effector, which could be as much as 50 inches away. McMaster-Carr features two main classes of high-current welding cable, Class M and Class K. Class M welding cable is significantly more flexible than Class K cable because it has many more strands and does not stay in the position it is left in, whereas Class K deforms plastically. Our implementation requires a Class M cable that is flexible enough to travel the length of the linkage without providing large amounts of resistance to changes in the cable’s path.

Additionally, with our spot welder providing a maximum of 9V, minimizing the voltage loss along the long stretches of cable that will connect the welder to the end effector is of peak concern. Resistivity of copper tends to decrease with cross-sectional area, so we chose the largest gauge of wire possible from McMaster’s catalog that still features a Class M option (part number 7940A81). This wire costs $8.94 per foot, and is sold in increments of 10 feet. Our budget must account for all of the other mechanical and electrical components necessary, including the spot welder itself. Spending nearly $180 for 20 feet of welding wire is not possible as a part of this budget, and so we must make do with 10 feet of cable. In the ideal case, as calculated above in the preliminary analysis section, a link length of approximately 30 inches would allow the end effector to reach any point within 40” x 40” operational area. However, a cabling run starting at the origin and running out to the end effector and back (as is necessary without mounting the welder onto the moving linkage somewhere) would automatically exhaust all 120 inches of cabling available, just to traverse exactly the distance between each link joint. There would be no slack left to allow for the cabling to adapt to the shape of the linkage as welds are performed across a module.

To address this multi-faceted problem, with the input from the finalized mechanical elements of the build design, we assume that each cabling run, the positive run and the negative run, is exactly the same length. With a 10-foot cable, that leaves 5 feet per cabling run, which should include extra slack for the placement of the spot-welder itself off to the side of the rigid base. When fully extended at our self-imposed limit of 150 degrees, the distance one run must travel is greater than simply twice the arm length. From the tip of the rigid base, the cables will need to travel at least 8 inches to ground level to reach the welder, with additional slack built in for the rotational capabilities required at the base pivot. Additionally, both cables are estimated to need to extend 6 inches further to have enough slack to reach the electrode probes at the tip of the end effector. This leads us to conclude that the arm length, of which there are 4, should not exceed 21 inches, such that there is enough welding cable remaining out of the 10 feet of purchased cable for the two >8-inch connections and two >6-inch connections required to be feasible. The arm lengths will take a minimum of 88 inches of cabling to traverse, leaving 16 inches of cable to travel from the base pivot to the ground, 12 inches of cable to travel from the second four-bar linkage to the end effector, and 10 inches of cabling as slack to allow it to adapt to the many degrees of freedom featured by our linkage design.

7.4 Joint Stackup Angular Deviation Analysis

The purpose of this analysis is to determine the minimum vertical distance required between joints across the twice-repeated four-bar linkage assembly. Our joint stackup is pictured below and includes a sleeve bearing, four thrust washers, and a needle-roller thrust bearing to ensure smooth, aligned rotational movement between the link arms (to which the shoulder bolt is fixed) and the rigid base, coupler, or end effector joint block. This stackup is very similar to the recommended joint stackups we gained expertise with in ME350, and has been proven as a low-tolerance solution for high-RPM movements with often significant applied moments and thrust loads from the cantilevered link arms utilized in the course. Shown below in **Figure 7.4.1** is the labeled joint stackup.

math

Figure 7.4.1: ME350-inspired Joint Stackup Applied to Four-Bar Linkage Concept

For this stackup, and its effect on our ability to fulfill Requirement #2 (explained in Section 4.2.2) will be analyzed by assuming the worst case tolerance scenario and calculating the resulting interaction between the shoulder bolt and the 1” bronze sleeve bearing. **Figure 7.4.2** below shows an exaggerated view of the result when a sleeve bearing with its maximum ID and minimum length is combined with a shoulder bolt with its minimum OD.

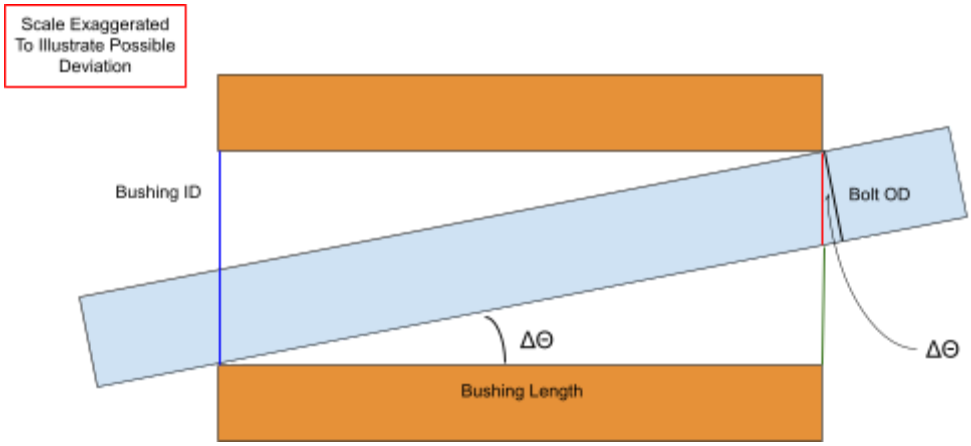


Figure 7.4.2: Exaggerated view of angular deviation with tolerance extremes on shoulder bolt OD and sleeve bearing ID.

We can clearly see that with a small shoulder bolt and large sleeve bearing, the bolt will tend to rotate in its housing as radial load is applied to it by the linkage. To quantify this angular deviation, calculations were performed using the diagram above along with the toleranced limits on the dimensions of the sleeve bearing and the shoulder bolt. The resulting angular deviation was used, in conjunction with details about the joint stackup between the sleeve bearing and the link, to determine the maximum angular deviation introduced into the system as a function of the vertical distance between the joint pivots. These calculations are expressed in great detail in Appendix section A.7, and **Figure 7.4.3** below illustrates this scenario.

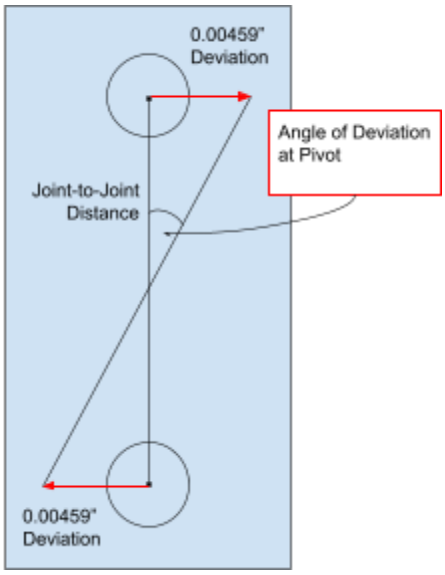


Figure 7.4.3: System angular deviation introduced from joints, side view

The result was a minimum vertical joint-to-joint distance of 1.05 inches, which we have increased to 3 inches as a conservative estimate to allow for a much greater range of motion with respect to the maximum angle the arms may reach. A shorter joint-to-joint distance will mean

that the link arms could collide with the shoulder bolts at a lesser angle of inclination. Additionally, this conservative value allows for some safety factor on the orientation angle requirement in case of manufacturing defects or out-of-tolerance parts, as it is extremely important that this requirement is met.

7.5 Analysis of Radial and Thrust Loads at Base

The purpose of this engineering analysis is to establish a set of mathematical relationships based on geometrical design parameters that can be used to determine whether our base pivot bearing selection can sustainably withstand the radial and thrust loads they will be subjected to. **Figure 7.5.1** displays a simplified diagram of the major weight forces of the linkage and end effector that the bearing will have to support. As a preliminary engineering judgment, we have determined that at least two rows of balls across at least one ball bearing will be necessary to support both the thrust and radial loads expected in our system, as a single row would not be able to break the moment load into two radial loads, and would likely rotate out of its housing or become misaligned.

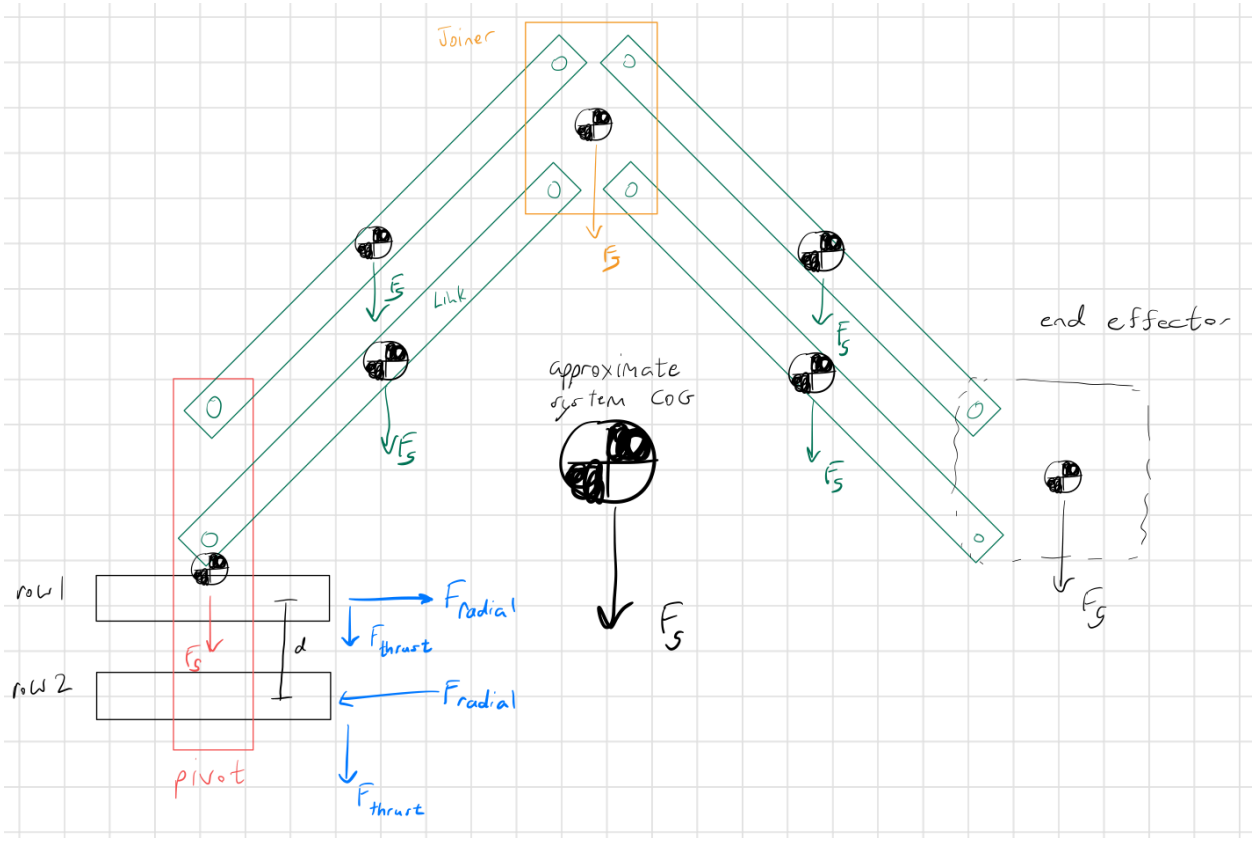


Figure 7.5: Expected loads on base pivot bearings.

The thrust load withstood by the system will remain constant, as it is purely equivalent to the mass of each component in the system multiplied by the gravitational constant. However, the moment load withstood by the bearings has the potential to change as a function of the distance

the linkage stretches away from the pivot, as the centers of gravity of the components shift further away from the bearings. If we assume that the joint locations on the end effector are approximately equal in height to the joint locations on the base pivot, the angle of inclination of the first four-bar linkage is approximately equal to the angle of inclination of the second four-bar linkage, reducing the degrees of freedom present in the problem. With this assumption, we define the following variables:

d = vertical distance between ball rows

L = link length

m_l = link mass

Θ = angle of inclination of four bar linkages ($\Theta = 90deg$) describes a vertically oriented link

j = lateral distance between joint points on the joiner

m_j = joiner mass

a = lateral distance between end effector joint points and end effector center of gravity

m_e = end effector mass

At our self-imposed lockout angle of 150-degrees, the angle of inclination of each linkage is $\Theta = 15\ deg$. A simple force balance allows us to compute the reaction moment that must be produced by the two rows of balls in the bearing(s).

$$\Sigma M_{bearing} = 0 = -m_l g * 2 * \left(\frac{L}{2} * cos(15deg)\right) - m_j g * \left(L * cos(15deg) + \frac{j}{2}\right) - m_l g * 2 * \left(\frac{3L}{2} * cos(15deg) + j\right) - m_e g * (2L * cos(15deg) + j + a) + M_{reaction,max}$$

The reaction moment can be produced by two radial reaction forces originating from each row of balls, separated by a distance d. These forces will be equal and opposite in direction.

$$M_{reaction} = F_{radial} * d$$

This way, once the rest of the linkage has been designed and these geometrical design parameters have been determined quantitatively, we can evaluate options for bearings based on their affordability and compatibility with our concept for a singular waterjet baseplate design, and increase the distance d between them such that the radial load sustained by the bearings is within the acceptable ranges.

With our now finalized build design, and with preliminarily-selected flanged single-row ball bearings from AMIBearings, we substitute our now-known masses of the links, end effector, joiner, and base pivot shaft, and compute whether the bearings can withstand the thrust and moment imposed by the linkage. Numerical calculations are included in the Appendix section A.7. Based on these results, we observe that each bearing will be withstanding approximately 210 lbs of radial loads and less than 4 lbs of thrust loads. This results in a load vector that is essentially perfectly radial, allowing us to use the flanged single-row ball bearings for their affordability, stability under high radial loads, and their high compatibility and ease of installation onto our base plate.

7.6 Determination of Pneumatic Cylinder Dimensions

The purpose of this analysis was to mathematically determine the required specifications for maximum pressure, bore diameter, and piston travel for the coupled pneumatic cylinders used in the build design.

First, empirical testing was conducted to approximate the level of force that needed to be applied to a cell to produce a high-quality weld. During this test, a dummy cell was placed on a scale, and three group members practiced performing 5 spot-welds each, while a second member looked on and recorded the maximum force measured by the scale. The full dataset is available in the Appendix section 7.6 A sample picture from the testing is shown below in **Figure 7.6.1.**



Figure 7.6.1. Example of trial of group member performing spot weld on scale. Approximately 16 lbs max measured during this trial.

Across all the trials we conducted, the mean force measured was 16.57 lbs with a standard deviation of 1.324 lbs. Applying the bounds of a typical normal distribution, we can expect the majority of force values to lie between 12.60 lbs and 20.54 lbs. As a conservative estimate, we will utilize the upper bound of this force range for the piston calculations. Assuming this force to be equally distributed between the two electrodes, we can develop mathematical relationships for the maximum pressure in the pneumatic cylinder as well as the expected minimum stroke necessary to sustain the necessary force without bottoming out.

Fundamental Variables:

$D = piston\ bore\ diameter$

$p = piston\ pressure$

$s = stroke\ distance$

Pressure equation: $p = F_{applied}/A_{piston} = \frac{F_{applied}}{\pi * \frac{D^2}{4}}$

Ideal gas equation assuming no temperature change: $p_1 V_1 = p_2 V_2$

At the start of a weld, with no force applied, the piston will be fully extended, with $F_{applied} = 0$.

At the height of force application before a weld, $F_{applied} = 20.54\ lbs\ /\ 2 = 10.27\ lbs$.

Therefore, at the very least, our chosen piston must be able to withstand a chamber pressure equal to $p_{max,piston} \geq \frac{10.27\ lbs}{\pi * \frac{D^2}{4}\ in^2}$

Additionally, the stroke of the piston s should be large enough such that in the fully compressed state, the piston has not bottomed out.

$V_1 = s * \pi * \frac{D^2}{4},\ p_1 = 14.7\ psi,\ p_2 = 14.7\ psi + \frac{10.27\ lbs}{\pi * \frac{D^2}{4}\ in^2},\ V_2 = \frac{p_1 V_1}{p_2}$

Our selection of McMaster-Carr's double-acting 5/16" bore piston meets these requirements, with a maximum pressure of 250 psi and a stroke of ½". With a bore of 5/16", the maximum pressure is expected to reach approximately 133.9 psi < 250 psi. Additionally, by performing the ideal gas calculation with $p_1 = 14.7\ psi$ and $p_2 = 14.7\ psi + 133.9\ psi = 148.6\ psi$, we obtain $V_2 = 0.0038\ in^3$, with the remaining stroke of 0.049" determined by dividing out the cross-sectional area $\pi\frac{D^2}{4}$. While we acknowledge that this represents a compression of over 90% of the piston's possible stroke, we are confident that in the majority of typical use cases, the piston will not bottom out. A sensitivity analysis of the percent compression as a function of the applied force, laid out in Appendix section A.6.4, shows that even with significant force variations within the range specified above, the piston's compression ratio remains in the range of 84 - 91%.

7.7 Analysis of Electrical Component Needs

To facilitate the operation of the welder and to enable the weld telemetry metrics, the welder must have five areas of functionality, all controlled by the microcontroller. They are as follows: load sensing (7.7.1), current sensing (7.7.2), current source (7.7.3), voltage sensing (7.7.4), and power supply (7.7.5). The load sensing is essential to our weld force requirement, informing the microcontroller as to when the applied force is within the acceptable range. The current sensing provides us the weld current as a function of time, which in tandem with the voltage across the weld as a function of time found in the voltage sensing circuit, can be used to find the total energy outputted into the weld. The current source is used to create a voltage differential across the weld, which is then read by the voltage sensing circuit to determine the weld resistance. The power supply is chosen to provide clean, reliable power to both the microcontroller and the analog components.

7.7.1 Load Sensing Circuitry

To accommodate the 44N maximum per probe force requirement, we must choose a load cell to meet the total force of 88N or ~20 lbs. We found the TE connectivity 0-55lb button load cell (FX292X-100A-0050-L) to meet these needs at an affordable cost [21]. This load cell is powered by a 5V supply and outputs a differential signal with maximum magnitude at 20mV/V for 100mV. For greater resolution, we desire to amplify the signal with a gain of 33 to match the 0-3.3V range of our Teensy 4.1 ADC [22]. To provide this, we chose the Texas Instruments INA333AIDGKR Instrumentation Amplifier with a gain resistor of 3KΩ [29]. This outputs a ground referenced signal that is first fed into an RC low-pass filter with a frequency cutoff of 800 Hz (20KΩ resistor, 10 nF capacitor) then into a diode overvoltage protection circuit. The frequency cutoff was chosen by using **Eqn 7.7.1**, where T_r is the 0-90% rise time of a signal and f_c is the cutoff frequency. The RC filter components were chosen using **Eqn 7.7.2**, where R is the resistance value and C is the capacitance. The final circuit is shown in **Figure 8.3.15.**.

$$f_c = \frac{0.35}{T_r} \tag{7.7.1}$$

$$f_c = \frac{1}{2\pi RC} \tag{7.7.2}$$

With an 800 Hz low-pass cutoff frequency, we filter signals with rise times lesser than ~0.5ms, which will not interfere with any relatively slow human inputs, but will remove high frequency noise. The diode protection circuit provides overvoltage protection for the ADC in the event that the amplifier outputs greater than 3.3V. This will be accomplished by connecting a schottky diode from ground to the signal wire, then another diode from the signal wire to the 3.3V bus. A 10KΩ resistor is in series with the signal to reduce the amperage to the 3.3V bus in the case of an overvoltage event.

7.7.2 Current Sensing Circuitry

To measure the current of the welder, we chose to use an in-series shunt with a differential voltage measurement circuit. When choosing the resistance of the shunt, we balanced the magnitude of the signal vs the power consumption. A higher resistance would produce a cleaner easy-to-read signal with a lesser need for amplification, but would also draw more power away from weld itself. Using Ohm's Law, we determined that the 1600A pulse would create a 0.16V signal with a shunt resistance of 100μΩ. This would only sap 1.7% of the power available from the 9V signal. When choosing an amplifier for this purpose, we had to consider the common-mode voltage of both the high side and low side of the welder. Because welders are electrically noisy with large swings in charge, it is not advisable to share a common ground between the welder and our microcontroller. To remedy this, we chose to electrically isolate the welder from the microcontroller. Drawing from a Texas Instruments build guide on automotive shunt-type current sensing, we chose the INA240A1 Instrumentation Amplifier with common-mode capabilities of -4 to 80V [23, 24]. With this amplifier on the high-side of the

welder, we can handle 13V of ground voltage differential. The INA240A1 outputs a ground referenced signal with a gain of 20V/V, bringing our 0.16V signal to 3.2V, just under our ADC maximum voltage. This signal is fed through an RC low-pass filter with a cutoff frequency of 160 KHz. This value was chosen because the square wave of our weld pulse has an approximate rise time of 10µs. Using **Eqn 7.7.1**, we find the frequency to be 35KHz. The 160 KHz filter, using a 100Ω resistor and 10nF capacitor, prevents noise with a rise time lesser than 2µs from impacting our data. This is then fed through a schottky diode protection circuit identical to the circuit presented in **7.7.1**. The final current sensing circuit is shown in **Figure 8.3.16.**

7.7.3 Current Source Circuitry

To test the resistance of the weld, we must provide a test current to produce a differential voltage across the weld. It is possible to use the existing current readings and voltage reading to read resistance during the weld itself, but we desire the ability to abort a weld prior to firing the main pulse. To enable this, we have chosen an LT3092 current source chip for its low price and easy implementation [25]. By using a 1Ω and 20KΩ resistor in parallel from the outputs of the LT3092, it will produce a 200mA current. Due to the isolation requirements of the system, the current source is fed from a 1S4E isolated 5V supply [26]. It is controlled on the low-side using a N-type MOSFET with a GPIO pin actuating the gate. In series with the 200mA current, there is a 10Ω ballast resistor. This resistor is there to take the brunt of the thermal load of the current. As we are expecting minimal voltage drop over the weld, the LT3092 would take the full 5V to 0V 1W load with the absence of the ballast. With the ballast resistor, a portion of the system power would be diverted. A diode is placed in series with the current source to prevent back-current during the weld pulse. The final current source circuit can be seen in **Figure 8.3.17.**

7.7.4 Voltage Sensing Circuit

The voltage sensing circuit provides valuable information for energy calculations and resistance measurements. In doing so, it needs to have dual sensitivity as the differential voltage during a weld and during the test current are drastically different. To accomplish the 0-9V reading, we will use an ISO224 Isolation Amplifier [27]. This amplifier boasts 5kV of isolation from the input side to the output side. As such it requires two power inputs, each referenced to the ground on either side. To accomplish this, we will again use the 1S4E isolated 5V supply [26]. The output side is referenced to the MCU ground as is supplied by the 5V bus. The output is in the form of a differential signal referenced to 2.5V. We then take the 2.5V+ and 2.5V– pair and feed it into an op-amp acting as a differential amplifier. This references the magnitude of the differential signal to 0V. Because the op-amp will be driven by the 3.3V bus, it also serves as overvoltage protection for the ADC. The signal is fed through an RC low-pass filter identical to the one found in the current sensing circuit (**7.7.2**). The gain of the ISO224 comes stock at ⅓ V/V. This works very well to remap the 0-9V signal to 0-3V for the ADC to read near full resolution.

To measure the current source produced differential voltage, the signal needs to be passed through an amplifier. We expect to see voltage differentials in the range of 0-50mV. As 200mA from the current source pass through the weld, we expect to see resistances in the range of 1-5mΩ, creating a maximum differential voltage of 1mV. However, we are unsure of contact resistances from the probes. As such, we are accommodating resistances up to 50mΩ, for a voltage of 10mV. This signal is passed through an INA333 with a gain of 1000V/V before passing through the ISO224 + OpAmp circuit identical to the 0-9V circuit [29, 27]. With the gain of the ISO224 at ⅓, the final signal exists from 0-3.3V, ideal for the ADC input. This is also passed through an RC filter identical to the one implemented on the 0-9V side. Once real data is collected, we are able to adjust the overall gain through the op-amp circuit to better fit the output signal to the range of the ADC. The final voltage sensing circuit can be seen in **Figure 8.3.18.**

7.7.5 Power Supply

To feed the microcontroller and analog devices with reliable clean power, we are using a SWI10B-5-NB-P5 switching power supply to convert wall power into a 5V DC output [28]. This has a power rating of 10W, which should be plenty for all the devices. The 5V bus is directed towards a pi-filter with a ferrite bead, 100pF, and 100nF capacitor. These components act as a low pass filter with high impedance for high frequency signals. This creates a clean power source that is provided to all of our analog components. This 5V is also fed into the VIN pin of the Teensy 4.1, which subsequently steps it down to 3.3V. This 3.3V bus supplies all of our op-amps and mosfets. The final power supply circuitry can be seen in **Figure 8.3.19.**

8. Build Design

The prototype for our solution will consist of manufactured and off-the-shelf components across four main subsystems, the base, the linkage, the electronic sensing system, and the end effector.

8.1 CAD of Final Build Design

Figure 8.1.1 below shows an isometric view of the full final build design. The design will be explained in more detail below, with manufactured and sourced components listed along with material selections and manufacturing process selections.

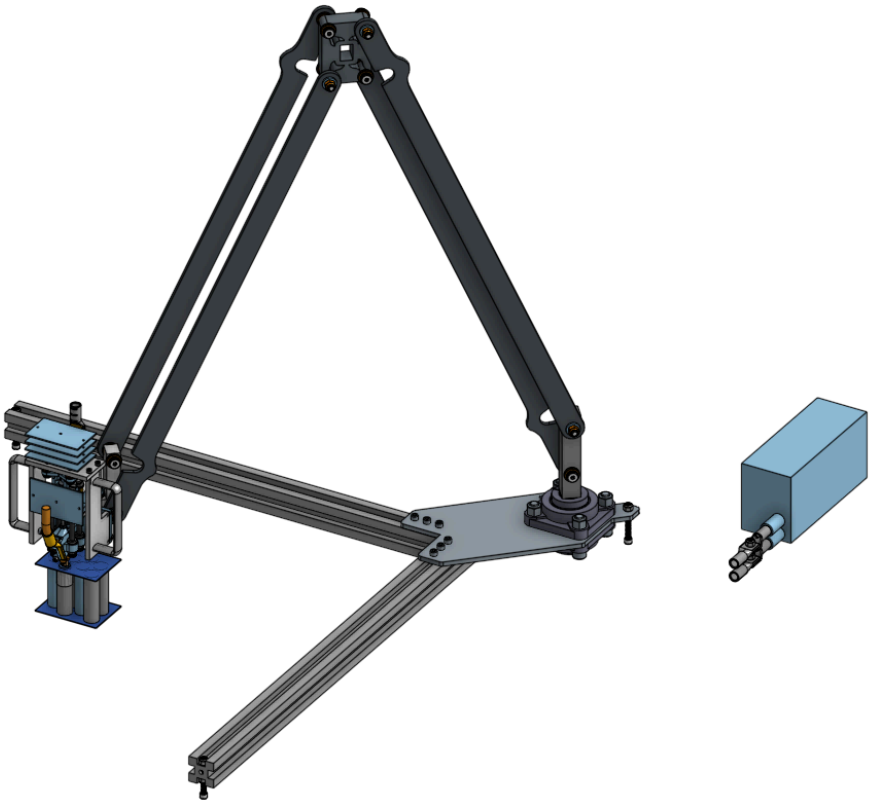


Figure 8.1.1. The full build design assembly interacting with a model of a small battery module. The spot welder is pictured off the side of the base pivot. Flexible cabling connections from the spot welder to the end effector are omitted for modeling purposes.

8.2 Subsystem Overview

Our four main subsystems help to satisfy the engineering requirements and specifications put forth in the above sections by individually supporting different parts of the spot-welding process. The base subsystem serves as the foundation upon which our linkage is built, and allows for user adjustability to ensure that the two four-bar linkages are always aligned with the normal vector of the cells to be spot-welded. Three adjustable screws, one at each corner of the triangular-shaped base subsystem allow for the base to be oriented to any plane in 3D space where the elevation difference between diagonally opposing corners of the operational area is up to 2.5 cm. A base

plate connects two aluminum extrusion channels at a perfectly perpendicular corner and provides mounting points for two beefy flanged spherical ball bearings, designed to withstand the radial forces imposed upon the base pivot point. **Figure 8.2.1** below displays the base subsystem.

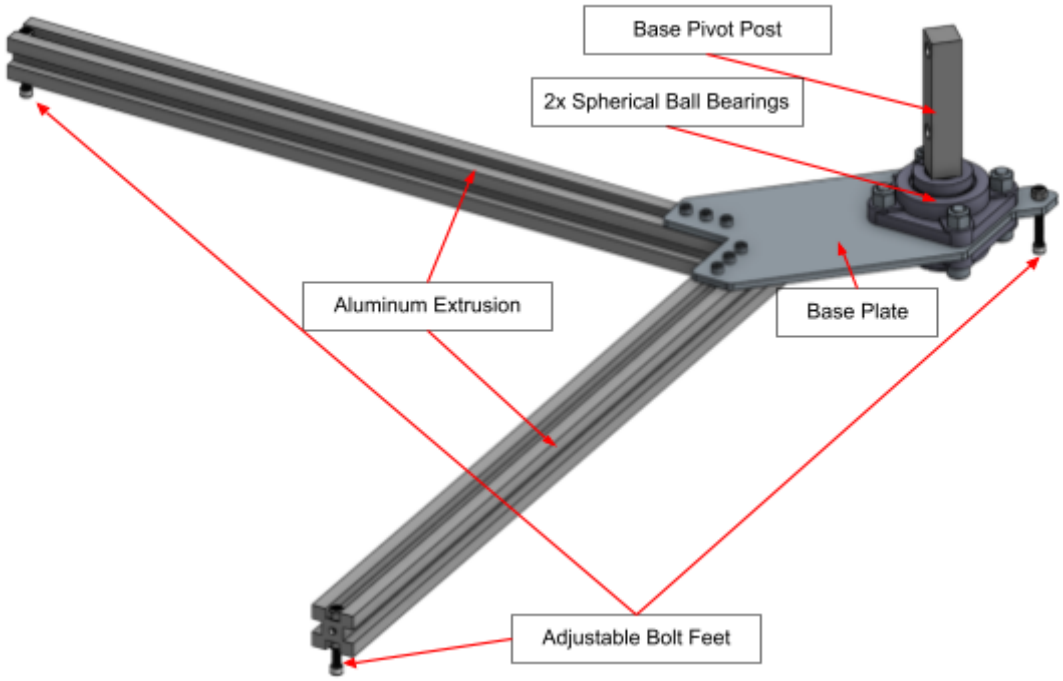


Figure 8.2.1 Labeled isometric view of base subsystem.

The linkage subsystem provides the 3 degree-of-freedom alignment system that assists the user in maintaining a constant orientation of the weld probes with respect to the cell terminals. Two independent four-bar linkages allow for movement in the radial and Z axes, while the rotating base pivot from the base subsystem allows for smooth movement in the theta-direction. All joints are composed of strong alloy steel shoulder screws and steel needle-roller bearings to ensure the smoothest joint operation possible. **Figure 8.2.2** below displays a singular link assembly, of which the build design contains four.

Figure 8.2.2 Labeled isometric view of a link subsystem.

The electronic sensing system provides real-time feedback about critical spot-welding parameters, including pre- and post-weld resistance values across the electrodes, weld current, and applied force on the electrodes. It is mounted to the end effector to minimize the length of wire leads, improving sensitivity and eliminating potential errors from wire resistances. A constant current source, multiple differential amplifier circuits, and a micro-Ohm scale shunt are the critical components that allow for this sensing to take place. Detailed circuit diagrams for the electronic sensing system can be found in sections 8.3.15 through 8.3.19.

Finally, the end effector provides the mechanical solution that assists the user in producing consistent, high-quality spot-welds. Two linearly-sliding sleeve bearing assemblies allow for independent movement of the two electrodes, while coupled pneumatic cylinders balance the user-applied load equally between the two. A load cell placed in series with the pistons records the applied force, transmitting it to the electronic sensing subsystem. Two ergonomic handles allow the user to apply force evenly and with minimal effort. **Figure 8.2.3** below displays the end effector subsystem.

Figure 8.2.3 Labeled isometric view of the end effector subsystem.

8.3 Manufactured Components

8.3.1 Base Aluminum Extrusion

This component is the base of the solution. The extrusions are joined together with the baseplate (8.2.2) to create a 90 degree corner, which is used to align the module to be welded with the solution. The extrusion also supports the rest of the solution above it. Aluminum extrusion is used as it is readily available for most project teams. Holes are drilled and tapped to mount directly to the base plate, and each aluminum extrusion contains a clearance hole at the tip for one of the three total adjustable bolts that allow for the base subsystem's angle of inclination adjustment.

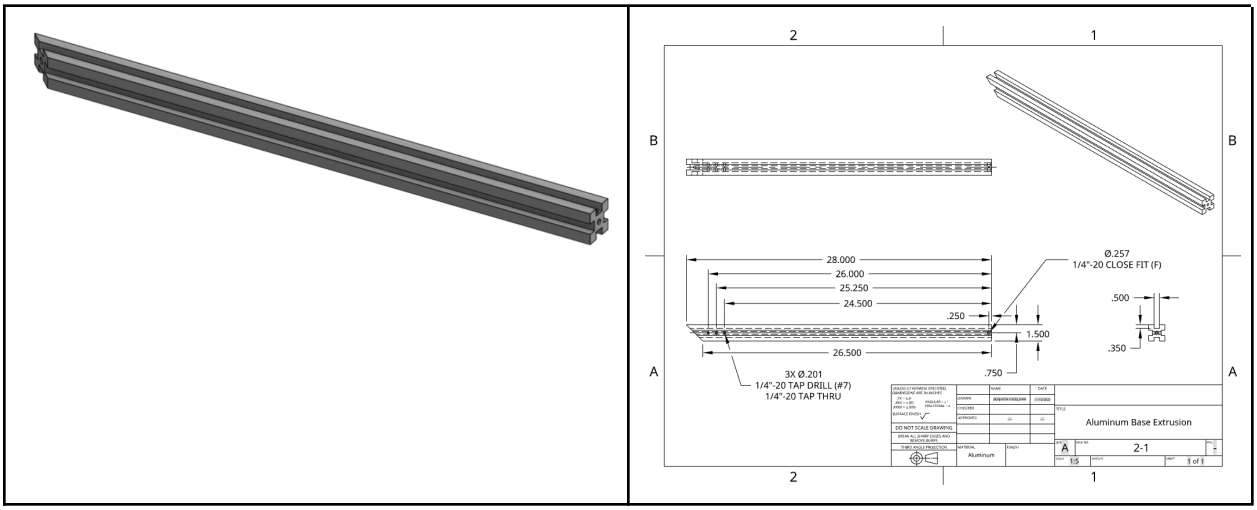


Figure 8.3.1. The isometric view and technical drawing for the base aluminum extrusion.

8.3.2 Base Plate

This component is the base on which the entire solution is built off. It has holes to join together two base extrusions, as well as holes to align pillow block bearings to create the center of rotation for the linkage system. Finally, it includes a clearance hole at the tip for one of the

adjustable bolts that allow for the base subsystem's angle of inclination adjustment. The base plate's shape lends itself nicely to waterjetting in the x50 Shop as a manufacturing method.

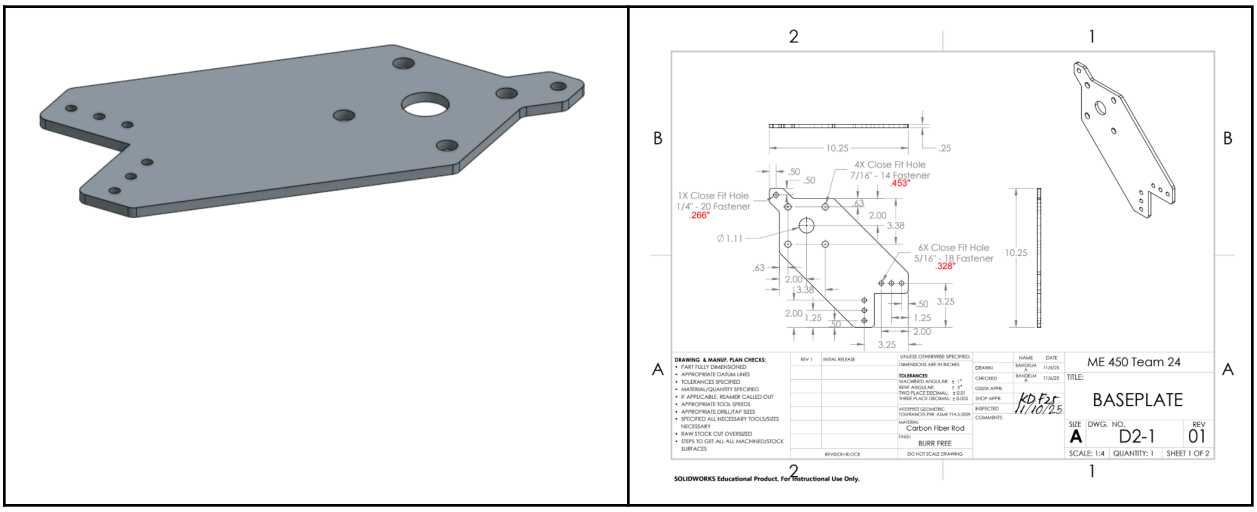


Figure 8.3.2. The isometric view and technical drawing for the base plate.

8.3.3 Base Pivot Post

This component sits in the pillow block bearings connected to the base, and rotates while connected to the linkage system. The location and size of the linkage holes is crucial to ensuring a good push fit with the sleeve bearings to maintain the alignment of the end effector. The piece must resist a bending moment from the force transferred from the end effector to the linkage, so the piece should be made of machined steel.

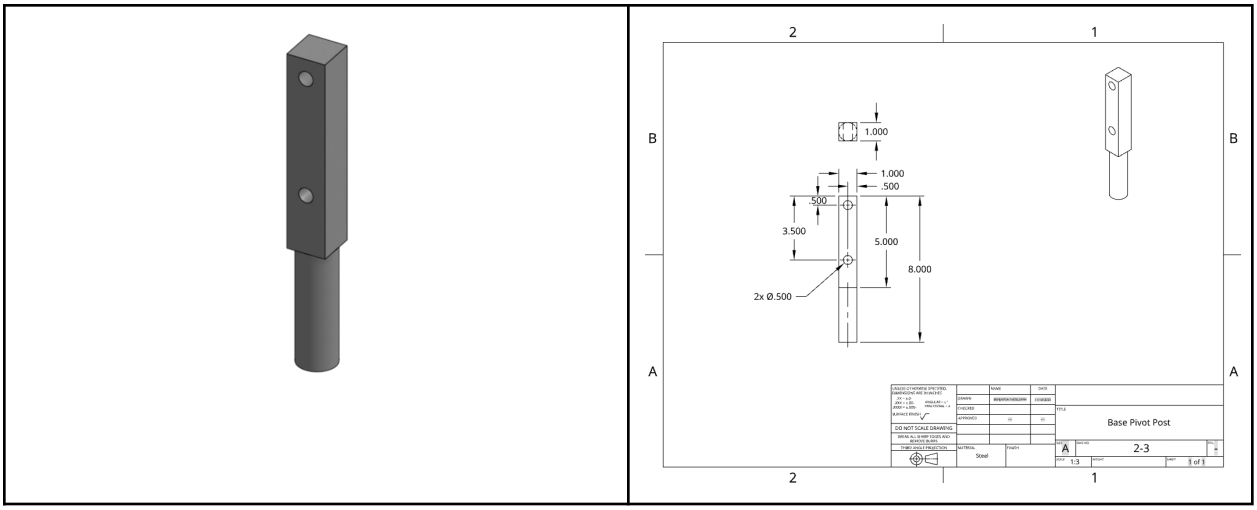


Figure 8.3.3. The isometric view and technical drawing for the base pivot post.

8.3.4 Linkage Arm

This component completes the 4 bar linkages to enforce verticality of the end effector to prompt good weld quality and alignment. Manufacturability of this part has been optimized by the team

so that all linkage arms can be cut on the waterjet and fabricated from 0.25” aluminum sheet, which is readily available from the SPARK workspace.

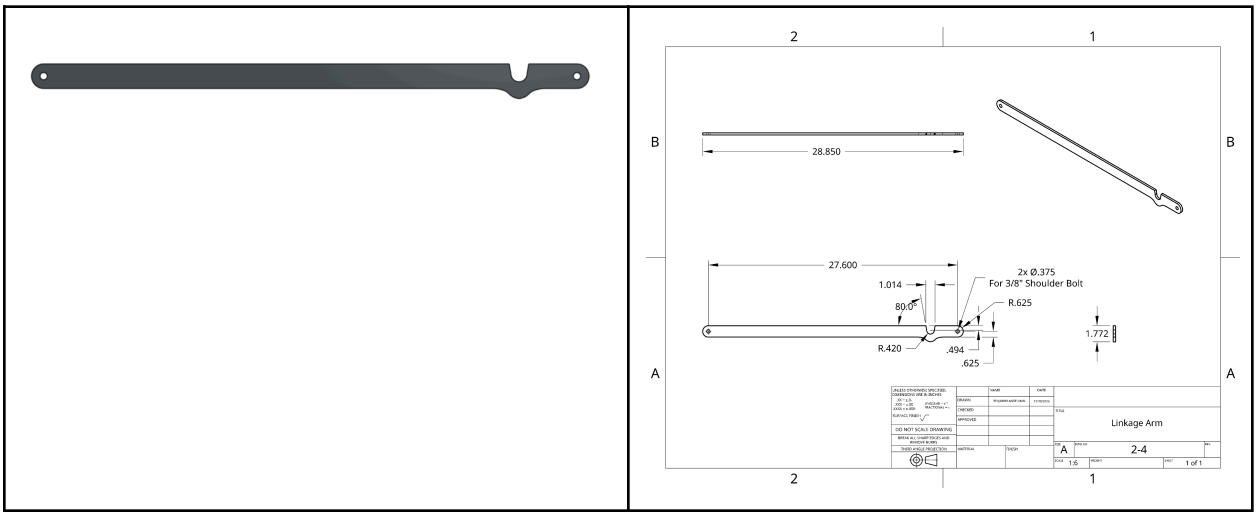


Figure 8.3.4. The isometric view and technical drawing for the linkage arm.

8.3.5 Linkage Joiner

This component joins together the two separate 4 bar linkages, also acting as a link itself to enforce motion. Due to the complex geometry to prompt weightsaving, and the open source intent of the project, this component should be 3D-printed using a robust filament such as PETG on an FDM printer. The tolerances of the four holes containing the long sleeve bearings will be important to ensure a snug fit such that the linkage is not thrown out of alignment by any angular deviations introduced at the joiner.

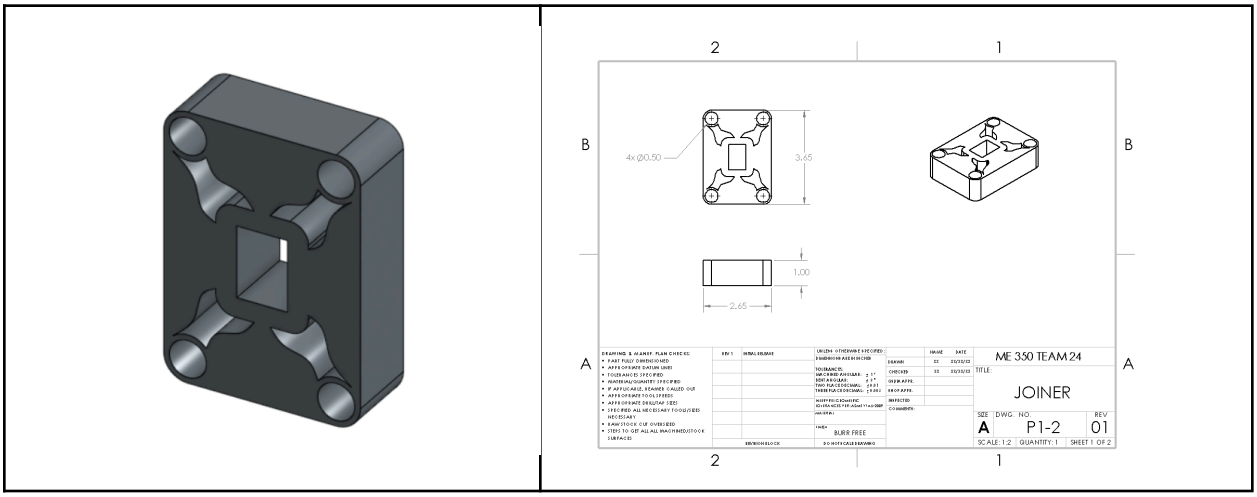


Figure 8.3.5. The isometric view and technical drawing for the linkage joiner.

8.3.6 End Effector Joint Block

This component serves as the output link of the linkage, and connects the end effector with a pivot point. This piece is critical to ensuring that the end effector has the necessary degrees of freedom. The piece must not deform under operation loads, as it directly enforces the angle of the welding probes relative to the battery pack, so this part will be made of machined aluminum. The tolerances around the three holes where the long sleeve bearings are meant to be press fit will be important to ensure the sleeve bearings stay snugly in place and do not move with respect to the joint block. Any failure to do this could compromise the end effector's alignment with the normal vector of the plane of the cell terminals.

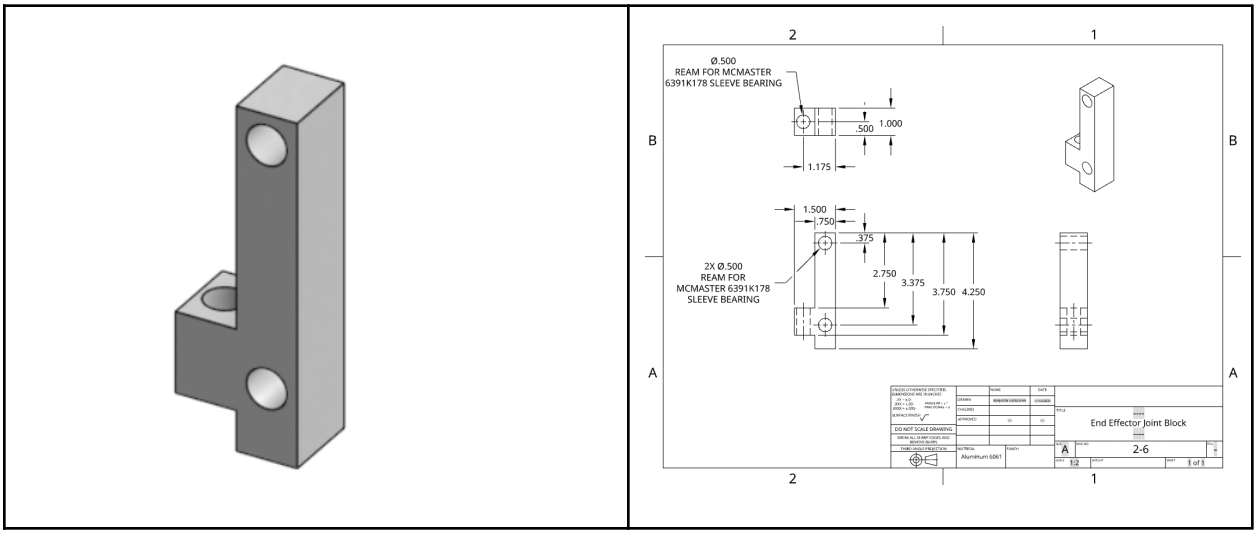


Figure 8.3.6. The isometric view and technical drawing for the end effector joint block.

8.3.7 End Effector Pivot Connector

This component attaches the main end effector structure to the joiner (8.2.5) and allows for rotation to align welds properly. This piece has complex geometry, so for the prototype stage it will be made using 3D printing with ABS or PETG on an FDM printer. The part could be made using CNC milling of aluminum, but the manufacturing time is not realistic given the timeline of the project.

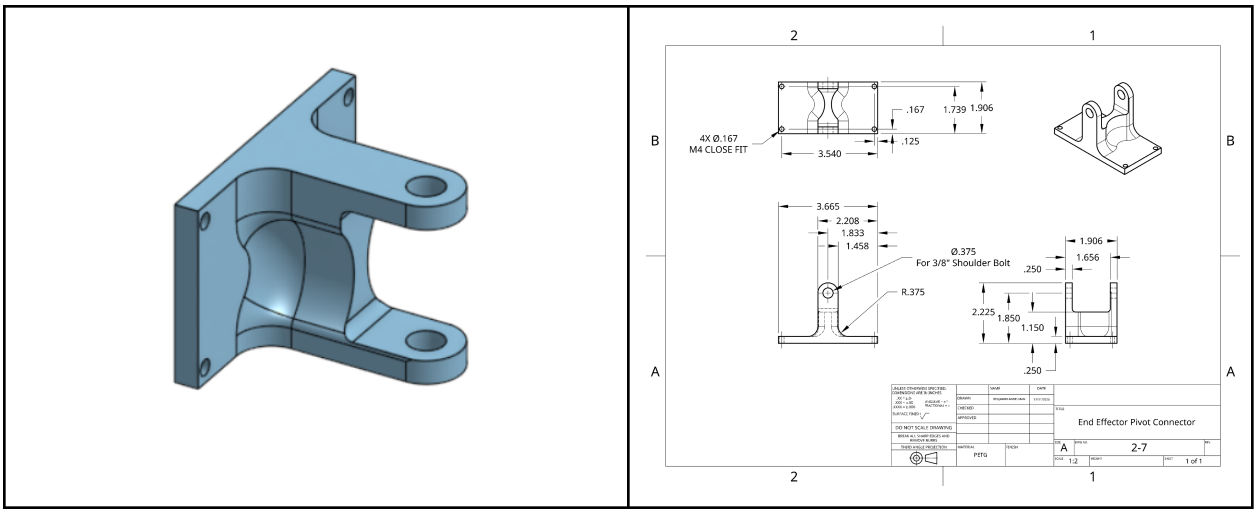


Figure 8.3.7. The isometric view and technical drawing for the end effector pivot connector.

8.3.8 End Effector Side Wall

This component provides rigid structure for the end effector and allows for attachment of the handles by which the user interacts with the end effector. As such, this piece needs to be strong in compression and bending, which lends itself well to a machined piece of aluminum. This piece can be made using the waterjet in the UG Shop, followed by a mill drilling and tapping operation to create the off-axis holes in the thickness of the plate. The dimensions of the smaller holes as seen in the isometric view are critical as they dictate the alignment of the end effector to the pivot, and thus to the linkage. The surface which these holes are on also needs to be made as smooth as possible, which we will achieve with grinding/polishing wheels.

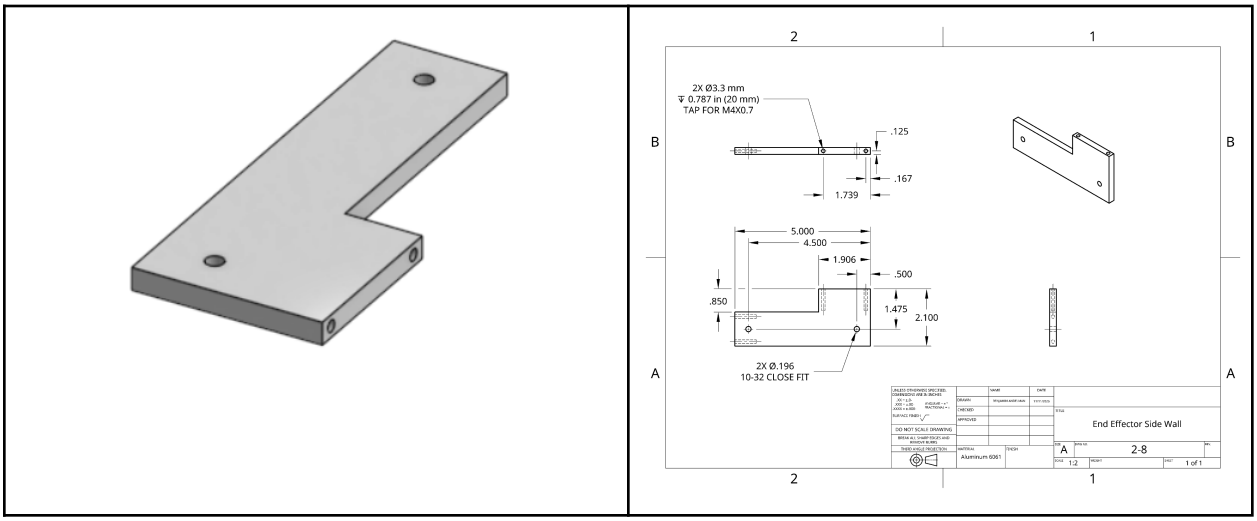


Figure 8.3.8. The isometric view and technical drawing for the end effector side wall.

8.3.9 Load Cell Top Plate

This component serves as the adapter between the load cell and the main structure of the end effector. Four tapped holes rigidly affix to four ¼” shoulder bolts arranged in a square, on which the 3D-printed load cell holder (see below) slides in order to bring the load cell in contact with the center of this component’s flat face. The four outer holes connect it to the end effector side walls, which in turn connect to the end effector pivot connector. The component’s profile makes it ideal for aluminum waterjet cutting. The four tapped holes for the shoulder bolt mounting will be made on the mill.

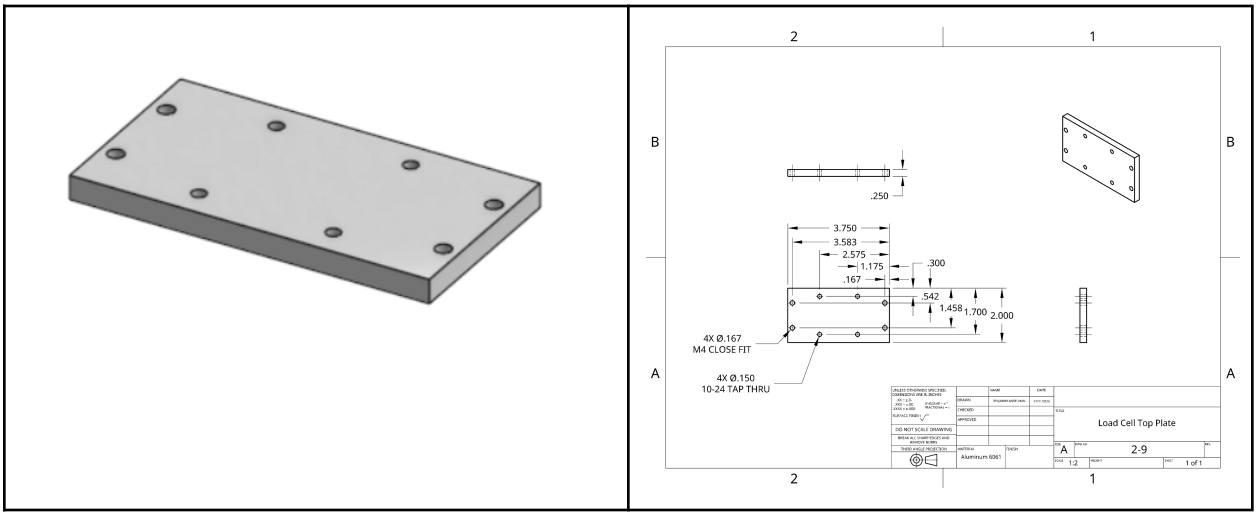


Figure 8.3.9. The isometric view and technical drawing for the load cell top plate.

8.3.10 Load Cell Holder

This component holds the load cell in a recessed hole on top, and contains four holes in which flanged sleeve bearings are inserted to allow this component to slide on the four ¼” shoulder bolts mentioned above in the Load Cell Top Plate description. Two rails extruded underneath the component allow for direct and secure attachment to the piston heads, effectively transferring the reaction force from the cell’s terminal into the load cell’s base. Tolerances around the four holes where the flanged sleeve bearings will be inserted will be important to ensure a snug press fit. It’s possible that this design will need to be modified to undersize the holes and subsequently ream them out to the correct dimension once printed. This part will be manufactured on a 3D printer with PETG filament for its stiffness and durability.

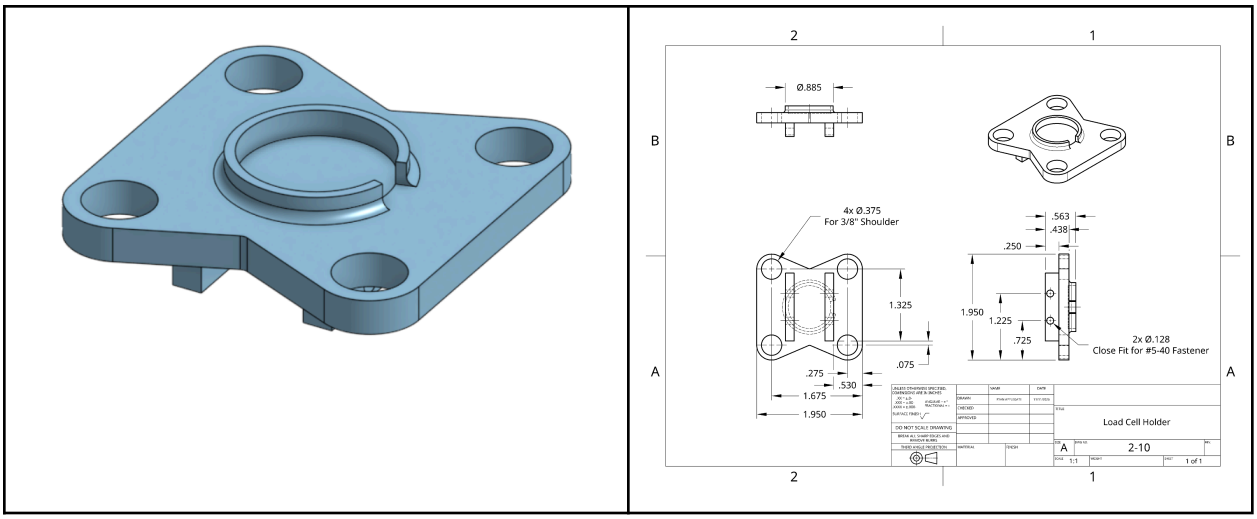


Figure 8.3.10. The isometric view and technical drawing for the load cell holder.

8.3.11 Piston Support - Fittings Side

This component attaches directly to the two coupled pneumatic pistons while leaving space for the 90-degree fittings to extend from the upper chamber. It also features two channels, aligned with the outlets for the lower chambers, for air to escape from those chambers during extension of the pistons. This component is used twice to connect the two pistons to the linear shaft guide below using two M4 bolts and to the load cell holder above using two 5-40 bolts. This piece will be manufactured using PETG filament on a 3D printer.

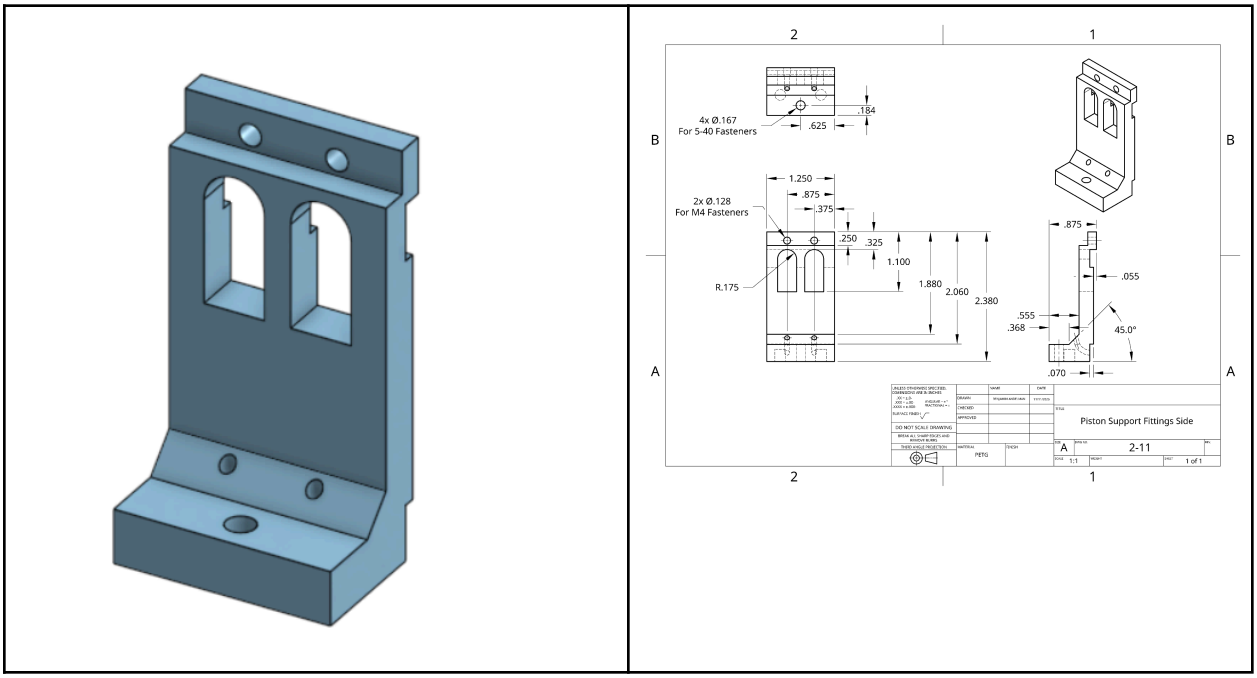


Figure 8.3.11. The isometric view and technical drawing for the fittings side piston support

8.3.12 Linear Shaft Guide

This component interfaces with the lower threaded mount points of the coupled pneumatic cylinders and simultaneously serves as the mount point for the four shoulder bolts that serve as the linear guides for the two electrodes' movement paths. Additionally, it features two holes for the two M4 bolts that connect it to the two piston supports. This component will be manufactured out of aluminum using the UG shop waterjet, as its planar shape lends itself to that manufacturing method. The tapped holes for the shoulder bolts will be done on the mill.

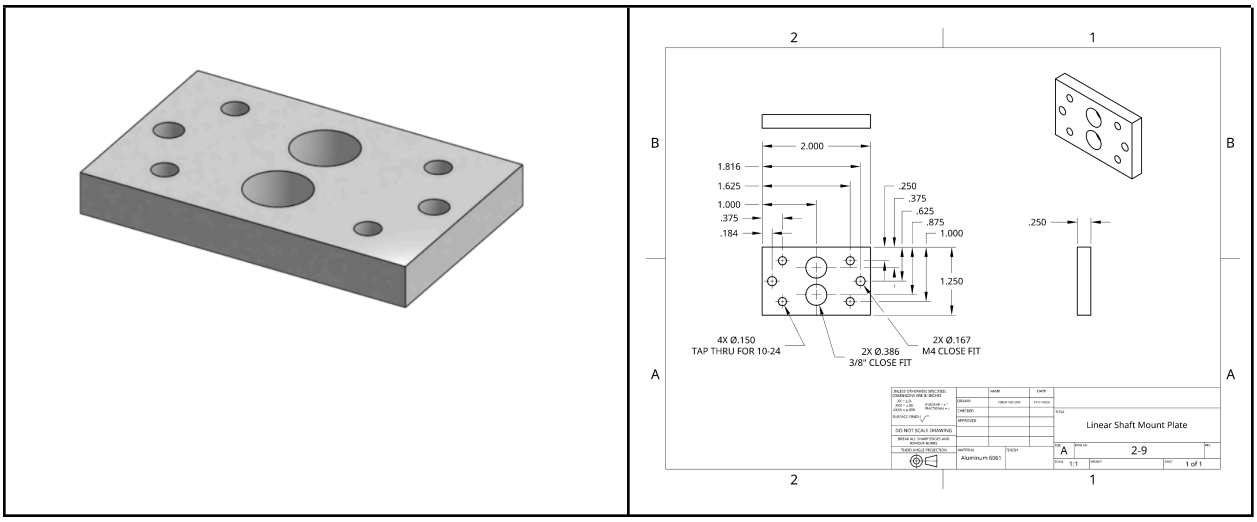


Figure 8.3.12. The isometric view and technical drawing for the linear shaft guide.

8.3.13 Straight Electrode Holder

This rather complicated component adapts the vertically-oriented electrode holder to the piston's threaded rod, while facilitating the connection of the electrode to the welding cable that will be spliced into the existing spot-welding circuit. It also contains two holes where two linear sleeve bearings will be inserted, so that the electrode can slide along its vertical axis without transferring lateral forces or moments into the piston. This component, with its complicated geometry, will be manufactured on a 3D printer with PETG filament for its stiffness. The tolerances of the linear sleeve bearing holes will be important to ensure a snug fit, but the retaining rings used with the bearings will provide a good backup option in case a press fit fails.

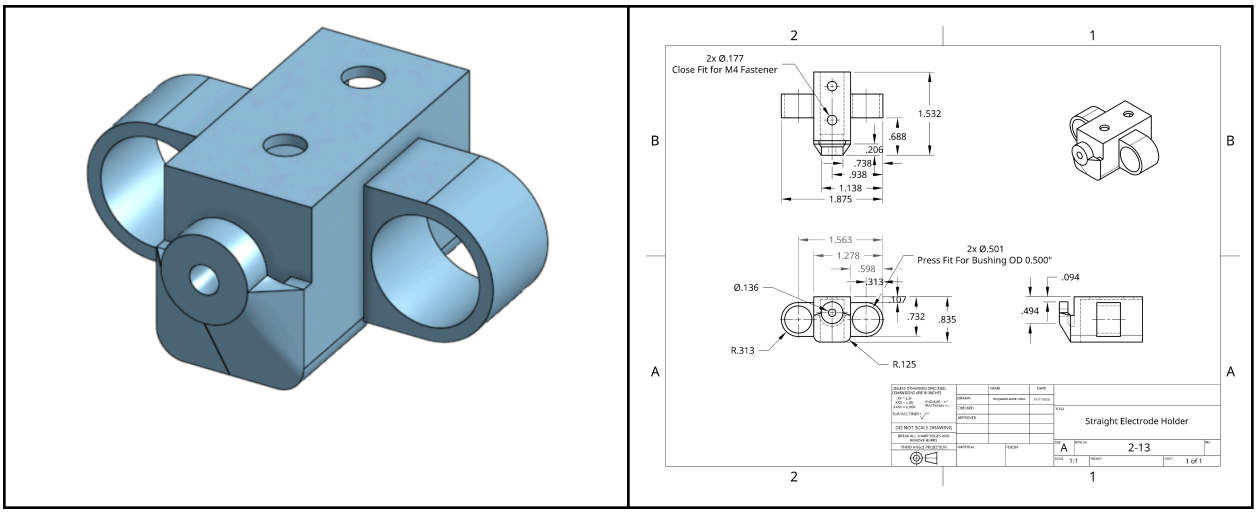


Figure 8.3.13. The isometric view and technical drawing for the straight electrode holder.

8.3.14 Angled Electrode Holder

This component performs the same functions as the straight electrode holder, but holds the second pointed electrode at a 65-degree angle with the horizontal plane, inserting it into the tight space on the cell terminal. It also transfers vertical force into the piston and any lateral forces and moments into two linear sleeve bearings. Finally, it facilitates the connection of the copper compression lugs to the welding cable to minimize resistance along the spot-welding circuit. Due to the geometrical complexity of the part, this component will be manufactured on a 3D printer using PETG filament. Similarly to the straight electrode holder, the tolerances around the two linear sleeve bearing holes are important to ensure a snug fit, though the bearings' retaining rings provide a good backup option in case a press fit fails.

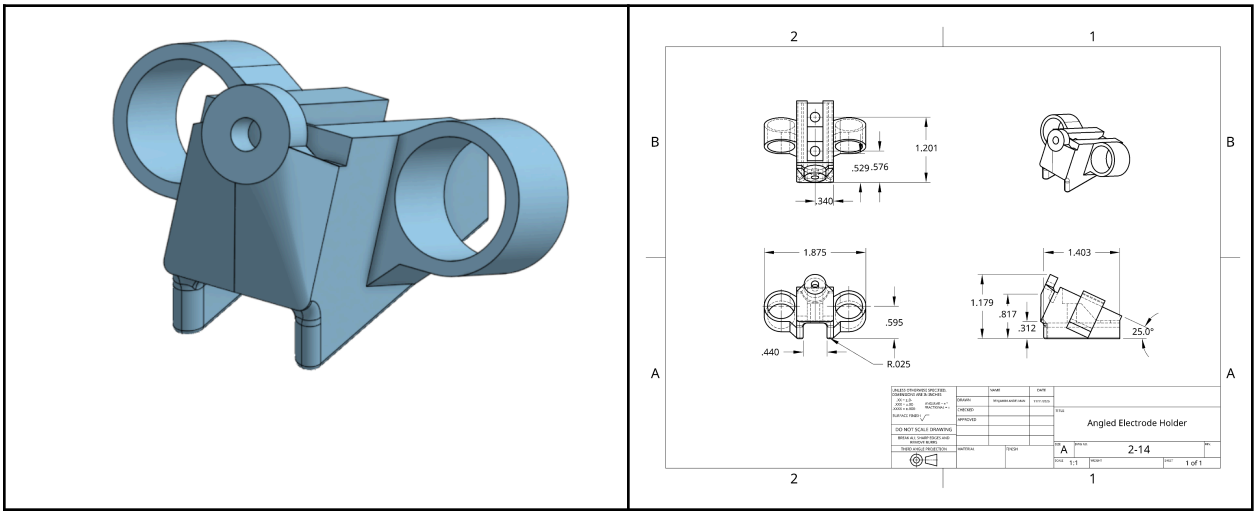


Figure 8.3.14. The isometric view and technical drawing for the angled electrode holder.

8.3.15 Load Sensing Circuitry

The load sensing circuitry uses a TE connectivity 0-55lb button load cell (FX292X-100A-0050-L) fed into an Texas Instruments INA333AIDGKR Instrumentation Amplifier [21, 29]. This is then outputted into a RC low-pass filter and a diode protection circuit before being read by the ADC.

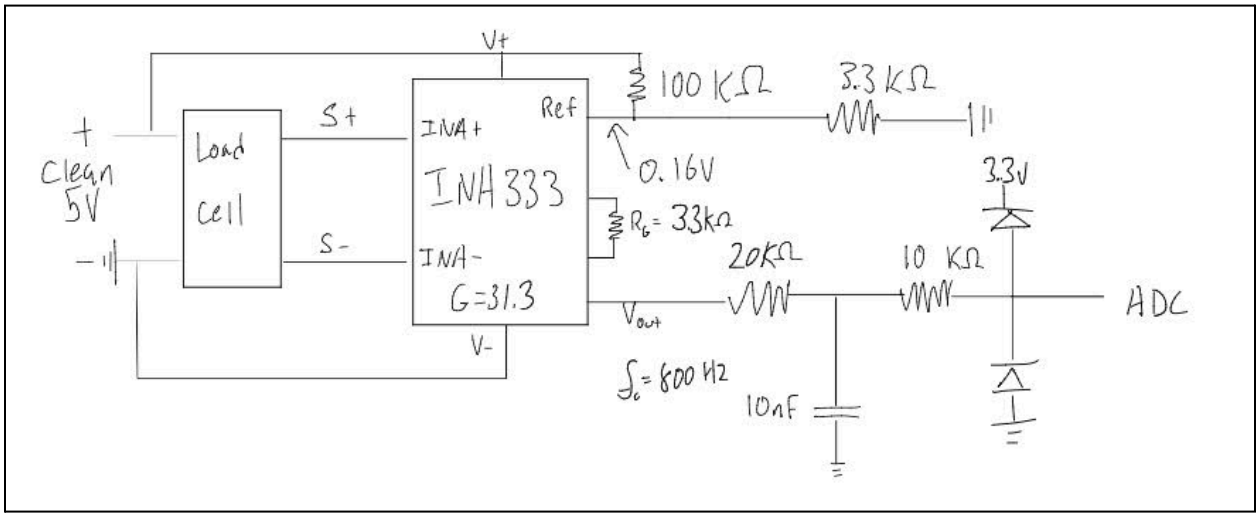


Figure 8.3.15. Circuitry Diagram for Load Sensing

8.3.16 Current Sensing Circuitry

The load current sensing circuitry uses a Vishay-Dale 100µΩ shunt in series with the weld path [30]. An INA240A1 Instrumentation Amplifier with a gain of 20V/V is used to read the differential voltage [24]. The output signal is passed through an RC low-pass filter and a diode protection circuit prior to the ADC.

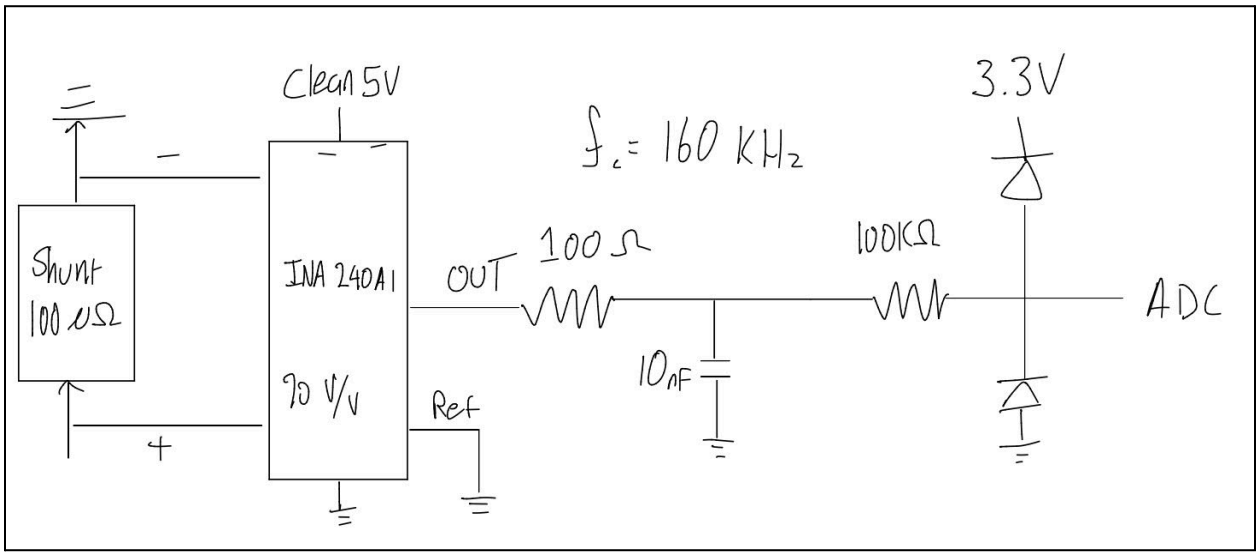


Figure 8.3.16. Circuitry Diagram for Current Sensing

8.3.17 Current Source Circuitry

The current source circuitry uses an 1S4E 5V isolated regulator to supply an LT3092 constant current source supplying 200mA [26, 25]. A schottky diode prevents backflow during a weld pulse. The circuit is controlled by an N-type MOSFET activated by a GPIO pin.

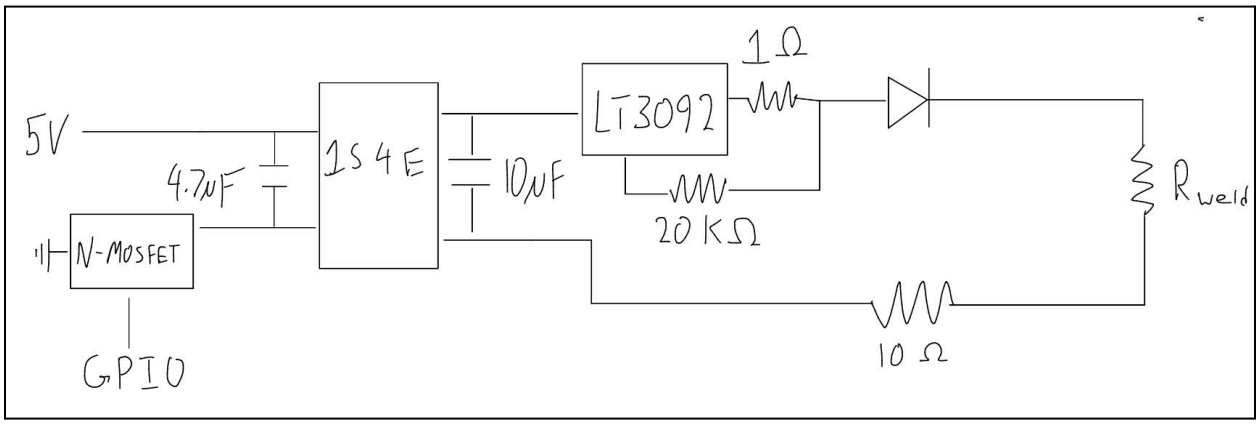


Figure 8.3.17. Circuitry Diagram for Current Source

8.3.18 Voltage Sensing Circuitry

The voltage sensing circuitry has dual sensitivity. The 0-9V reading uses an ISO224 isolation amplifier with a gain of ⅓ V/V [27]. The differential output signal is fed into an differential amplifier that level adjusts to signal to ground. The signal is then passed through a RC low-pass filter prior to entering the ADC. The 0-50mV reading uses the same circuitry with an additional INA333 instrumentation amplifier with a gain of 1000 V/V [29]. The INA333 and weld sides of the ISO224's are fed isolated 5V power from a 1S4E voltage source [26].

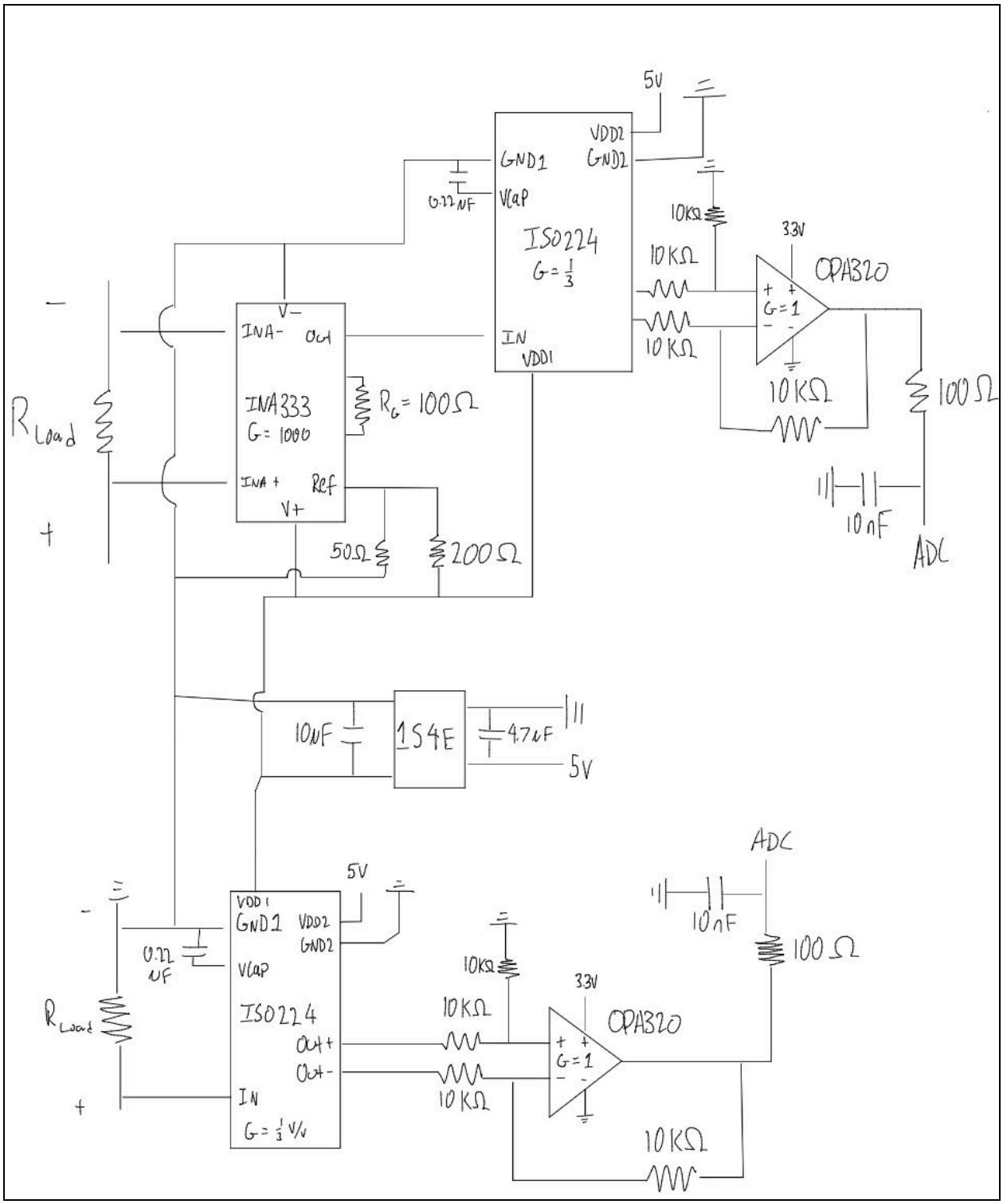


Figure 8.3.18. Circuitry Diagram for Voltage Sensing

8.3.19 Power Supply Circuitry

The power supply uses a SWI10B-5-NB-P5 switching power supply to convert wall power into a 5V DC output [28]. The 5V bus is passed through a pi-filter with a ferrite bead, 100pF, and

100nF capacitor, which acts as a high frequency noise filter. This 5V power is used for all analog components as well as the microcontroller. The microcontroller outputs the 3.3V bus necessary for powering op-amps and MOSFETs.

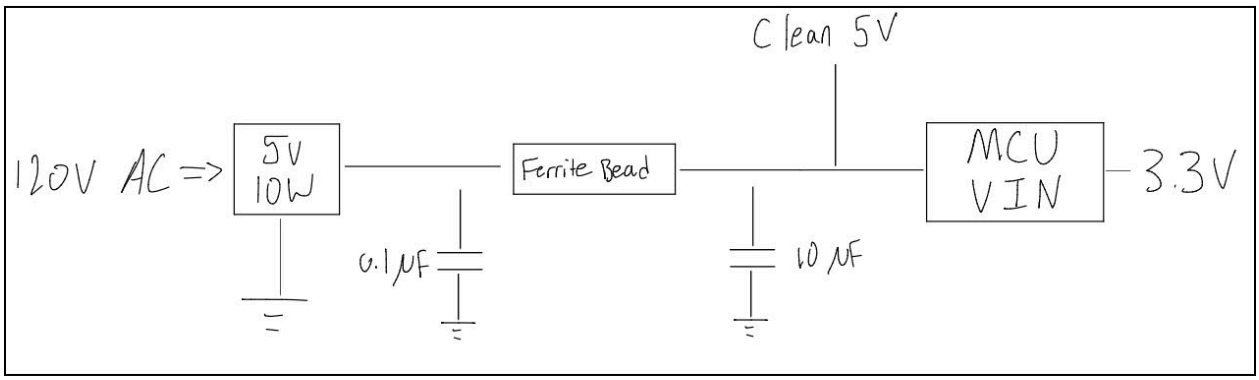


Figure 8.3.19. Circuitry Diagram for Power Supply

8.4 Off-the-Shelf Mechanical Components

All of the subsystems require careful selection of hardware to join pieces together and ensure the correct degrees of freedom. The table below summarizes the mechanical components that will be purchased to complete the build design.

Table 8.4.1. This table summarizes the purchased hardware for the base subsystem.

Part Description	Supplier	Part Number	Unit Cost	Quantity
Concentric Collar Locking Pillow Block Bearing for 1” Shaft	AMI Bearings	UEF205-16	$15.50	2
M12 x 1.75 Socket Head Screw	McMaster Carr	91090A626	$0.96	4
M12 x 1.75 Hex Nut	McMaster Carr	90591A181	$0.23	4
¼”-20 x 1 in Socket Head Screw	McMaster Carr	91251A542	$0.25	6
¼”-20 x 2 in Socket Head Screw	McMaster-Carr	9044A125	$0.53	3

Table 8.4.2. This table summarizes the purchased hardware for the linkage subsystem.

Part Description	Supplier	Part Number	Unit Cost	Quantity
⅜” Shoulder Bolt x 1.75” Shoulder Length	McMaster-Carr	91259A630	$2.35	9

1” Oil-Embedded Bearings for ⅜” Shaft	McMaster-Carr	6391K178	$2.32	9
5/16”-18 Locknut	McMaster-Carr	90630A115	$4.13	9
Oil-Embedded Thrust Washer for ⅜” Shaft	McMaster-Carr	5906K565	$1.14	36
Needle-Roller Thrust Bearing for ⅜” Shaft	McMaster-Carr	5909K25	$3.27	18

Table 8.4.3. This table summarizes the purchased hardware for the end effector subsystem.

Part Description	Supplier	Part Number	Unit Cost	Quantity
Threaded-Hole-Mount Oval Pull Handle	McMaster-Carr	1897A56	$5.62	2
10-32 x 0.75 in Socket Head Cap Screw	McMaster-Carr	91251A345	$0.16	4
Linear Sleeve Bearing for ¼” Shaft	McMaster-Carr	6673K11	$11.18	4
Retaining Rings for ¼” Linear Sleeve Bearing	McMaster-Carr	9968K22	$0.44	8
¼” Shoulder Bolt, 2 in Shoulder Length	McMaster-Carr	91259A103	$2.62	4
5/32 OD Hard Plastic Tubing (350 psi rated)	McMaster-Carr	5548K82	$0.37	25
Push-to-Connect Tube Fitting for Air	McMaster-Carr	5779K284	$6.57	2
Double-Acting Air Cylinder 5/16” Bore ½” Stroke	McMaster-Carr	6498K945	$40.49	2
M4 x 18mm SHCS	McMaster-Carr	91290A164	$0.16	7
5-40 x 1 in SHCS	McMaster-Carr	91251A080	$0.15	2
M4 x 30mm SHCS	McMaster-Carr	91290A180	$0.21	3
¼” Shoulder Bolt, ⅜” Shoulder Length	McMaster-Carr	91259A535	$1.73	4

M4 x 12mm SHCS	McMaster-Carr	91290A148	$0.12	4
5-40 Hex Nut	McMaster-Carr	90480A006	$0.04	6
M4 Thin-Profile Hex Nut	McMaster-Carr	90695A035	$0.04	6
Flanged Sleeve Bearing, ¼” Shaft	McMaster-Carr	6338K411	$1.25	4
¼”-20 x 0.75 in	McMaster-Carr	91251A540	$0.23	4
¼”-20 x 0.5 in	McMaster-Carr	91251A537	$0.16	4
¼”-20 Lock Nuts	McMaster-Carr	90630A110	$0.18	4

Table 8.4.4. This table summarized the purchased electrical hardware for the spot-welder

Part Description	Supplier	Part Number	Unit Cost	Quantity
600V AC/DC 2/0 Wire Gauge Welding Cord	McMaster-Carr	7940A81	$8.94	10
Tin-Plated Copper Compression Lug	McMaster-Carr	6926K342	$12.88	2
Tin-Plated Copper Compression Lug	McMaster-Carr	6926K324	$8.11	6
AWithZ 14.6 kW Spot Welder	AWithZ (fulfilled by Amazon)	P20B	$289.99	1

8.5 Off-the-Shelf Electrical Components

The build design requires a carefully selected combination of electrical components to achieve desired capability like voltage sensing and resistance sensing across the weld. The table below summarizes the purchased electrical components for the build.

Table 8.5.1. This table summarizes the purchased electrical components for the build.

Part Description	Supplier	Part Number	Cost	Quantity
Solderable Prototype Board	Digi-Key Standard	DKS-SOLDERBREAD-02	3.19	6
5V Power Supply	Bel Power Solutions	SWI10B-5-NB-P5	8.57	1
DC Jack to Leads	Tensility International	10-01097	2.66	1

	Corp.			
Ferrite Bead	Laird Signal Integrity Products	28L0138-40R-10	0.23	1
100 pF X7R Ceramic Capacitor	Vishay BC Components	K101K10X7RF5UH5	0.21	1
10 nF X7R Ceramic Capacitor	Vishay BC Components	A103K15X7RF5TAA	0.23	4
100 µΩ 4-Terminal Shunt Resistor	Vishay Dale	WSBS8518L1000JK	16.16	1
Current-Sense Amplifier	Texas Instruments	INA240A1D	3.81	1
SOIC-8 to DIP Adapter	Adafruit Industries LLC	1212	2.95	3
100 Ω Metal Film Resistor (1%)	Vishay BC Components	MBB02070C1000FCT00	0.10	5
Schottky Diode	STMicroelectronics	1N5711	0.10	4
100 kΩ Metal Film Resistor (1%)	Yageo	MFR-25FRF52-100K	0.10	3
Isolated 5V DC–DC Converter	GAPTEC Electronic	1S4E-0505S1-5U	1.30	1
4.7 µF X7R Ceramic Capacitor	TDK Corporation	FK24X7R1E475KR000	0.45	1
10 µF X7R Ceramic Capacitor	TDK Corporation	FG14X7R1A106KRT06	0.56	1
ISO224 Isolated Amplifier (⅓ V/V)	Texas Instruments	ISO224ADWVR	15.66	2
0.22 µF X7R Ceramic Capacitor	TDK Corporation	FG18X7R1H224KRT00	0.28	2
OPA320 Precision Op-Amp	Texas Instruments	OPA320AIDBVR	2.47	2
SOT-23-6 to DIP Adapter	SparkFun Electronics	717	1.25	2
10 kΩ Metal Film Resistor (1%)	Yageo	MFR-25FRF52-10K	0.10	8
INA333 Instrumentation Amplifier	Texas Instruments	INA333AIDGKR	4.54	2
VSSOP-8 to DIP-8	Chip Quik Inc.	PA0042	3.19	2

Adapter				
50 Ω Metal Film Resistor (1%)	Yageo	MFR25SFBE52-5 0R	0.10	1
200 Ω Metal Film Resistor (1%)	Yageo	MFR-25FTF52-20 0R	0.10	1
LT3092 Programmable Current Source	Analog Devices Inc.	LT3092ETS8-TR MPBF	6.40	1
SOT-23-8 to DIP Adapter	Chip Quik Inc.	PA0089	3.19	1
10 Ω Metal Film Resistor (0.6 W)	TE Connectivity Passive Products	LR1F10R	0.10	1
1 Ω Metal Film Resistor (0.6 W)	Vishay BC Components	MBB02070C1008 FCT00	0.10	1
20 kΩ Metal Film Resistor (¼ W)	Yageo	MFR-25FRF52-20 K	0.10	1
50 lb Button-Type Load Cell	TE Connectivity Measurement Specialties	FX292X-100A-00 50-L	20.50	1
3.3 kΩ Metal Film Resistor (1%)	Yageo	MFR-25FTE52-3 K3	0.10	1
300 Ω Metal Film Resistor (1%)	Vishay BC Components	MBA02040C3000 FRP00	0.10	1

9. Final Design

The final design is, first and foremost, the product that will be delivered to SPARK Electric Racing to address the problem that was given to the team to solve. It is also the design that will be shared and documented on an open-source scale. Our build design, described in *Section 8*, served as a prototype, but upon testing required change to the design of the end effector to meet the specifications of our solution.

9.1 Relation to Build Design

During testing of the build design, it became clear that the cylinder equalization mechanical in the end effector would not work. There were issues with alignment and sealing the tube connection which did not hold up the forces during a weld. The team decided to keep the rest of the build solutions, and just change the design of the end effector. The cylinder equalization was swapped out for a mechanical linkage, utilizing an equalization bar. Beyond this redesign, our final design also changed the manufacturing methods for certain parts.

We also took the redesign chance to change the manufacturing method of the end effector pivot. The end effector pivot did not have enough dimensional accuracy being 3D printed, so it was manufactured again by milling a block of aluminum to create the features. Upon seeing the increase in tolerance and performance of the pivot, the team identified other 3D printed parts to change the material or manufacturing method of. The electrode holders were originally going to be made using Fused Deposition Modeling (FDM) in PETG, but there is concern that PETG is weaker than conventional engineering materials such as aluminum and other materials used in additive manufacturing such as PA-12. In addition, the FDM process creates parts with anisotropic properties that are significantly weaker in the layer height directions. The electrode adapter needs to be made of an insulative material, so staying with plastic is the best way to go. The material and manufacturing changes for our build design parts can be found in the table below.

Table 9.1.1. A summary of the changes to certain manufactured parts from the build design to final design.

Part Name	Part Number	Material Change	Manufacturing Change
End Effector Pivot	2-7	PETG → Aluminum	FDM → Milling
Straight Electrode Adapter	2-13	PETG → PA-12	FDM → SLS
Angled Electrode Adapter	2-14	PETG → PA-12	FDM → SLS

9.2 Final Design Functional Explanation

This section of the report serves to provide a high level overview of how the solution is used to complete a spot weld on a battery. Please see *Section 8 - Build Design* for more detailed explanations on the individual components.

9.2.1 Degrees of Freedom

The motion of the solution is constrained by rotation about the pillow block bearings built into the base (θ axis) and the extension of the end effector in the rotated 2D plane (r and z axes). **Figures 9.2.1.1 through 9.2.1.3** show the motion capabilities to sweep from one corner of the welding area to the opposite corner. Notice how the pivot on the end effector allows for the end effector to stay constrained relative to the base extrusions, ensuring the probes are lined up properly with the current collector tabs placed on the cell terminals, which remain in the same orientation across the module for battery design convention.

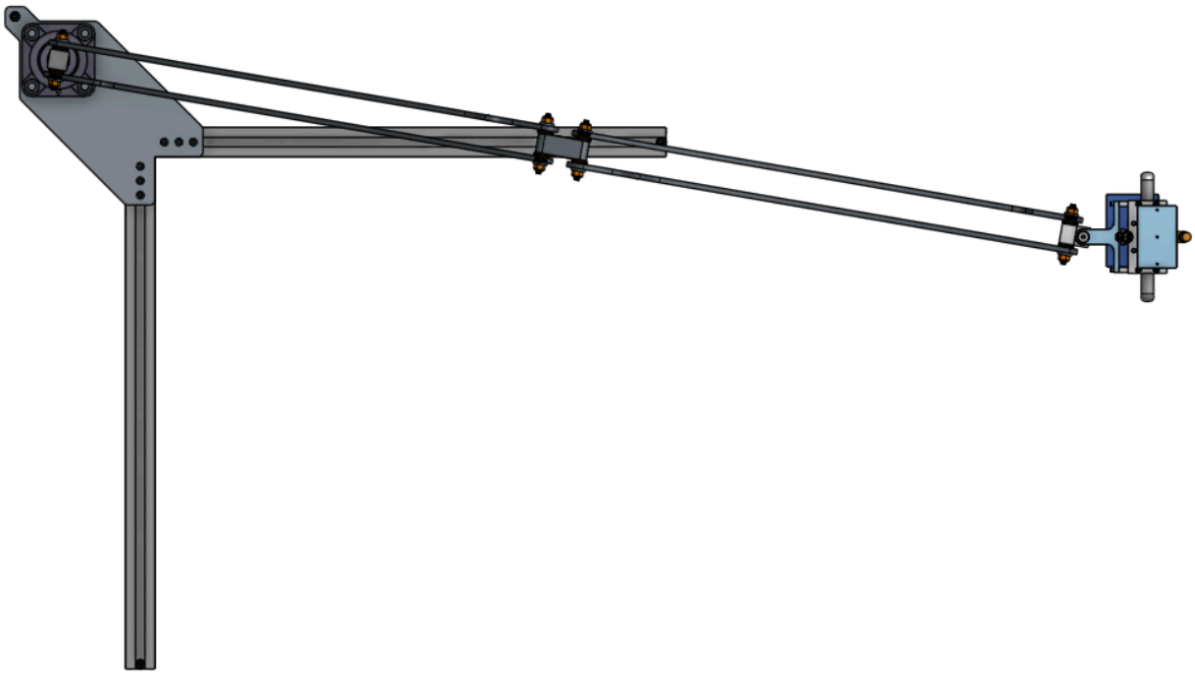


Figure 9.2.1.1 The linkage is fully extended and the linkage is then rotated to reach the furthest point in the top right of the welding area.

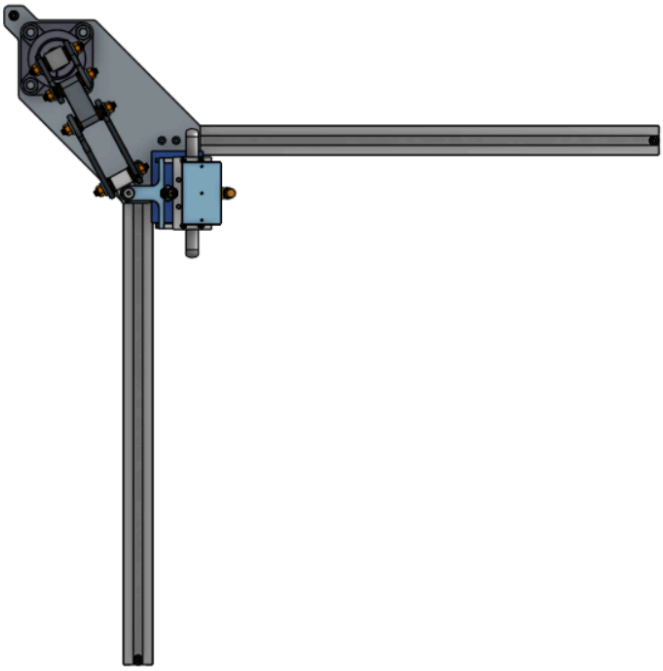


Figure 9.2.1.2 The linkage is fully retracted and the linkage is slightly rotated to reach the closest point in the top left of the welding area.



Fig 9.2.1.3 The linkage is again fully extended and the linkage is rotated about the base to reach the furthest point in the bottom left of the welding area.

9.2.2 End Effector Functionality

The purpose of the end effector is to provide an ergonomic, assistive interface by which the user can consistently apply a high-quality spot-weld to the terminal of a 21700 format lithium-ion battery cell. It also must be adaptable to multiple different current collector orientations and different elevations of current collector and cell terminal surfaces, while allowing the user to apply measurable, equivalent vertical force to both spot-welding electrodes. **Figure 9.2.2.1** below shows an isometric view of the effector.

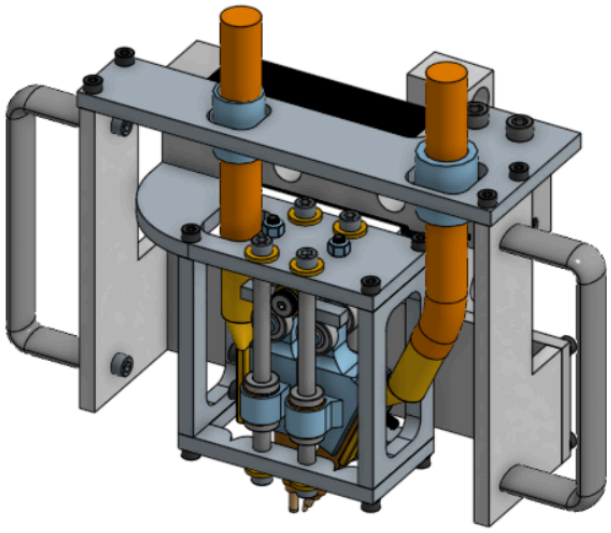


Figure 9.2.2.1. Isometric view of end effector

The end effector features two vertically-oriented aluminum handles that aid the user in applying a downward force onto the cell terminals to aid in the execution of a good weld. These handles are attached to one end of a shear load cell. The other end of the shear load cell is rigidly connected to a housing that contains the electrode adapted on sliders. These adapters slide and push against an equalizer, or “seesaw”, bar which pushes down the other electrode, helping to ensure full contact between both electrodes and the battery or current collector respectively. When force is applied to the handles and the electrodes are making full contact with the cell, the shear load cell is receiving the full force of the weld. To best understand the functionality of the end effector, we look to **Figure 9.2.2.2** which displays the path of the vertical load as it travels through the electrodes, across the equalizer bar, through the load cell, and into the rigid end effector frame.

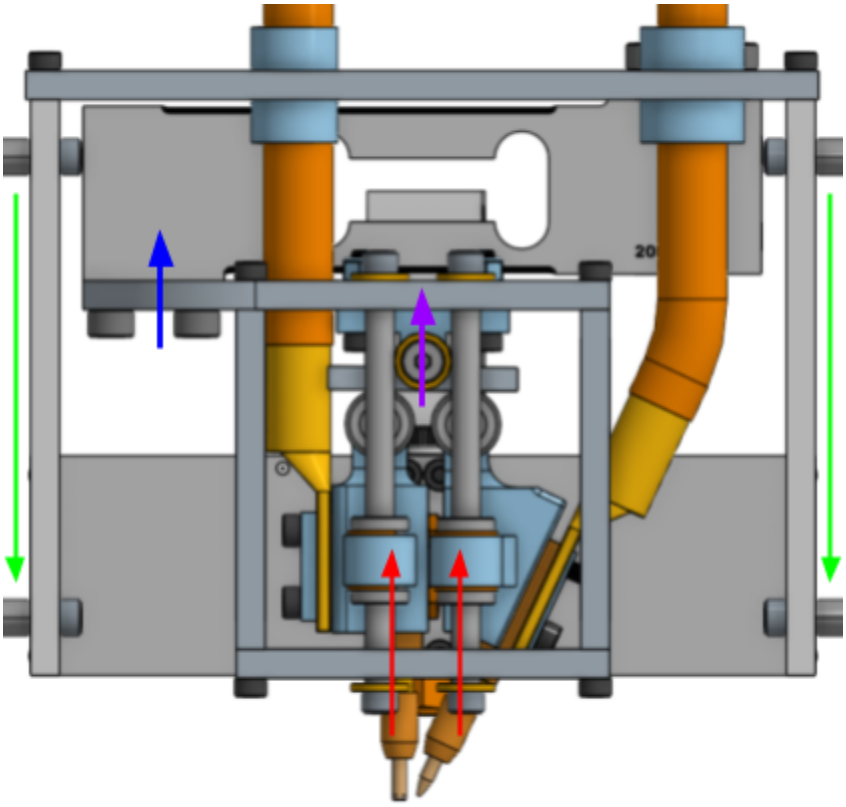


Figure 9.2.2.2. The flow of vertical forces through the electrode adapters (red), onto the equalizer bar (purple), and to the load cell (blue) as the handles are being pushed down (green).

Once the displacements of the electrodes have been balanced. The equalizer bar will be in full contact with the sliding electrode adapters. The electrode adapters will transfer all lateral forces to the equalizer bar, while any planar forces or moments will be absorbed by the rods which the adapters slide on, as seen in **Figure 9.2.2.3.** The equalizer bar is rigidly connected to the top plate, which in turn is boiled to the shear load cell, so all forces of interest from the weld are directly transmitted into the load cell.

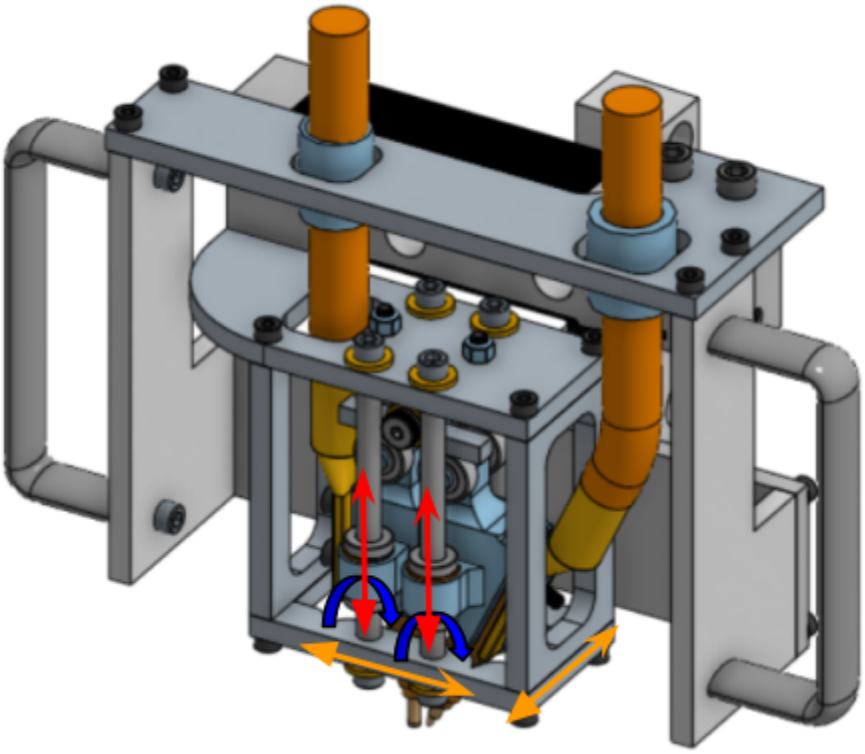


Figure 9.2.2.3. Axial forces (red) are allowed to create linear motion along the rods, while lateral forces (orange) and moments (blue) around the X- and Y-axes are resisted by the linear sleeve bearings on the rods.

9.2.3 Supporting Electronics

The supporting electronics were implemented into TINA-TI for virtual testing before they were manufactured. The virtual circuits for load sensing, current sensing, voltage sensing, test current source, and power supply can be seen in the figures below.

Drawing from SPICE simulation results, the voltage sense circuit and load sense circuit had to be modified. The simulation showed that the high sensitivity voltage sensing circuit using the INA333 as a pre-amp failed to accurately capture inputs on the extreme low or high end of the desired range. This was due to the INA333 not being a rail-to-rail amplifier, which was not considered during the build design. This was remedied by replacing the INA333 with an OPA320 with a resistor network for a non-inverting gain of 100 V/V. The downstream differential OPA320 was adjusted to a gain of 2 V/V for a total gain of 66.6 V/V. We also observed that the resistor divider circuit providing a reference voltage for the INA333 in the load sensing circuit was failing to maintain 0.16 V. This was due to the INA333 reference pin drawing enough current to sway the output. This was remedied by placing an OPA320 as a unity gain buffer with the resistor divider circuit as the input voltage to the op-amp.

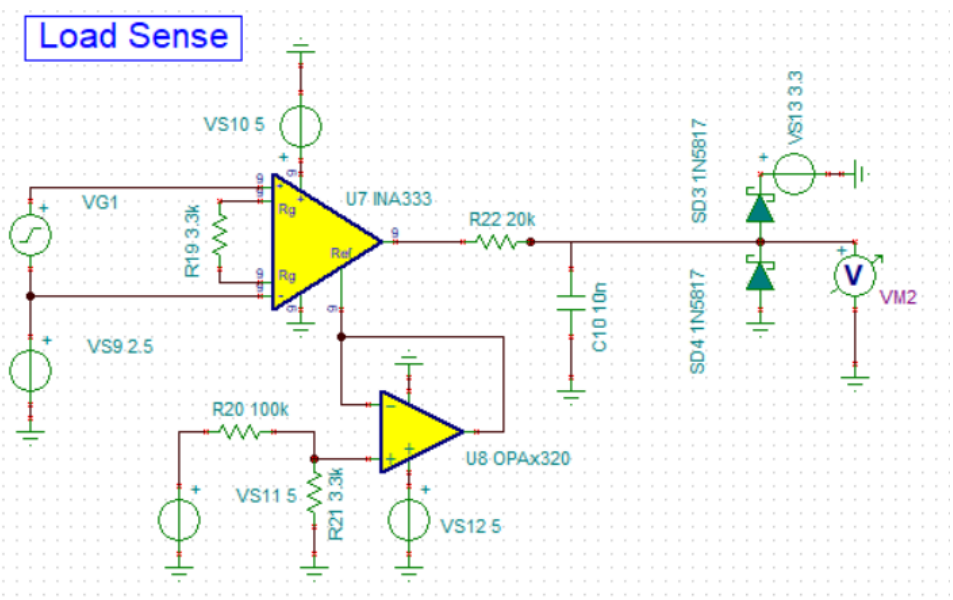


Figure 9.2.3.1. The virtual circuit representation for the load sensing circuit.

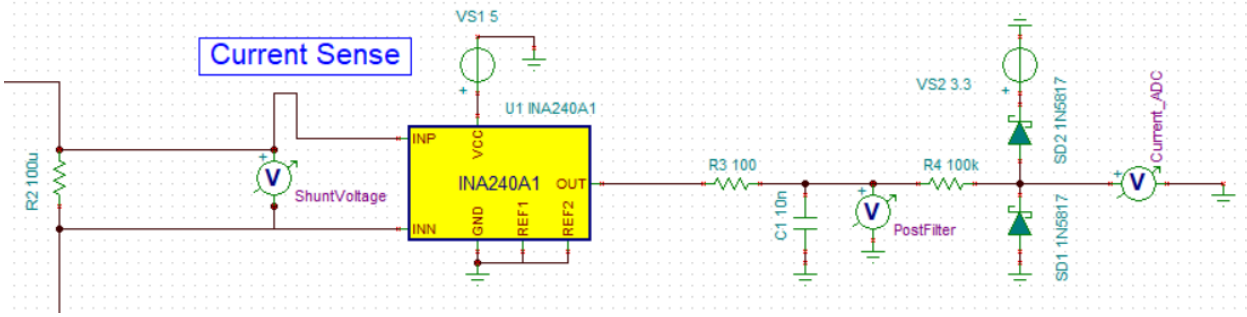


Figure 9.2.3.2. The virtual circuit representation for the current sensing circuit.

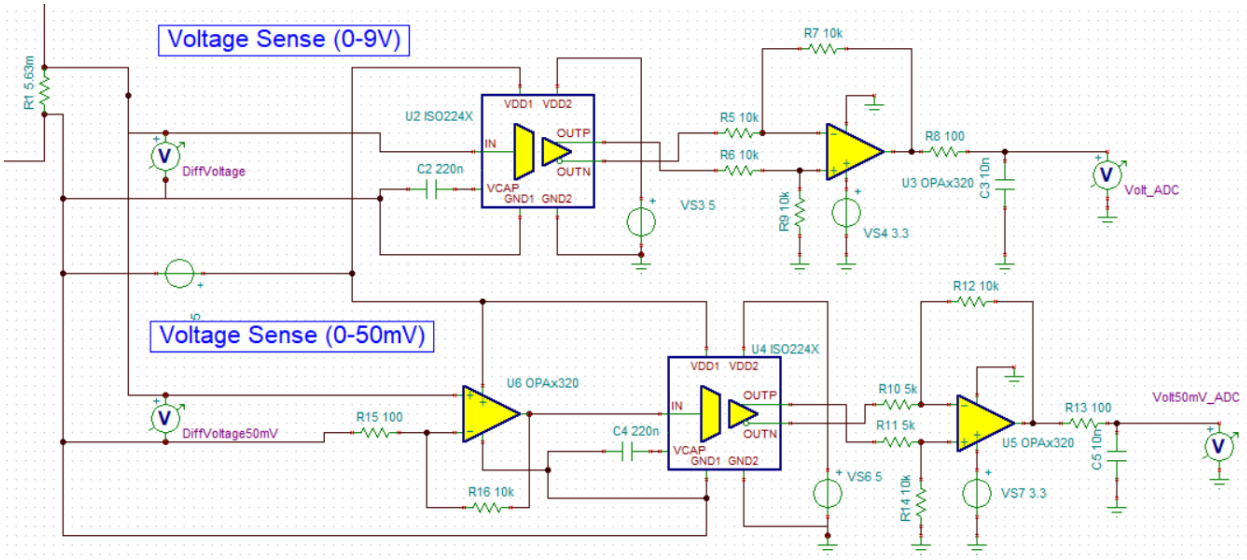


Figure 9.2.3.3. The virtual circuit representation for the voltage sensing circuit.

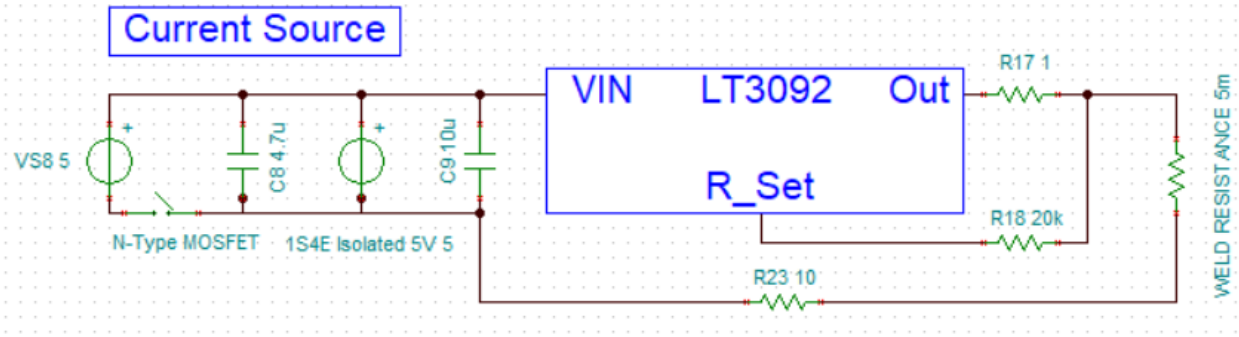


Figure 9.2.3.4. The virtual circuit representation for the current source circuit.

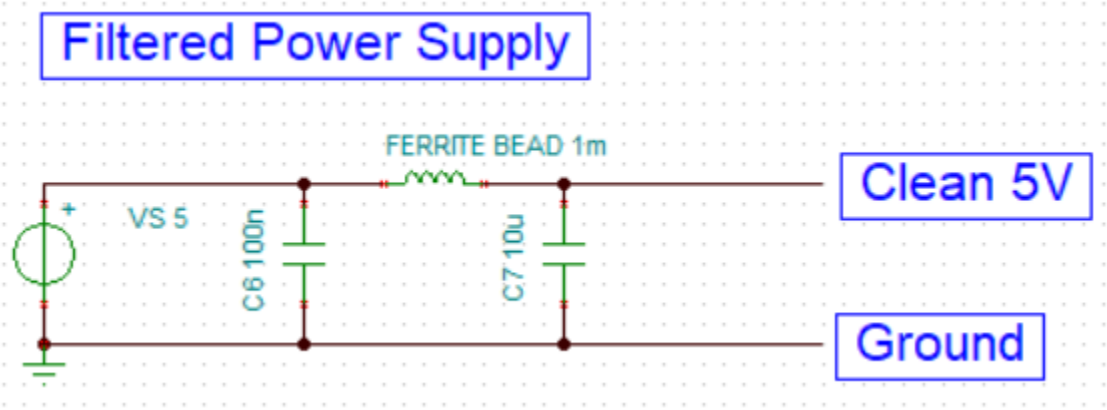


Figure 9.2.3.5. The virtual circuit representation for the power supply circuit.

10. Verification and Validation

10.1 Verification Plans

The following verification plans address the requirements and specifications that we consider to be physically testable once our device is fully assembled. These include requirements and specifications from both our needs and wants in **Table 4.1.1** and **Table 4.1.2**. The requirements and specifications that are unable to physically be tested will be discussed in **section 10.2**. The goal of the testable verification plans is to provide a way to quantifiably test, based on the specifications for each requirement, how well our device will perform. With our extensive engineering analysis, robust CAD assembly, detailed circuit analysis, and precision manufacturing, we have confidence that these physical tests will confirm our theoretical analysis and meet all of our requirements and specifications successfully. Verification plans in list form are available for quick reference in appendix **section A.8**.

10.1.1 Weld Location Accuracy Verification

The first requirement and specification we must verify is how accurately our device is able to move into the proper weld position at each cell location. This will be tested by placing

cylindrical cells in each corner of the 32” x 32” work area, as well as in 20 randomized intermediate locations, and ensuring the device is able to reach each distance. Once the distance is confirmed, the end effector orientation will be assessed as to how well it is able to be rotated into our ideal welding position on the current collector. The specification that we will be measuring is a 0.5 mm tolerance to the dimple location on the current collector. This can be accomplished by having our current collectors pre-setup with these dimple zones established, and with the 0.5 mm radius of tolerance illustrated around the dimple. If the device falls within this radius of tolerance we will count that as a pass and move onto the next cell location. We will consider this verification plan to be a success if it is able to reach all 24 locations without falling beyond the radius of tolerance at any locations.

We have high confidence that our device will be able to pass this verification test. Our initial engineering analysis in **section 7.2** and **section 7.3** of determining the link length guarantee that we will be able to reach the maximum radius in the work area, as well as all locations in between. As for the end effector orientation, it has been designed in order to be able to rotate ±90 degrees from its starting position. This will allow for it to be rotated into the proper position at any location in the work area. In addition, the device is human-operated and therefore we don’t have to design any sophisticated controllers to reach this radius of tolerance. Instead, we will ideally be able to perfectly align the controller to fit into this tolerance ourselves and therefore pass the verification test without any issues of controller malfunction.

10.1.2 Weld Probe Orientation Verification

The second requirement and specification we must verify is how reliably our end effector is able to remain normal to the cell plane. There will be cells placed in the four corners of the work area as well as in 20 randomized locations within. The device will then be moved to each location and a digital level will be mounted on the top of the end effector to measure the deviation from being normal to the cell plane. This will verify the specification requiring deviation no greater than a cone of tolerance of 2 degrees at each cell location. This verification will be considered a success if the end effector remains within that cone of tolerance at all 24 locations within the work area.

We have high confidence that this verification test will be a success due to our design being a dual parallel four-bar linkage. Based on theory this will ensure that the end effector will be held normal to the cell plane naturally, and that any deviations from this will be due to tolerancing. We have confidence that our design is robust and all joints analyzed properly to allow for it to fall within our 2 degree cone of tolerance, based on our engineering analysis in **section 7.4**.

10.1.3 Weld Force Application Verification

For this requirement and specification we must verify the robustness of our device while being placed under a minimum weld force load threshold. This will be tested by using an embedded load cell in the end effector that will measure the force we apply per weld. The entire welder

must be able to sustain and transmit at least 44 N of force per weld probe (88 N total) without any deformation or instability anywhere in the device. The verification plan will utilize the same setup as the previous two, performing welds at the four corners and in 20 intermediate positions at this force requirement. Visual checks will be performed at each weld location to ensure the device appears to comfortably handle it. It will be a successful verification if it is able to be stable and unaffected by the loads at each location.

We have high confidence that our device will be able to pass the verification test due to our engineering analysis. Our analysis of the radial and thrust loads at the base from **section 7.5** give us an understanding as to how well our bearings at the base will be able to handle these loads acting on them while welding. The only area of concern would be the weld probe tips, as each has to comfortably handle 44N without deflection. Our initial FEA of our previous design of the end effector showed a millimeter of deflection. The design has since been changed to do a better job of handling the applied force.

10.1.4 Weld Quality Verification

For this requirement and specification we must verify the quality of each weld created under the prior specifications of location accuracy, orientation, and minimum force. From here we have our established “ideal” spot weld for our device that will allow for a high quality weld nugget. In order to test this, we will perform one spot weld nugget per cell and sheet of current collector in order to isolate the nugget. Using a force gauge, we must ensure that the nugget is able to withstand 25N of force in both axial and shear. This will indicate that the nugget has established a strong connection between the cell and current collector. Repeat this 10 times and ensure that each weld is able to withstand the force requirement.

We have high confidence for this verification test due to preliminary manual testing at welds created with upwards of 70N of force. Although this weld probe force is slightly below our requirement of 88 N, we were seeing welds that performed very well in both shear and axial pull tests. We were unable to use a force gauge to quantify the result, however this allowed for a good indication of how strong the welds will be once we reach the force requirement from the verification test.

10.1.5 Spot Welding Rate Verification

For this requirement and specification we must verify that our device is able to perform spot welds more efficiently than the prior manual welding process. This will be tested by having members of the SPARK Battery Team (both with and without prior manual spot welding experience) perform a timed operational trial run. We will ensure that they are properly trained on how to use our device and what our requirements are for a successful spot weld (from the SOP), and enforce these procedures during the time trial. We will prevent them from knowing they are being timed to see how many they are able to do naturally. This will prevent any rushing

from the user that would in return cause a lapse in quality of the weld. The specification threshold each user must meet is at least 6 spot welds per minute. Have at least three different users perform and compare the results.

We have moderate confidence in this verification test as we are truly unsure as to how much more efficient this device will be due to the added steps of end effector orientation and required force application. Therefore, if because of this we were forced to fall short of our 6 welds per minute specification, that would suffice due to the improved quality and consistency of the welds outputted. We could also reassess any ergonomics that could be changed in order to make the movement easier, but we have confidence in the way we have it designed now to be able to be comfortably moved around the work area.

10.1.6 Stability Verification

For this requirement and specification we must verify that the welding device frame plane is parallel to the cell plane. It must be adjustable by at least 2cm of elevation difference between the two opposite corners of the welding device frame, and there must be a tolerance of no more than 2 degrees of angular offset between the welding device plane and the cell plane. This will be verified by first placing a digital level on the battery pack and then zeroing it out to set that as the reference plane. From here that level will be moved to the welding frame, which will then be adjusted to align within our tolerance of 2 degrees.

We have high confidence that this will work, as being adjustable within that range will be enough to account for any cell plane deviations. It will also allow us to ensure that once our battery pack is flipped over on the already welded side of the current collector that it can be re-leveled to account for any offsets from the weld nuggets. This ensures that the two planes are aligned within our 2 degrees of tolerance, which is also crucial for the weld probe orientation specification that requires being normal to the cell plane.

10.1.7 Weld Energy Consistency Verification

For this requirement and specification we must verify the pre and post-weld resistance and exergy expended per weld of 12 consecutive welds within a 95% confidence interval. This confidence interval will be obtained by sampling 30 successful welds using the standard manual welding method, paired with the circuit analysis done for our device in order to record the data. With this confidence interval obtained we will be able to compare how well our device is able to perform in comparison to the manual baseline.

10.1.8 Ease of Maintenance Verification

For this requirement and specification we must verify how quickly we are able to disassemble all moving parts on the tool head. Part of this specification is that only two distinct tools should be required as well as being able to be completed in under 10 minutes. This will be verified by

providing 3 different users with our SOP section of tool head maintenance, and then timing them to see how long it takes to disassemble the device. The same thing will be done for the reassembly of the device.

We have moderate confidence in verifying this specification. Our end effector is designed to be easily disassembled and reassembled using no more than two distinct tools, however the time will be dependent on the user and how well they may already know the operating procedure for maintenance. The first time disassembling and reassembling will take much longer than the second time and beyond. But overall this device will be easily reassembled and disassembled for user convenience and motivation to keep things in working condition.

10.1.9 Easy Setup and Use Verification

For this requirement and specification we must verify how easily we are able to get an entire battery module into the operating area. The specification calls for 60 seconds for initial placement of cells and 10 additional seconds per current collector. We will verify this by setting up a dummy battery cell and making sure it is able to be quickly set up for ease of use.

We have high confidence in verifying this specification as our device is designed to be in the open without any constraints blocking the working area. This will allow for easy access to all sides of the work area and allow for easy alignment of the current collector.

10.1.10 Theoretical Circuitry Verification

Prior to fabrication, all circuitry schematics will be recreated in LTSpice, or a similar circuitry simulator. Each component will be examined for DC response to ensure that the data collected is accurate and that the electrical components are protected from over-voltage and over-current conditions. Next, a full scale simulation of the entire circuit will be performed, with a simulated square wave weld pulse including artificially added noise. This will test the robustness of the system against external EMI from the welder.

10.1.11 Physical Circuitry Verification

Once a physical circuit is built, we will provide test inputs similar to those expected from actual use and monitor the outputs of each circuit to determine if our outputs resemble the expectations from the simulations.

10.2 Non-Physically Testable Verifications

The following additional requirements will be verified differently than the previous physically testable requirements. For our open-source requirement, we will ensure that 100% of all materials that are necessary for the manufacturing, assembly, and operation of the machine are released to the public domain. We will also make sure that we release an extensive SOP that will ensure that the user is able to easily follow and begin spot welding immediately upon setup. The

cost will be verified by constant BOM tracking as we proceed with part selection and ordering. We have been keeping track of our spending since the beginning and are on track to stay below our budget of $2000. The system dimensions requirement is verified by designing our device to be able to accommodate all locations within the 32” x 32” work area. Our analysis has been conducted to account for this as well as our CAD design and therefore it is verified already. For our safety requirement, we will ensure we have an emergency disconnect of all power to the weld device located at the terminal connection of the weld probes.

10.3 Verification Results

10.3.1 Weld Location Accuracy Verification Result

The location accuracy was tested via the method described in **section 10.1.1.** The cells were placed in our required work area of 32” x 32”, and at a maximum joiner angle of 150 degrees, the device was successfully able to reach the maximum radius seen in Figure 10.3.1.1.



Figure 10.3.1.1. Cell boundaries for location accuracy verification test.

The device was also able to reach the other corner extremes of the work area successfully, as well as 20 intermediate positions not pictured above. At each of these locations the end effector’s ability to be positioned in the proper orientation with the current collector was also verified. The current collectors had the 0.5mm tolerance dimple zone pre-setup on them and the device was able to be positioned precisely within the dimple at each location. The device did not fall beyond the radius of tolerance at any location and therefore it passed this verification test.

10.3.2 Weld Probe Orientation Verification Result

The weld probe orientation was tested via the method described in **section 10.1.2**. With the four cells placed in each corner extreme the device was moved to each location and the orientation of the end effector with respect to the level battery plane was assessed as seen in figure 10.3.2.1.

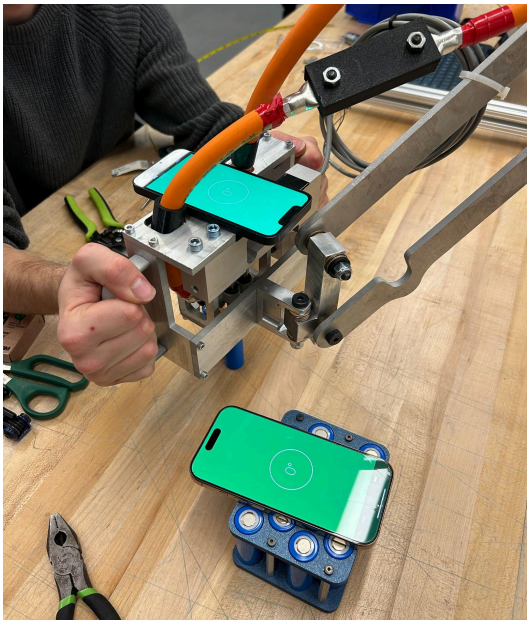


Figure 10.3.2.1. End effector orientation at maximum position relative to level battery pack

At the maximum radius pictured above and at all 20 intermediate locations the device passed and fell within our 2 degree cone of tolerance specification. However when testing at the minimum weld location we did not pass as pictured below in figure 10.3.2.2.

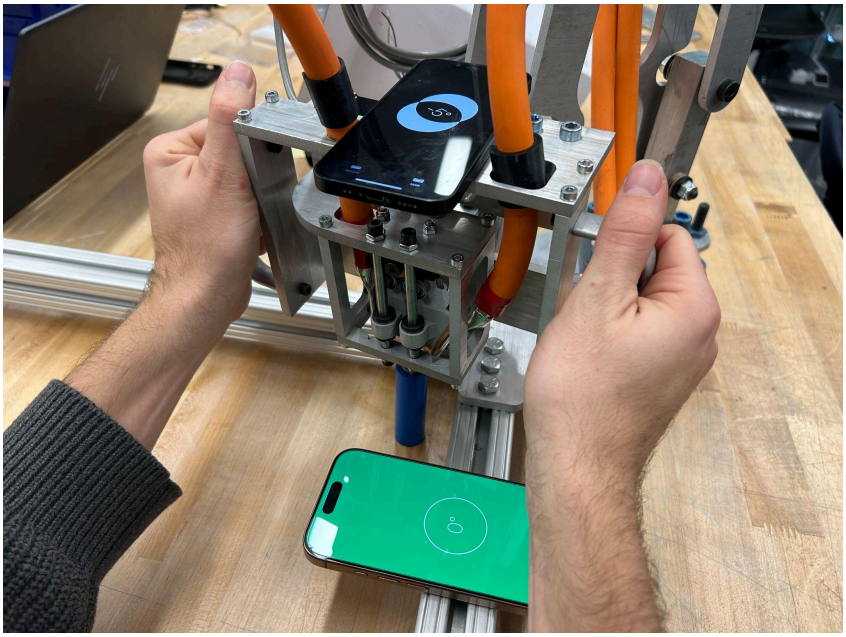


Figure 10.3.2.2. End effector orientation at minimum position relative to level base

This failure is due to linkage lock out occurring at this location, as the links begin to overlap each other and the four-bar mechanism loses its effectiveness. This lockout forces the end effector to follow the movement of the linkage arms and hence causes a massive deviation,

exceeding our cone of tolerance. This could have been prevented with more engineering analysis focused on the minimum extreme and not just on the maximum. In the future the base pivot point would need to be extended further back to prevent this lockout from happening, and the link lengths increased as needed to still meet the maximum reach radius requirement.

10.3.3 Weld Force Application Verification Result

The weld force was verified via the method in **section 10.1.3.** Cells were placed in the four corners as well as 20 intermediate positions, with a bathroom scale placed beneath them as pictured in figure 10.3.3.1.

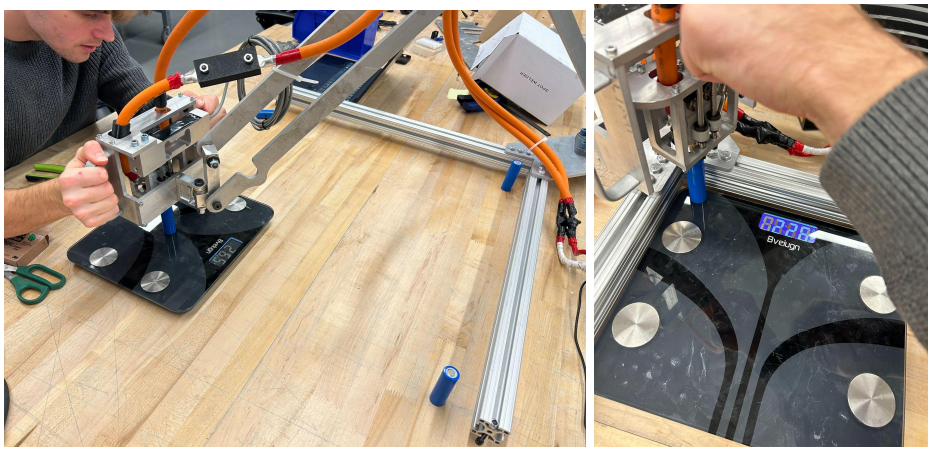


Figure 10.3.3.1. Force test at maximum and minimum linkage position

At each cell location the device greatly exceeded the minimum force requirement of 88N (20lbs), reaching upwards of 50lbs. This proves the device to be stable and able to sufficiently handle forces well beyond what is required, therefore passing this verification test.

10.3.4 Weld Quality Verification Result

The weld quality was verified via the method in **section 10.1.4.** We created a weld nugget using the device after meeting the prior specifications with a force of at least 88N. This singular nugget was then tested axially and in shear by using 5lbs of weights and an extra half a pound to exceed this requirement. The weights were tied to the current collector to best approximate shear and axial loading respectively. The setup is pictured below in figure 10.3.4.1.

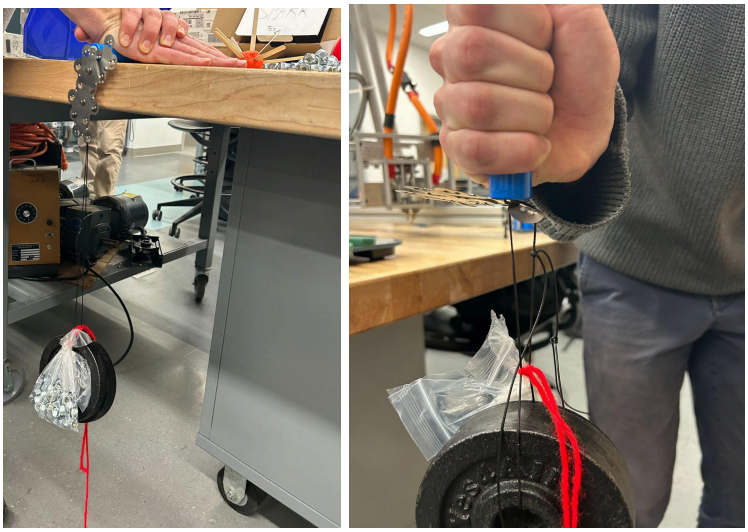


Figure 10.3.4.1. Shear and Axial tests with 5lbs on single weld nugget

The weld nugget successfully handled the 5.5lbs loaded in both shear and axially. By exceeding our required load of 22.2N (5lbs) our device has successfully passed this verification test.

10.3.5 Spot Welding Rate Verification Result

The weld quality was verified via the method in **section 10.1.5.** A rectangular current collector was cut out and laid across 3 battery cells. This gave the opportunity for a member of the group to test the time it took to create 6 welds. The group member was able to complete 6 welds in 19.4 seconds, which passes the verification test. The setup of the current collector and cells can be seen below in figure 10.3.5.1.

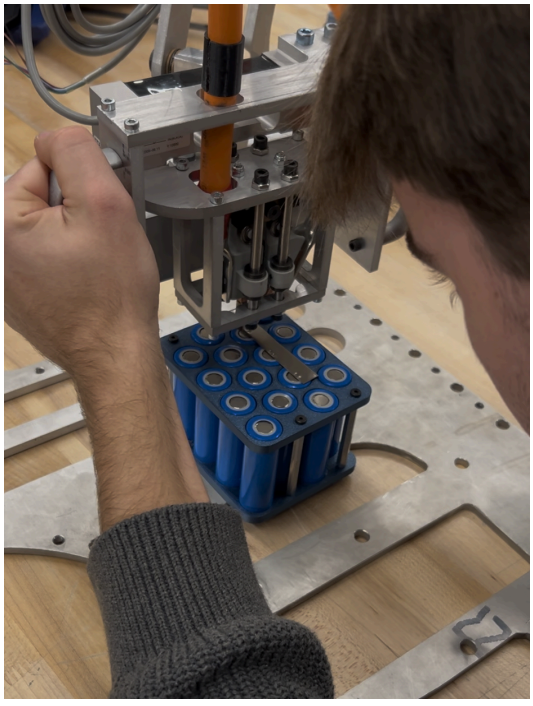


Figure 10.3.5.1. Rate verification process setup

Welding Rate Verification Video

10.3.6 Stability Verification Result

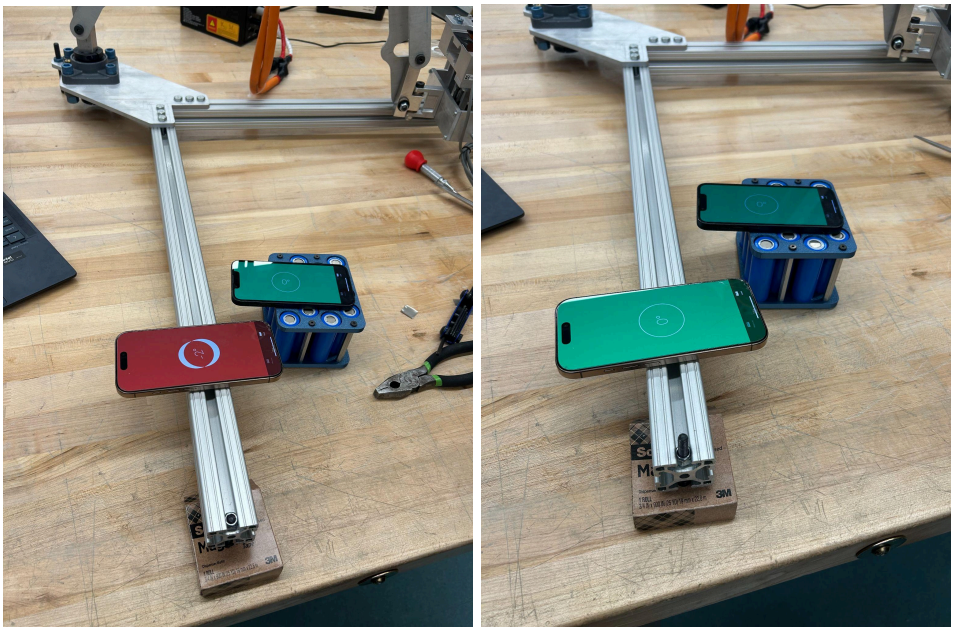


Figure 10.3.6.1. Verification of ability to adjust base to account for offset table and battery pack. An uneven working area was simulated by adding a cardboard box underneath one corner, and then the base's feet were adjusted to re-level the linkage with the cell plane.

10.3.7 Weld Energy Consistency Verification Result

Unfortunately, during physical verification performed according to 10.1.10, our circuits did not behave as expected. This prevented us from obtaining energy use measurement to enable this verification plan.

10.3.10 Circuitry Verification Results

The first step to verify the circuits' performance was to apply a DC test current to each circuit. The current source circuit was excluded as no public SPICE model was available. A nominal voltage of 3V was given to the low sensitivity voltage sense circuit. A current of 533 A was passed through the current sense circuit. These both represented a third of the total capacity of the spot welder. The results shown below corroborate that the circuits have the desired gains as a third of full power produced output signals of 1V, which is a third of the input range of the ADC.

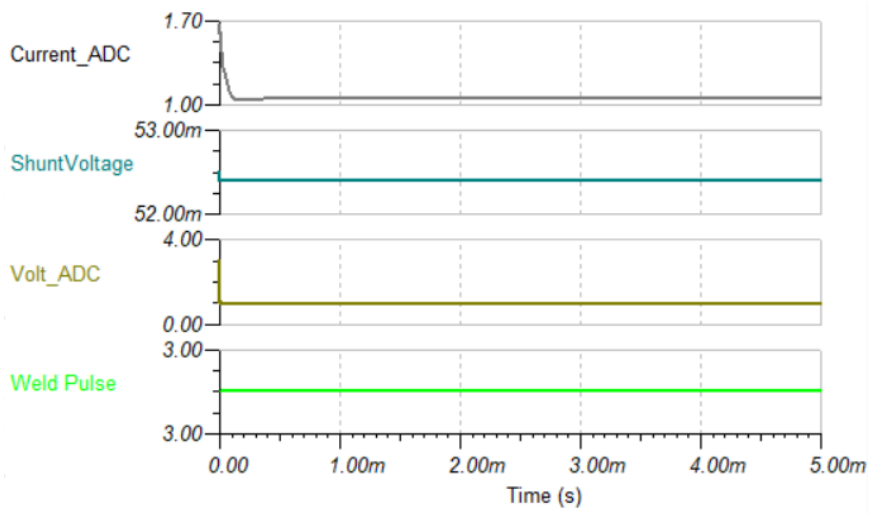


Figure 10.3.10.1. Current and voltage (low sense) measurements with a 3V DC input.

For the high sensitivity voltage sense circuit, a 200mA test current was passed through the simulated weld bead, producing a reading of 75mV. This confirmed the designed total gain of 66.6 V/V.

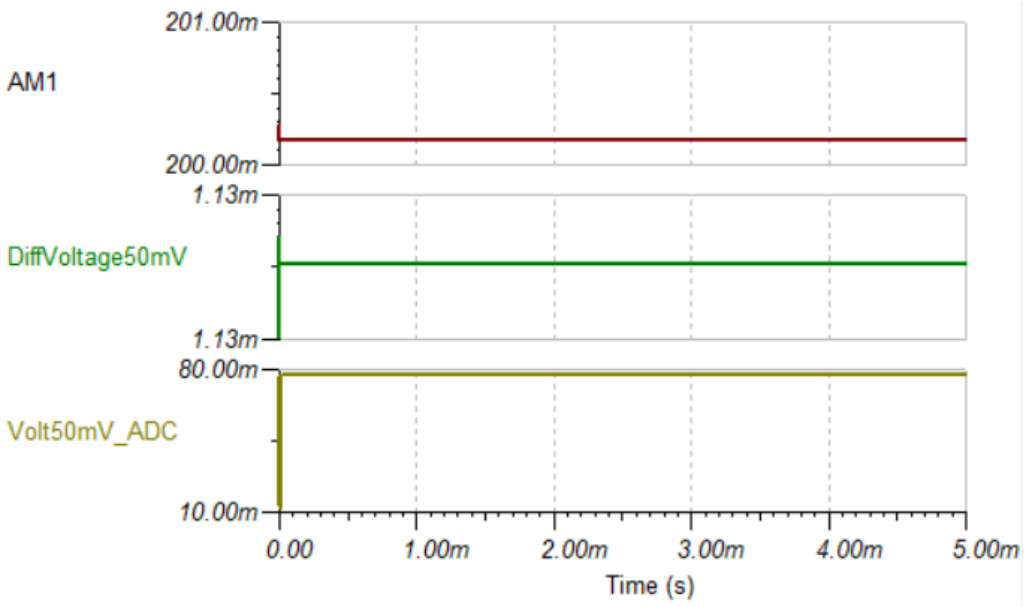


Figure 10.3.10.2. Voltage (high sense) circuit with a 200mA test current.

To test the load sense circuit, a 50% workload of 5 mV was inputted. This produced an output of 1.68 V, which confirms the designed gain of 333 V/V.

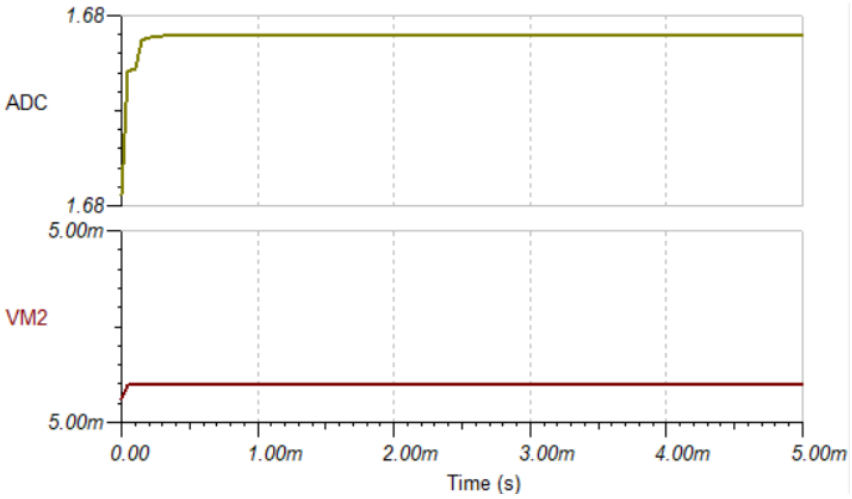


Figure 10.3.10.3. Load sense circuit with a 5mV test input.

Next, the overvoltage protection of each circuit was tested. This was verified by supplying an abnormally high input voltage and observing to see if the output voltage exceeded the 3.3V threshold that would cause damage to the ADC. All circuits passed inspection.

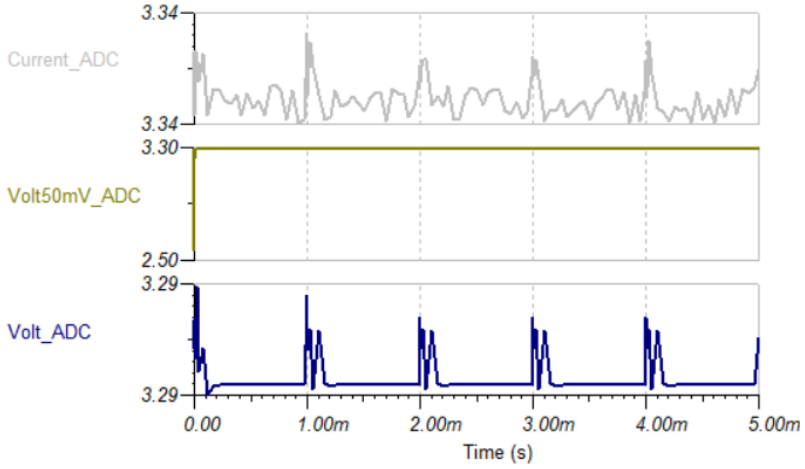


Figure 10.3.10.4. Current sense and voltage sense circuit with a 20V test input.

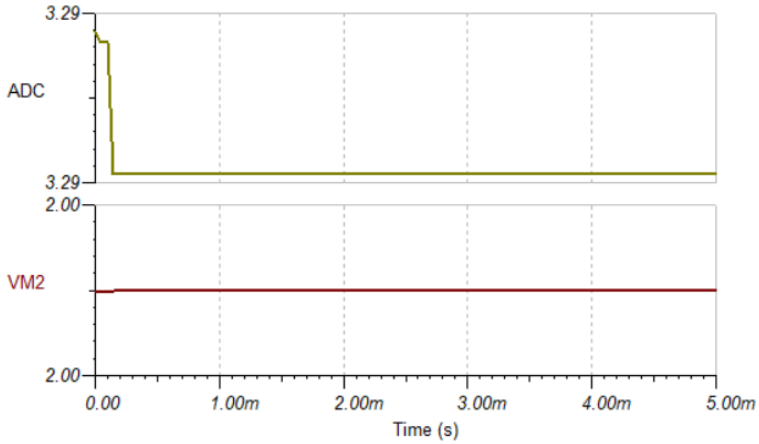


Figure 10.3.10.5. Load sense with a 2V test input.

With all circuits performing well under DC conditions, we now move on to square wave inputs with artificial noise. The square wave provided had an amplitude of 3V, a width of 10ms, and a rise/fall time of 10 microseconds. An 300 KHz noise signal with an amplitude od 20mV was also added. All outputs successfully rejected the noise and tracked the square wave nicely. On the current readout, we can see some rounding, but not a worrying amount.

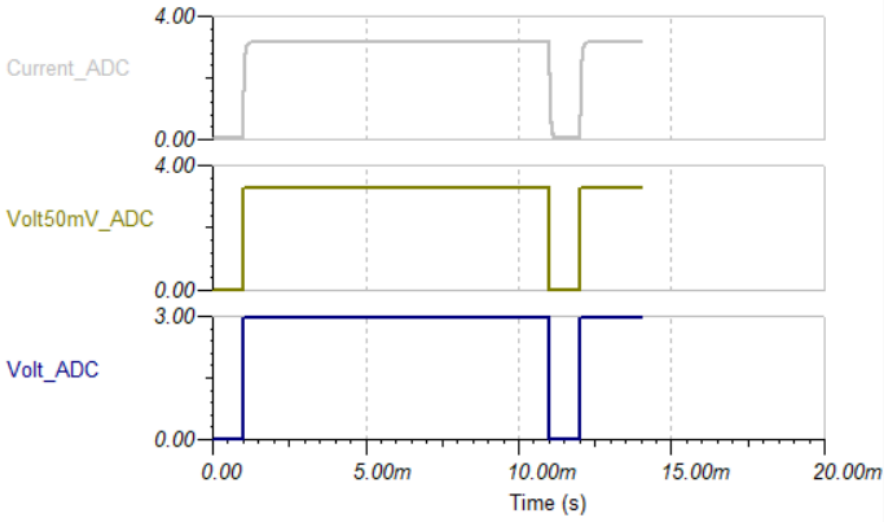


Figure 10.3.10.6. Current and voltage sense with a square wave test input.

The load sense circuit is not subject to square waves, but was still tested for noise rejection. The applied noise, shown as VG1, has an amplitude of 1mV and a frequency of 5 KHz. The circuit performed well, rejecting the noise and outputting the expected DC value.

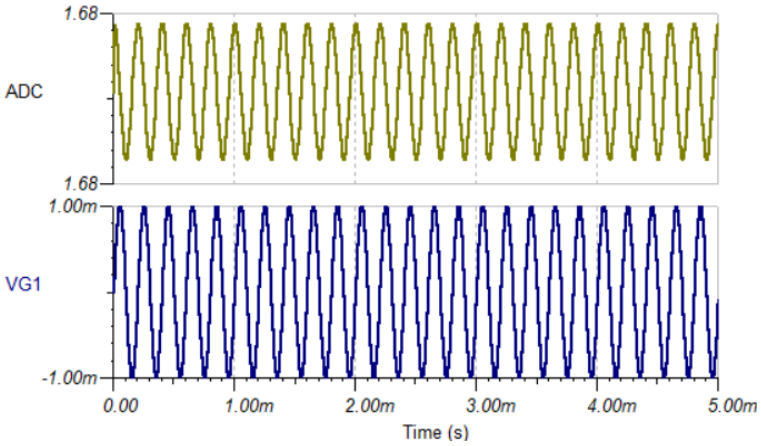


Figure 10.3.10.7. Load sense with a noisy DC test input.

10.3.11 Physical Circuitry Verification Results

Physical verification of these circuits was performed by providing a DC input signal with normal amplitude. Each ADC output was measured with a multimeter. The results for each circuit are summarized in the table below.

Table 10.3.11.1. Test procedure and findings from physical verification of circuitry.

Circuit	Observations	OK/NOK
Power supply	A 5V input corresponded to a stable 5V output.	OK
Voltage Sense	The low sensitivity voltage sense circuit was passed a 5V input. This caused an output of 1.66 V, verifying our ⅓ V/V gain. The high sensitivity circuit was tested with a voltage divider circuit producing 0.063 V. The output of the circuit was 4.16 V, verifying the 66 V/V gain. This was tested with the final op-amp being powered at 5V not 3.3V, which allowed for the overvoltage condition.	OK
Current Sense	Using a voltage divider circuit, we created an input voltage of 0.126V for the current sense input. We observed an output of 4.2V. This was measured without connecting the Schottky diode overvoltage protection to the 3.3V bus, temporarily allowing for a higher reading. This number indicated a gain of 33 V/V which is substantially larger than the 20 V/V fixed gain of the INA240A1.	NOK
Load Sense	With the circuit powered and the load cell attached, we started applying a slowly oscillating load between 10-20 lbs. We did not observe any activity from the circuit output. With the oscilloscope connected directly to the load cell, we observed the oscillating voltage output. The buffered reference voltage performed according to plan, indicating that the problem was arising from the INA333 chip and surrounding circuit.	NOK
Current Source	The current source did not produce the 200mA current. We supplied the circuit with 5V and observed that the 1S4E isolated 5V supply powered up with the closing of the MOSFET, but the LT3092 did not produce a current. More bizarrely, the voltage differential between the open ends read as 5V, even when power was cut to the system. It did not slowly discharge in a capacitive manner.	NOK

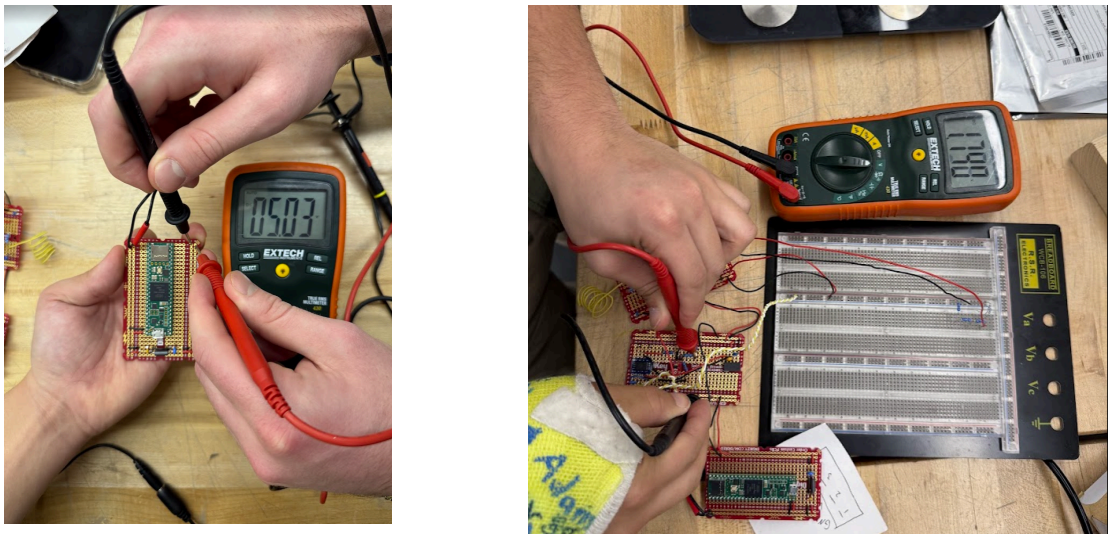


Figure 10.3.10.8. Circuits undergoing experimental testing.

Unfortunately, three out of five circuits malfunctioned during the demo. This was especially confusing as all connections were triple checked without any apparent errors. All the faults were near areas using surface mount chips on adapter boards. This observation is not damning, as we see no apparent mistakes in these areas either. With only a few days left, we were unable to remedy the circuity, and as such, were unable to continue with validation plans reliant on them. Most notably, ease of use and energy use telemetry were impacted.

10.4 Validation Plan

In addition to the verification plans described above, we are also taking into consideration validation of our device. Due to this device being delivered to our project team SPARK Electric Racing, we will be able to receive feedback from members of the battery team directly, some of whom we interviewed and some whom we didn't. There is a new battery build cycle approaching and the goal is for our device to be used for this build cycle. By having a true application of our device, we can gain authentic and honest feedback from the battery team as to whether or not our device allows for a better welding experience both for quality and consistency of the welds, as well as for user comfort. This validation will be important in determining how successful the outcome of the project is, and whether or not it truly makes a difference for SPARK.

We will also encourage our open-source users to provide feedback as to how beneficial our device is to their specific applications. This feedback will be taken into consideration for future iterations of the device.

11. Discussion

11.1 Problem Definition

With more time and resources, we would like to complete more interviews with individuals who have experience with manual spot welding EV battery packs. Ideally this would include members of other student project teams as well people that manufacture EV battery packs as their full-time job. The latter group could really provide insight to the pain points of manual spot welding, as they would be experiencing it day after day on repeat. These new insights would surely help our team refine our problem definition as well as improve our user requirements.

11.2 Design Critique

Due to the time constraint of the ME450 class, there were many design errors realized in the physical prototype that the team did not have time to address. The design of the double four bar linkage has each long link on opposite sides of the short link, making the linkage susceptible to torsion loads. The center coupler piece should be changed to include hardstops, as well as be machined instead of 3D printed to increase hole location accuracy. The design of the housing for the sliding electrode adapters should also be revised to not rely so heavily on precision machining of 2 plates. Even though our team used a mill to drill the holes and reamed them, the profile was cut on a waterjet and just that small roughness threw off the location of the holes. This caused binding when the adapters would slide, which was solved by giving the rods more tolerance in their hole fits. Ideally, this housing should be redesigned so that precision machining is not needed, as we do not expect other student project teams to have access to more than a typical waterjet, manual mill, and manual lathe.

Our supporting circuitry is especially impactful as many of our welder control objectives rely on it. We believe that the possible assembly challenges when working with proto-boards caused our circuits to fail. For a second iteration, we would like to create a custom PCB layout such that the assembly process is straightforward.

11.3 Risk

The process of manual spot welding is inherently dangerous due to the high amount of energy expended in single spot welds, as well as all the danger associated with lithium-ion batteries. While our solution does make the process safer by making it more consistent, an inexperienced user could put the probes in the wrong location, press too hard, and puncture the cell. There is also the risk that a weld created using our solution does not hold up in its service life, and if it were to break off, the heat generated by the separation of the battery and the terminal could cause thermal runaway and thus catastrophic failure of the battery. The team is committed to ensuring that neither immediate or eventual failure occurs for users of our solution, so a rigorous SOP will be released along with the materials for manufacturing our solution when it becomes Open Source.

12. Reflection

12.1 Social Context

12.1.1 Public health, safety, and welfare

Public health is highly relevant to the project. Manual spot welding battery cells has posed significant safety risks for the users, including cell punctures, thermal runaway, and even fire hazards. Our design directly improves public health and safety by enforcing correct use, that being within the ideal force and orientation bounds to minimize the chance of an accident. Additionally, we included emergency stops and real-time feedback to reduce the likelihood of dangerous failures further.

12.1.2 Global context and benefit in a global marketplace

This is relevant due to the open-source nature of our project. Many student teams, research groups, and small startups face the same issues that SPARK does with our welding methods, those being primarily limited budgets and access to industry standard solutions. We hope that we have accomplished a solution for groups like this to be used globally.

12.1.3 Social impacts associated with manufacture, use, and disposal

Our project has positive social impacts primarily through the fact that it improves weld consistency, limiting the amount of damaged or scrapped lithium-ion cells and thus reducing hazardous waste and lowering the risk of improper disposal. A possible negative impact our project could have is that, through it being open-source, we enable possible inexperienced users to build battery packs. This risk, however, is mitigated through the inclusion of a detailed standard operating procedure and proper safety information.

12.1.4 Economic impacts associated with manufacture, use, and disposal

Our project was aimed to be affordable and efficient. The product significantly reduced labor time and material waste compared to the manual welding process, lowering the overall cost for battery manufacturing that would heavily affect student teams and small organizations. Additionally, our total cost being under $2000 allows for broader participation in electric vehicle development without requiring expensive industrial equipment.

12.1.5 Tools used to characterize societal impacts

We used several tools to evaluate our societal impacts. Firstly, we used stakeholder interviews and stakeholder maps to identify safety, usability, and ethical concerns across different user groups. We also applied life-cycle cost considerations to assess the affordability, maintenance, and material waste we would be producing. Finally, we benchmarked against the existing industry standard solutions to help contextualize the economic and accessibility impact of the final design.

12.2 Culture, Privilege, and Identity

12.2.1 Differences between team members

The team shared a common academic and technical culture as mechanical engineering students that have experience with hands-on design, analysis, and student project teams. This background allowed for a strong baseline for communication, expectations, and technical experience. Going through a very similar university through this point, all team members were able to contribute meaningfully to CAD, analysis, prototyping, and documentations without any major barriers. Differences in our individual strengths, styles, and prior experiences influenced how tasks were approached. Some members focused more on mechanical design and analysis, while others emphasized the electronics, controls, or documentation. These differences proved to be beneficial, as they encouraged more broad exploration of concepts and overall made the design process more thorough. Overall, the similarities in our privilege and educational background allowed for less friction in our processes, while the differences allowed for improved creativity, division of labor, and general robustness of our final solution.

12.2.2 Differences with the sponsor

The sponsor, Cameron Trumpy, influenced the design process through both his expertise and positional authority as our primary stakeholder and end user. As an established student-engineer with extensive hands-on experience with battery manufacturing, his knowledge shaped our team's priorities toward safety, reliability, and ease of use rather than just theoretical optimization alone. Power differences were present in that, ultimately, our constraints and overall success was defined by our sponsor. However, cultural and identity similarities, like the fact that we are all engineers working for the same team at the same institution, facilitated a sense of open communication and collaboration rather than a top-down flow of information. This balance allowed the sponsor to use his experience to guide the design while also allowing our team the autonomy to explore and iterate upon our own solutions. The result is a design that closely aligns with both real user needs and operational realities.

12.3 Inclusion and Equity

Power dynamics existed between the design team, stakeholders, and end users primarily due to differences in experience and roles in the process rather than traditional authority. While the team ultimately acted as the designers and final decision-makers, the stakeholders helped influence through their lived experience with battery manufacturing and extensive history of spot welding. The end users have practical knowledge of safety risks, inefficiencies, and failure modes that the design team would not have known about or addressed prior to consulting with them. This created a dynamic where the stakeholders and end users had greater contextual authority while the team retained control over the technical implementation and final design decisions.

The team's own identity and experience shaped perspective in that all the members are also affiliated with SPARK, allowing for overlap between designer and user roles. This reduced the distance between the team and the end users. Compared to the end users, the design team initially approached the problem more analytically, whereas users emphasized the safety, consistency, and ease of use from their experience with the repetitive, hands-on welding experience. Compared to other team members, individual perspectives varied based on prior exposure to elements like manufacturing or electronics, influencing which risks or requirements were emphasized during discussions.

To include diverse viewpoints, the team conducted structured stakeholder interviews and intentionally allowed interviewees to describe their experiences in open-ended terms rather than guiding them toward predefined solutions. Input from multiple stakeholders across different teams and roles was combined into shared user requirements rather than treated as isolated opinions. Within the team, concepts were generated individually before group discussion, ensuring that quieter or less dominant voices were represented in the solution space prior to convergence.

When balancing differing ideas from stakeholders and team members, the team relied on explicitly defined requirements, engineering specifications, and verification criteria rather than personal preference or authority. Conflicting viewpoints were evaluated against safety, cost, usability, and feasibility metrics, allowing decisions to be justified transparently. This approach helped prevent dominance by either sponsor preferences or individual team members and ensured that selected ideas directly supported project goals.

Cultural similarities among team members, such as shared engineering education, access to university resources, and familiarity with student project team environments, enabled efficient collaboration and reduced communication barriers. Differences in working styles and technical focus, however, influenced how problems were approached and ultimately strengthened the design by encouraging iteration from multiple perspectives. Similarly, cultural similarities with the sponsor, including shared institutional context and student-led engineering culture, facilitated open dialogue and mutual respect. Differences in experience level, particularly the sponsor's deeper practical knowledge, influenced the final design by grounding decisions in real operational constraints. Together, these dynamics resulted in a design process that balanced inclusivity, technical rigor, and user-centered decision-making, producing a final product aligned with both engineering standards and stakeholder needs.

12.4 Ethics

Ethics came into question during solution development mainly related to safety and responsibility. Since lithium ion battery cells are volatile, misuse of our solution may lead to serious hazards such as cell puncture and fire. One ethical challenge was balancing the goal of making the system cost effective for small groups and open-source with the reality that

inexperienced users might misuse it. Our team addressed this problem by prioritizing safety features in the design, like controlled force application, enforced probe orientation, emergency stops, and real-time feedback. We were also committed to thorough documentation and standard operating procedures to promote safe use and limitations of the system.

If the project were to enter the marketplace, more ethical issues could arise related to liability, misuse, and unintended applications. Commercial distribution could lead to use outside of our intended application, potentially by users without training in battery safety. There would also be ethical considerations surrounding product responsibility, such as giving warnings, training materials, and safeguards are provided to prevent harm. Intellectual property issues could also arise if modified versions of the open-source design were distributed without maintaining our original commitment to safety.

Our team's ethics align with the professional ethics displayed by the University of Michigan, particularly in safety, honesty, and responsibility to the public. Our standards emphasize the importance of public welfare and clearly communicating risks and limits of our system. Our project shows the importance of focusing on professional ethical standards early in a design cycle, especially when designing systems that interact with hazardous materials. We highlight the engineering responsibility to consider impacts beyond immediate technical performance.

13. Recommendations

The first recommendation would be to mill every part of the housing with the end-effector, as waterjetting any features reduces the tolerance to the point where the sliding bearings bind up as the ground shafts are not perfectly centered. We also recommend introducing additional light weighting features in the linkage arms, joiner, and end effector plates to reduce their final weight and make the end effector easier to move. For the supporting electronics, we recommend remaking all the circuits as PCBs to simplify the building process and to also condense the circuits compared to their current protoboard versions. Making sure that the circuits are working is very important for mitigating the risks mentioned in Section 11.3, as they give important feedback to the user about the force and quality of their weld, which could directly avoid immediate failure or failure of the welds while in service.

14. Conclusion

This project addressed a critical problem faced by student-led project teams and startups that design and build their own custom cylindrical cell lithium-ion battery packs. These custom battery packs are assembled using a manual spot-welding process that is slow, inconsistent, and poses safety risks due to the variations that occur in each weld. Upon interviewing our stakeholders on the SPARK Electric Racing battery team, we discovered that these variations stem from changes in electrode orientation, electrode placement, and the electrode force applied at each welding location. While industrial automated welding solutions do exist to address these inconsistencies, their high cost and complexity make them unobtainable for student teams and

startups. The objective of this project is to bridge the gap between the cheap unreliable manual method and the industrial solutions by developing a low-cost, accessible, and open-source assistive device that improves weld consistency, efficiency, and safety while remaining affordable and accessible for student project teams and startups.

Upon developing this problem objective, we developed our requirements and specifications that needed to be addressed for a successful solution. These requirements and specifications are seen in table 4.1.1 and table 4.1.2. From these requirements and specifications we then began our concept generation process where, through an initial morphological chart, we discovered two potential solutions that would successfully address our requirements and specifications. These two solutions were a human-powered dual four bar linkage solution, or an automated gantry solution. After making additional morphological charts and utilizing design heuristics, we systematically decided on the human-powered dual four bar solution using a pugh chart, and began our engineering analysis and design process from there.

This final solution uses a dual four-bar linkage to enforce electrode orientation to be normal to the cell plane all throughout the work area, allowing for two-dimensional movement. Through additional engineering analysis the link lengths and joint distances were calculated in order to be able to reach our desired maximum radius while keeping the maximum flexion of the linkage at 150 degrees. The end effector incorporates an equalizing seesaw mechanism that ensures even probe contact at all cells and as well as a load cell that will allow for real-time force indication when we are at the desired force of 88N. The end effector also was designed to have integrated circuitry for voltage and current sensing to get the energy expended at each weld, as well as the necessary load sensing circuitry. Together, all of these components work together to make the welding process safer, more consistent, and more reliable while maintaining a simple, human-powered process with real time weld quality metrics.

This solution was then evaluated through verification tests that addressed the specifications for each of our requirements. Our location accuracy, weld probe orientation, and force application verification tests were to determine the mechanical functionality of our design, all of which passed each test. The quality of the nuggets were verified using shear and axial loading, both of which passed. The spot welding rate greatly exceeded our expectations with 6 welds in 19.4s (expected to be 6 welds in 60s). Additionally, the stability, ease of maintenance, and ease of setup and use verification tests all passed. Unfortunately during our circuitry verification tests we ran into some issues with the load sensing circuitry. This led to not only this circuit being unsuccessfully verified, but also our weld energy consistency verification test to be unable to be performed. Despite this, the remainder of the circuitry was able to be tested and verified that they matched the results of the LTspice simulations. This circuitry bug for the load cell will be addressed by SPARK Electric Racing next semester.

Overall, this project successfully delivers an easy use and robust alternative to manual spot welding that bridges the gap between fully manual process and expensive industrial automation. Our solution improves welding consistency, reduces safety risks, and increases productivity while remaining affordable (<$2000), maintainable, and open-source. Future work needs to be done to fix the circuitry to be implemented into the end effector, but overall the current outcome of this project represents a high-quality, well-validated engineering solution that meets the needs of its stakeholders and fulfills the project's objectives.

15. Acknowledgements

The team would like to thank SPARK Electric Racing for sponsoring our project, especially Cameron Trumpy who provided insight and guidance to the team throughout the design process. The team would like to thank Jason Siegel for his insight into all things EV battery pack related and testing which inspired our verification plans. We would also like to thank our ME 450 section advisor Shorya Awtar for his constant feedback on the design process and sharing his knowledge of precision mechanical design. Finally, we would like to thank the University of Michigan Battery Lab staff for meeting with our team and explaining how industry and cutting edge research in battery technology affected our project.

16. References

[1] ME450 Design Process Slides

[2] C. L. Dym and P. Little, *Engineering Design: A Project-Based Introduction*, 4th ed. New York, NY, USA: John Wiley, 2000. [Online]. Available: https://search.lib.umich.edu/catalog/record/004198336

[3] D. Wynn and J. Clarkson, "Models of designing," in *Design Process Improvement*, J. Clarkson and C. Eckert, Eds. London, U.K.: Springer, 2005. [Online]. Available: https://doi-org.proxy.lib.umich.edu/10.1007/978-1-84628-061-0_2

[4] "FANUC R-1000iA/80H Robot," FANUC America, [Online]. Available: https://www.fanucamerica.com/products/robots/series/r-1000ia/r-1000ia-80h.

[5] AMADA Weld Tech, "Custom Resistance Welding Systems," AMADA Weld Tech. [Online]. Available: https://amadaweldtech.com/product/custom-resistance-welding-systems/.

[6] AMADA Weld Tech, "Jupiter Laser Welding System for battery tab welding," AMADA Weld Tech. [Online]. Available: https://www.amadaweldtech.eu/products/laser-welding/laser-welding-systems/jupiter-laser-welding-system-battery-tab-welding.

[7] ISO, *Quality requirements for welding – Resistance welding of metallic materials,* ISO 14554-1, Geneva, 2016.

[8] AWS, *Recommended Practices for Resistance Welding,* AWS C1.1M/C1.1, Miami, FL, 2019.

[9] ISO, *Safety of machinery – General principles for design – Risk assessment and risk reduction,* ISO 12100, Geneva, 2010.

[10] AMADA Weld Tech, "Resistance Welding Fundamentals," 2023. [Online]. Available: https://amadaweldtech.com/wp-content/uploads/2023/04/Resistance-Welding-Fundamentals.pdf. [Accessed: Sep. 29, 2025].

[11] EMS Clad, "EMS Step-Weld Test Report," 2020. [Online]. Available: https://www.emsclad.com/wp-content/uploads/sites/12/2023/02/EMS-Stepweld-test_62227.pdf. [Accessed: Sep. 29, 2025].

[12] Adam Heiler, personal interview, Sep. 16, 2025.

[13] Morgan Duvel, personal interview, Sep. 16, 2025.

[14] Giovanna Celi, personal interview, Sep. 16, 2025.

[15] Cameron Trumpy, personal interview, Sep. 16, 2025.

[16] Andrew Dailey, personal interview, Sep. 23, 2025.

[17] Daniel Kedroske, personal interview, Sep. 23, 2025.

[18] ME450 Concept Generation Slides

[19] "History | BOLT at Virginia Tech," BOLT at Virginia Tech, [Online]. Available: https://www.vtbolt.com/superbike.

[20] "REV3 – EVT," RIT-EVT.com, [Online]. Available: https://rit-evt.com/rev3.

[21] TE Connectivity, "20009605-06 Datasheet," [Online]. Available: https://www.te.com/usa-en/product-20009605-06.datasheet.pdf.

[22] PJRC, "Teensy 4.1 Development Board," [Online]. Available: https://www.pjrc.com/store/teensy41.html.

[23] Texas Instruments, *TIDUD33A Reference Design User's Guide*, [Online]. Available: https://www.ti.com/lit/ug/tidud33a/tidud33a.pdf.

[24] Texas Instruments, *INA240 Precision Current Sense Amplifier Datasheet*, [Online]. Available: https://www.ti.com/lit/ds/symlink/ina240.pdf.

[25] Analog Devices, *LT3092 1.5 mA to 200 mA 2-Terminal Programmable Current Source Datasheet*, [Online]. Available: https://www.analog.com/media/en/technical-documentation/data-sheets/lt3092.pdf.

[26] GAPTEC Electronic, *1S4E-1.5U Isolated DC-DC Converter Datasheet*, [Online]. Available: https://gaptec-electronic.com/datenblaetter/1S4E_1.5U.pdf.

[27] Texas Instruments, *ISO224 Precision Isolation Amplifier Datasheet*, [Online]. Available: https://www.ti.com/lit/gpn/iso224.

[28] Bel Power Solutions, *SWI10B-N Series 10 W AC-DC Power Supply Datasheet*, [Online]. Available: https://www.belfuse.com/media/datasheets/products/power-supplies/SWI10B-N.pdf.

[29] Texas Instruments, *INA333 Precision Instrumentation Amplifier Datasheet*, [Online]. Available: https://www.ti.com/lit/ds/symlink/ina333.pdf.

[30] Vishay Intertechnology, *WSBS8518 Power Metal Strip® Resistor Datasheet*, [Online]. Available: https://www.vishay.com/docs/30134/wsbs8518.pdf.

17. Bios

Benjamin Andelman is a senior studying mechanical engineering with a robotics concentration, originally from Silver Spring, MD. He has always had an interest in pulling apart mechanisms and trying to understand how they work, as well as improve them. This interest has been transformed into design, manufacturing, and testing through various experiences at the University of Michigan. None is more influential than his involvement with SPARK Electric Racing, where he now serves as the mechanical director. The development of an electric vehicle capable of going 200 mph completely from the ground up has been a consistent source of work and interest for him. He also conducts research for the EMBiR lab at the University of Michigan, where he developed a patent-pending automated robot mixing device.

Vincent Bourgeois is a senior studying mechanical engineering with a robotics concentration, originally from Thompson, CT. He knew he wanted to become a mechanical engineer since high school where he purchased his first project car, a 1993 BMW 325is. Learning how vehicles work from this project sparked his interest in pursuing engineering. After working three internships in manufacturing and design engineering, his future goals are to work in a manufacturing environment where there is a mix between hands-on and design work. Fun fact about him is that his childhood home used to have a 100 foot waterslide into a lake in his backyard.

Matthew Gibson, a senior studying mechanical engineering, HAILs from Redwood City, CA. Ever since he was a child, he made mad contraptions and ordered chemicals from Amazon that his parents promptly seized. As he grew older, his desire to create and work with his hands was directed towards transportation. He made frankenstein electric scooters and started an ultralight aircraft design team in high school. Since arriving at the University of Michigan, he has been a member of SPARK: Electric Racing on the aerodynamics team. In the future, Matt hopes to start his own mobility focused company and eventually become a high school physics teacher.

Ryan Applegate is a fourth year mechanical engineering student with humble beginnings in Hamilton, NJ. His passion would be SPARKed at an early age, taking apart Nerf blasters and replacing their springs with unnecessarily large ones to improve performance. His interest more recently has shifted to the development of autonomous robotics, combining principles of computer science with knowledge of mechanical engineering.

Esben Nielsen is a senior in mechanical engineering with a minor in computer science, hailing from Matawan, NJ. His interest in mechanical engineering was piqued by his involvement in VEX Robotics in high school, where he took his team to the world championships in senior year as captain. Since then, he has delved into his education at the University of Michigan, joining the SPARK electric racing team and rising to the rank of president after three years. He is interested in pursuing a career in aerospace structural dynamics after completing his master’s degree in

mechanical engineering. His dream is to attend MIT for his master's degree, conducting research in the area of flexible structural dynamics, and his dream job is to work at Lockheed Martin's Skunkworks facility, designing the next generation of advanced propulsion technologies.

APPENDIX A

A.1 Concepts Generated - Esben Nielsen

A.1.1 Initial Ideas - Text Descriptions

1. 3-axis gantry type table with spot-welder
    a. Table containing battery module moves in one axis, tool head with spot-welder probes is on single axis gantry and contains Z axis movement as well
    b. Table moves in both axes, tool head with spot-welder probes contains Z axis movement as well
    c. CoreXY motion system with belts, utilizes two stepper motors with interlinked belts
    d. Rack and pinion used for all axes
    e. Stiff cables linked together with pulleys used for all axes
    f. Z-axis specific ideas (also applicable to single-axis solution below)
        i. Single pneumatic piston with pressure regulator used for dual position Z-axis - device hooked up to high-pressure air supply - solution utilizes a flow regulator as well to ensure that actuation of the piston is not too fast
        ii. Motor actuated Z-axis but stops once a spring senses enough travel to indicate that correct force has been achieved
2. Human-Powered spot-welder
    a. Probes of spot-welder are combined into a single mount instead of separate and loose and device is hand-held size - ensures correct alignment
    b. Integrated spring and gyroscope / orientation sensor onto probe ends ensures correct force application - weld is not issued until force level is reached and correct orientation is attained
3. Single axis device that applies correct alignment of probes to each other
    a. User moves battery to correct position, actuates welder to perform perfect weld with integrated pneumatic pump to provide exact application force, along with distance and angle between probes set by geometry
4. Crimping device to grab onto cell, force current collector into contact with cell terminal and join them together

A.1.2 Expanded Ideas Using Design Heuristics

Idea 1: improvement upon "Z-axis specific ideas … " - idea 1.f from A.1.1
Design Heuristic 14: attach independent functional components
Description: dual pneumatic pistons with dual solenoids and pressure regulators, singular air supply, one attached to each probe. Allows individual customization of applied forces for terminal probe and current collector probe.

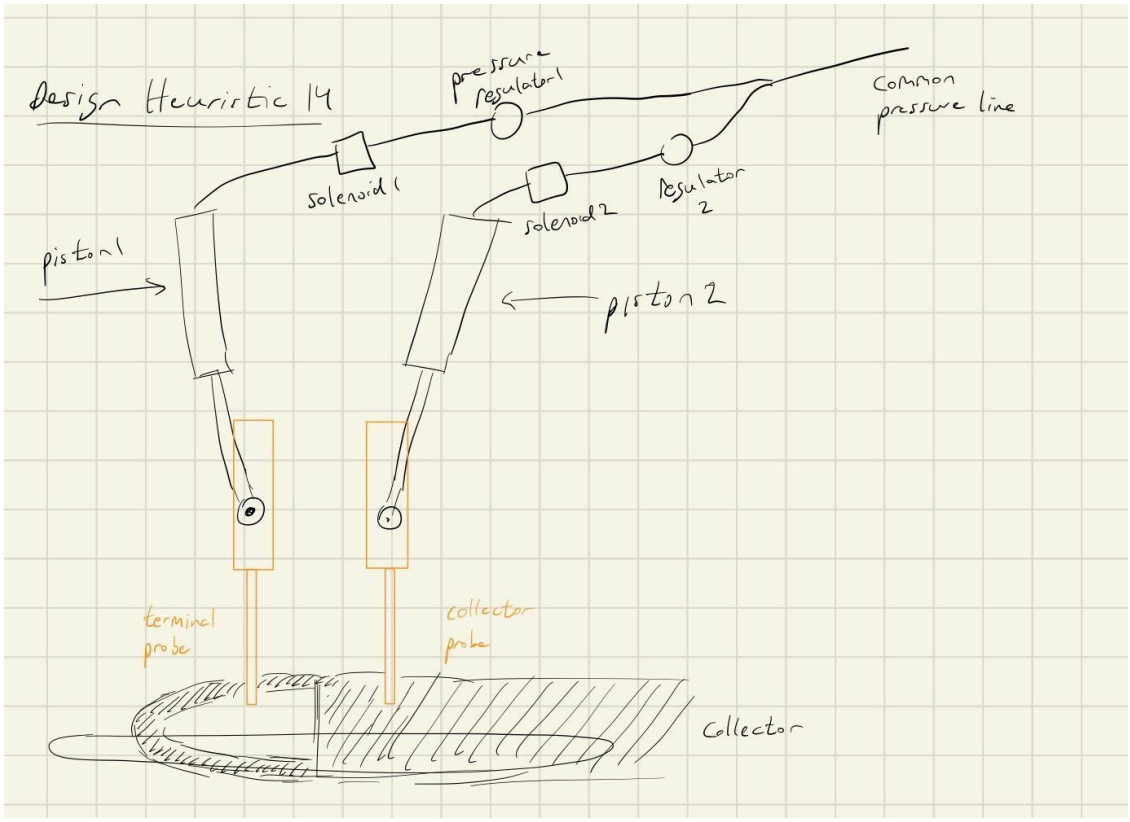


Figure A.1.2.1: Drawing of Double Cylinder Pneumatic Force Application Solution

Idea 2: bounced off of human-powered spot-welding device above with sensors incorporated
Design Heuristic 50: provide sensory feedback
Description: device issues haptic vibrational feedback when and during all times when correct force has been applied so that user knows that a weld can be issued, and makes a consistent noise (like a continuity sensor) when the correct probe orientation range has been attained. The device contains a button to issue the weld, but is only active when the device is both vibrating and making noise (indicating both weld conditions have been met).

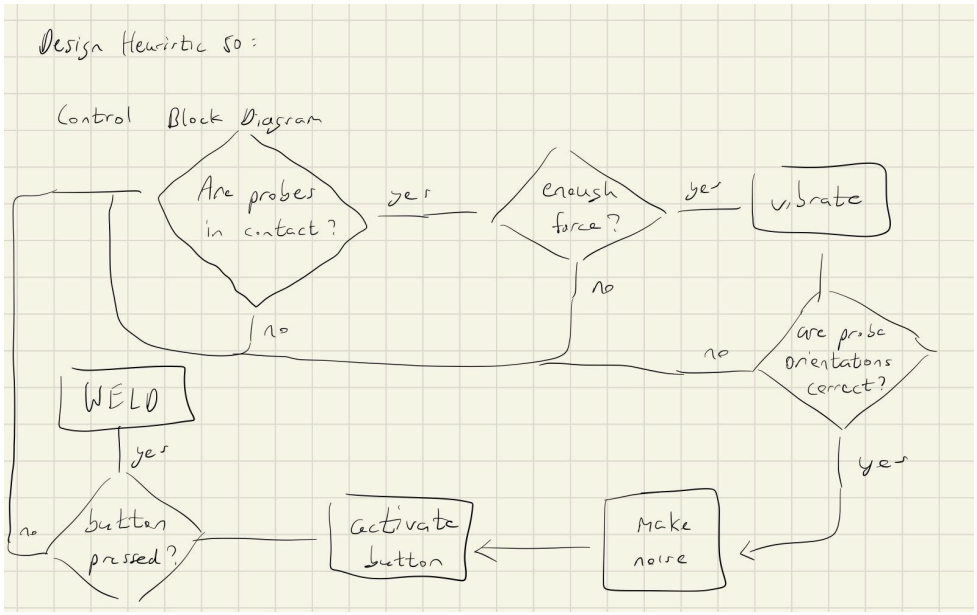


Figure A.1.2.2: Control diagram of force and orientation feedback-controlled weld enabling.

Idea 3: Independent idea, likely will utilize design components from gantry idea in A.1.1
Design Heuristic 76: utilize opposite surface
Description: When spot-welding cylindrical cells, current collectors need to be attached to both ends of each cell, meaning that there are twice as many welds needed as there are cells. In current ideas, I've always imagined the module laid flat in the 2D plane. However, if we could place the module upright, laying on the side of the cells, we could have access to both sides of the cell at the same time, enabling multiple welds to be accomplished at the same time.

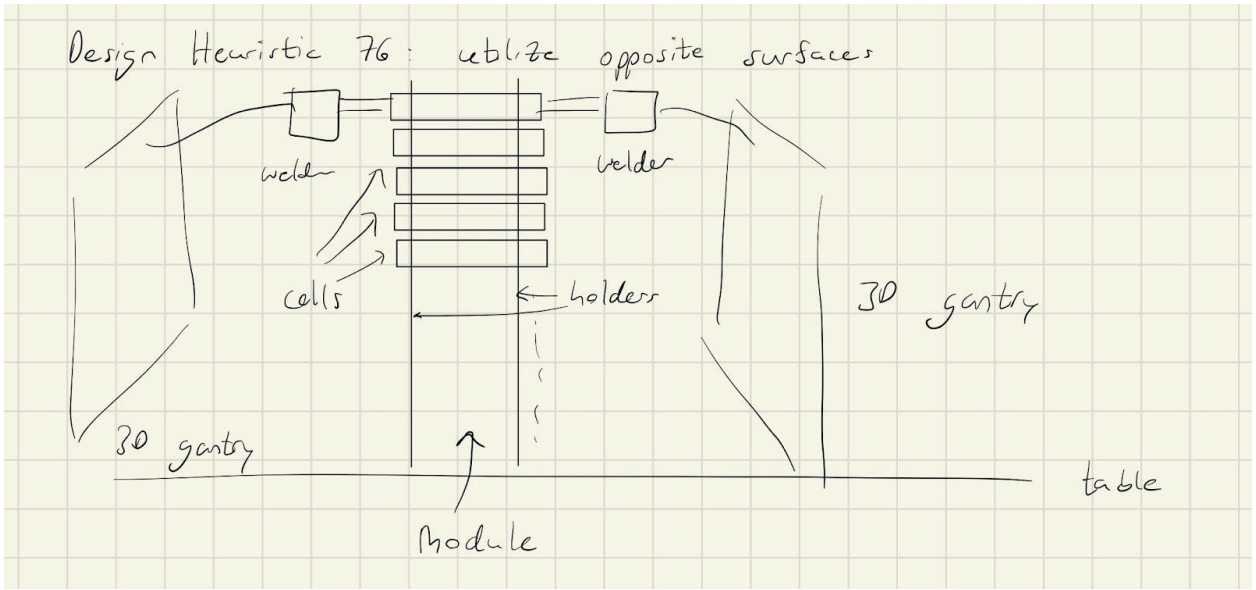


Figure A.1.2.3: Drawing of Double-sided Gantry Welder with vertically placed battery module.

A.1.3 Expanded Ideas Utilizing Functional Decomposition

Table A.1.3: Three-Function Decomposition Table

Function	Possible Solutions		
Move quickly between terminal/collector attachment points along continuous X and Y axes	Move spot-weld probes by hand	Use dual polar coordinates-aligned systems	
Join current collector with cell terminal	Spot-welding	Cell sheath that slides over cell and terminals	
Hold current collectors tight onto cell terminals	Use vacuum to hold collectors	Use air jets from spot-weld head	Use physical clamps

Idea 4: Independent idea that modifies the way current collectors are attached, inspired by "physical clamps" from function #3: "Hold current collectors tight onto cell terminals" Description: instead of utilizing electricity to weld current collectors to cell terminals, a sort of sheath could be developed that slides over the cell horizontally, and utilizes tension along the length of the cell to pull metal end caps into contact with each cell terminal. These end caps could be made of extremely weldable material, allowing for easier joining to be done with the current collector geometry instead of welding directly to the cell terminal.

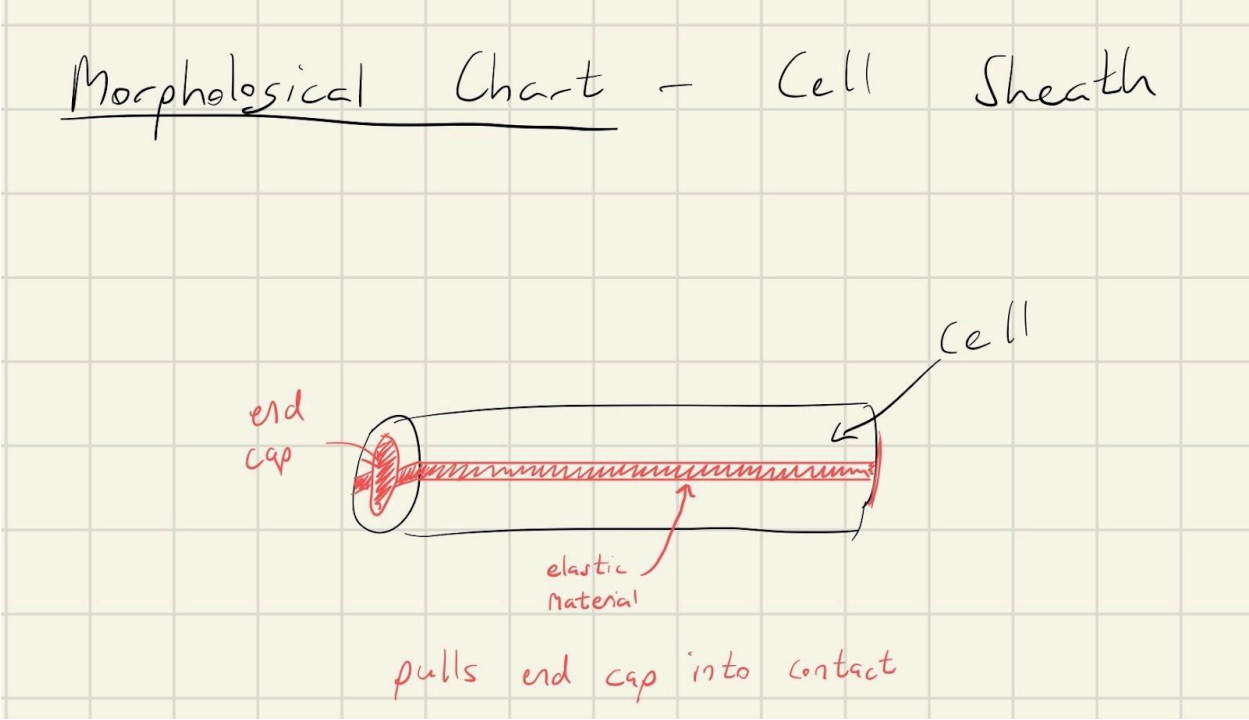


Figure A.1.3.1: Drawing of cell sheath idea, utilizing elastics to pull current collector into contact with cylindrical cell.

Idea 5: Improving upon gantry (1) or human-powered (2) idea from A.1.1
Description: holding current collectors in their originally placed position is a major issue, and could be solved by using a vacuum underneath the cells to pull the current collectors into place.

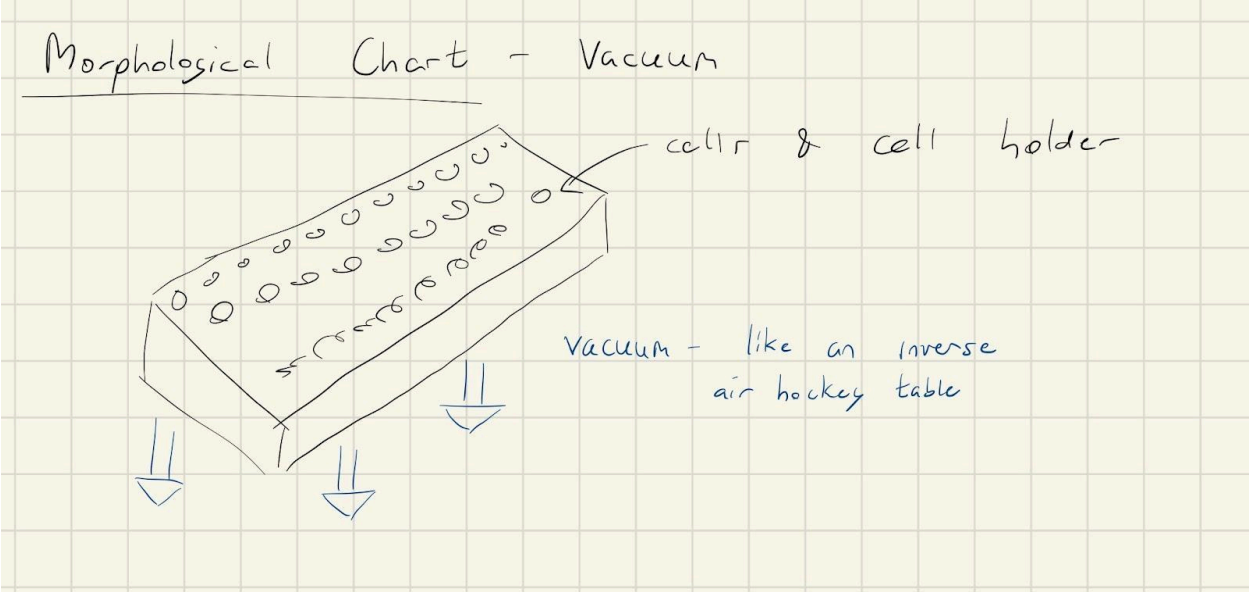


Figure A.1.3.2: Drawing of vacuum-pressurized module bed, utilizing negative pressure to ensure placement and stability of current collectors.

Idea 6: Improving upon gantry idea from A.1.1, and with pneumatic pistons considered
Description: holding current collectors in their originally placed position is a major issue, and could be solved by utilizing a part of the air supply used to fire the Z-axis pistons to provide downward-pointing air jets that apply pressure normally to the surface of the current collector, forcing it to stay in place on the cell terminals
Drawing:

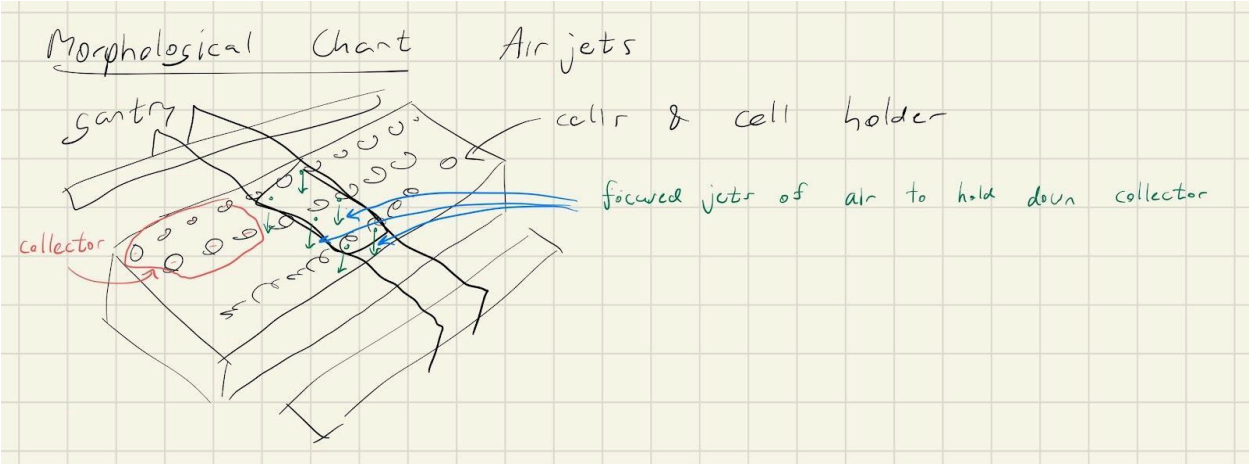


Figure A.1.3.3: Drawing of air-jetting toolhead, utilizing downward-facing air jets to pressure current collector material into place.

Idea 7: Improving upon gantry idea, only requires most basic components
Description: simple, user-operated clamps that can be used to hold down the current collector during the first few welds of a cell group, and that can be removed once the collector is securely in place.

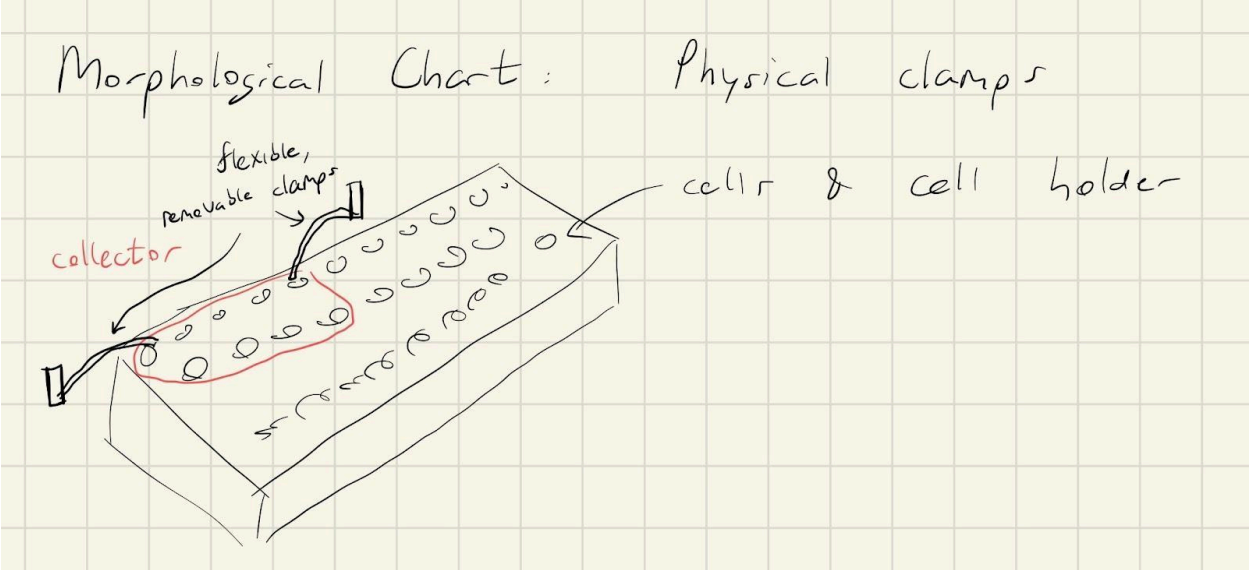
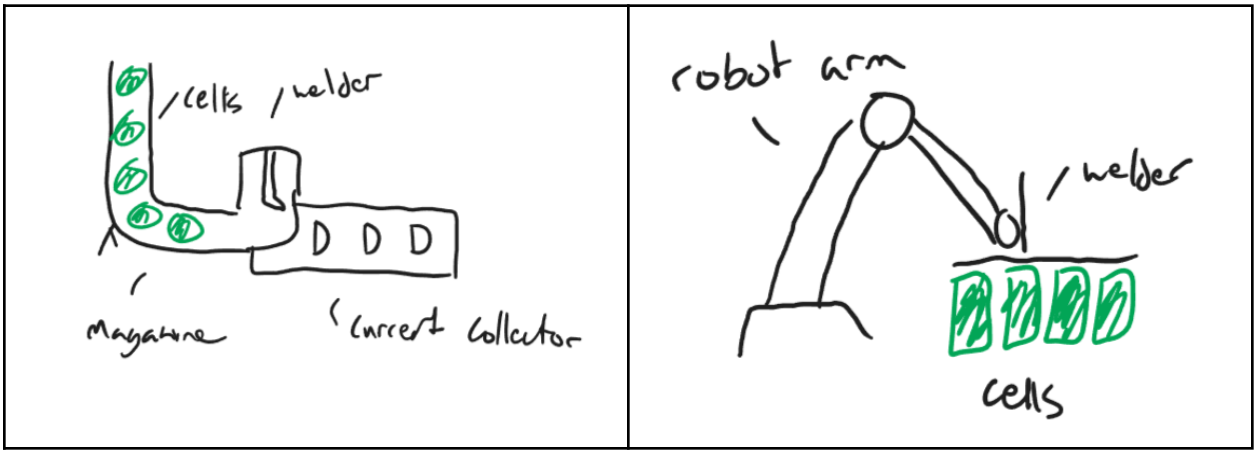


Figure A.1.3.4: Diagram of clamped current collector module bed design, utilizing flexible clamps to provide downward force onto top surface of current collectors to hold them in place.

A.2 Concepts Generated - Benjamin Andelman

Table A.2.1. The preliminary concepts for solutions to the ME450 design problem, communicated by a mixture of descriptions and sketches.



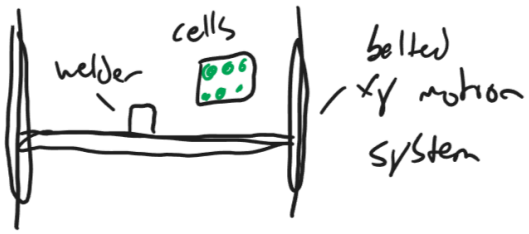
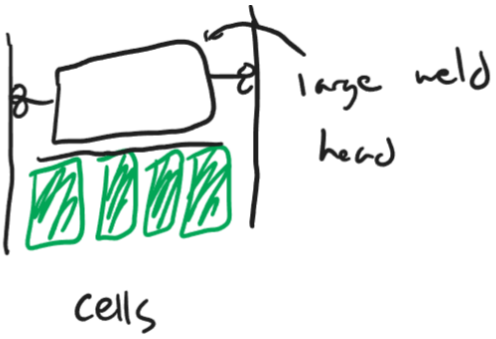
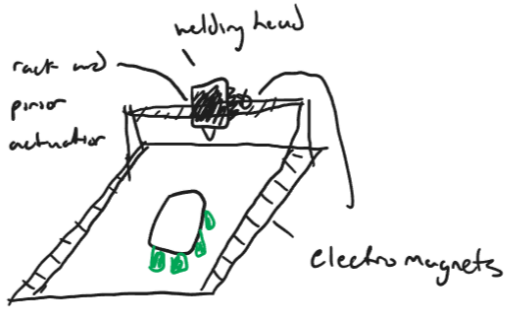
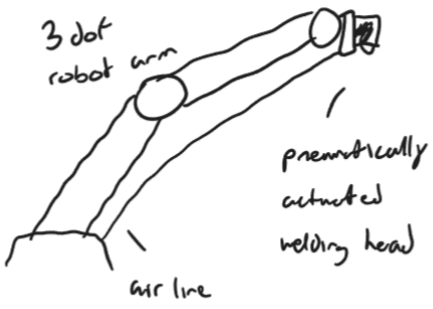
A hydraulic movement system to guide the welding head to where the spot weld goes	
	A motion system to move the welding head that uses electromagnets
A heated chamber to weld the welding material flux then apply to each cell	
A motion system to move the the welding head that uses compressed air	A manual low friction sliding rail assembly with a manual pull down welding head

Table A.2.2. A collection of more refined/complete concepts that were achieved using functional decomposition.

Have an adjustable XY frame made with slotted extrusion to adjust to module size, use crank handles to handle XY motion and a rack and pinion system to lower the welding head, big red button to push to activate the rack and pinion	
Use the 3 DOF robot arm base, but incorporate a spring-plunger system on the welding head so the arm can press down with force to weld and have a cushion	Use a belted drive in the rigid XY frame and a rack and pinion to lower the welding head, but have the user control it with a joystick
Use linear screws to control the motion on a rigid XY frame	Using the rigid XY frame, use cables to move the motion and have the welding head be lowered pneumatically
Using the adjustable XY frame, use pneumatic cylinders to adjust the frame size, as well as to move in XY, rack and pinion to press down the welding head	Attach a rack and pinion sliding system to the end effector of a 3 DOF robot arm, so that the robot lines up the weld then the rack and pinion complete the weld

A.3 Concepts Generated - Vincent Bourgeois

Initial Ideas

A.3.1 Gantry design (3D printer style) utilizing guide rails for x-y motion for the spot welder, and some sort of additional z-axis control in place

A.3.2 Scara robot style arm utilizing pivots for x-y motion with spot welder attached on the end

A.3.3 Higher degree of freedom robot arm utilizing a mix of pivots and guide rails for great degrees of freedom with the spot welder being able to rotate.

A.3.4 A design where the spot welder itself is fixed and the cells move into the correct location instead

A.3.5 A design with multiple spot welders to increase maximum output efficiency

Improved Ideas using Morph Chart and Design Heuristics

Morph Chart

Sub Functions	Solutions ->		
Reduce time	Tuned PID control	Tuned Stepper Motor	Multiple welders
Increase reliability	Robust design	Generate maintenance plan	Have operator do occasional checks
Increase safety	Add current sensor for welder	Add visual system to assist with alignment checks	Include safety plan in SOP

Design Heuristics

Using design heuristic cards, I am also able to generate new ideas. Using card #4 of adding to an existing card, I could add the spot welder to an existing 3D printer gantry design. Using card #42 of making components attachable and detachable, I could make a design where the spot welder could be swapped out and therefore have the ability to create other types of welds if needed. Using card #74, we could attempt to make this design using repurposed/recycled materials. This was never really considered prior and wouldn't have been without the use of the cards.

A.3.6 Spot welder attached to an existing 3D printer gantry design with a tuned stepper motor
A.3.7 Multiple spot welders attached to gantry design with robust design and visual system
A.3.8 Gantry designed welding system with current sensor for weldsRobot arm with multiple degrees of freedom with advanced tuned PID control
A.3.9 Robot arm with visual system to do alignment checks of the weld
A.3.10 Robust welder design that is rigid and the cell pack is moved instead

A.4 Concepts Generated - Ryan Applegate

Initial Ideas

A.4.1 XY Gantry with Spring-Loaded Z Probe - Simple x-y CNC-style motion with simple probe downforce control.

A.4.2 Rotating Table with Fixed Welder - Similar design to 2.1, just use rotational movement to position battery modules under a stationary spot-welding head.

A.4.3 Articulated 2-DOF Arm - Robotic arm with pneumatic Z-actuator for weld pressure.

A.4.4 Magnetic Cell Clamp System - Use magnetic fixtures to hold collectors flat during welding.

A.4.5 Laser Alignment Guide - Laser crosshairs project weld positions for operator verification.

Additional Designs Generated Using SCAMPER Technique

A.4.6 *Substitute* - Replace stepper motors with belt-driven linear actuators for cheaper XY movement.

A.4.7 *Combine* - Integrate laser alignment with camera vision to auto-correct weld errors.

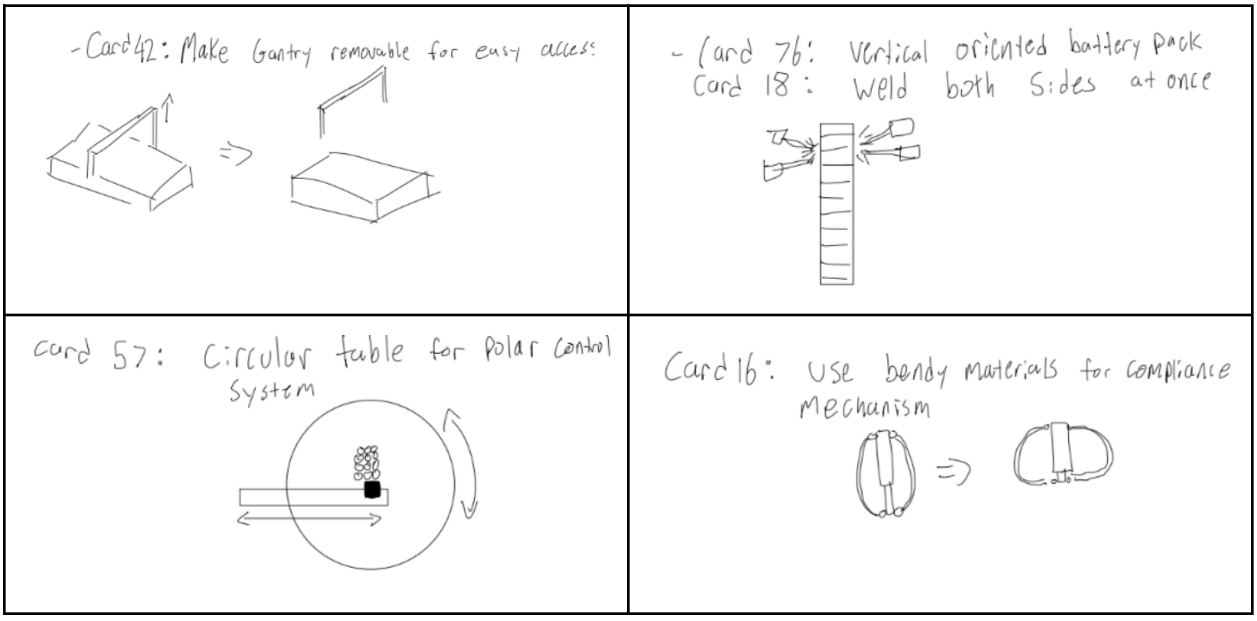
A.4.8 *Adapt* - Borrow a 3D printer frame (Prusa/Ender style) and retrofit with a welding head.

A.4.9 *Modify* - Scale up for multi-head welding, allowing two welds simultaneously.

A.4.10 *Reverse* - Instead of a moving welder, move the pack under a fixed welder using conveyors.

A.5 - Concepts Generated - Matthew Gibson

Table A.5.1 Concepts Generated using Design Heuristics



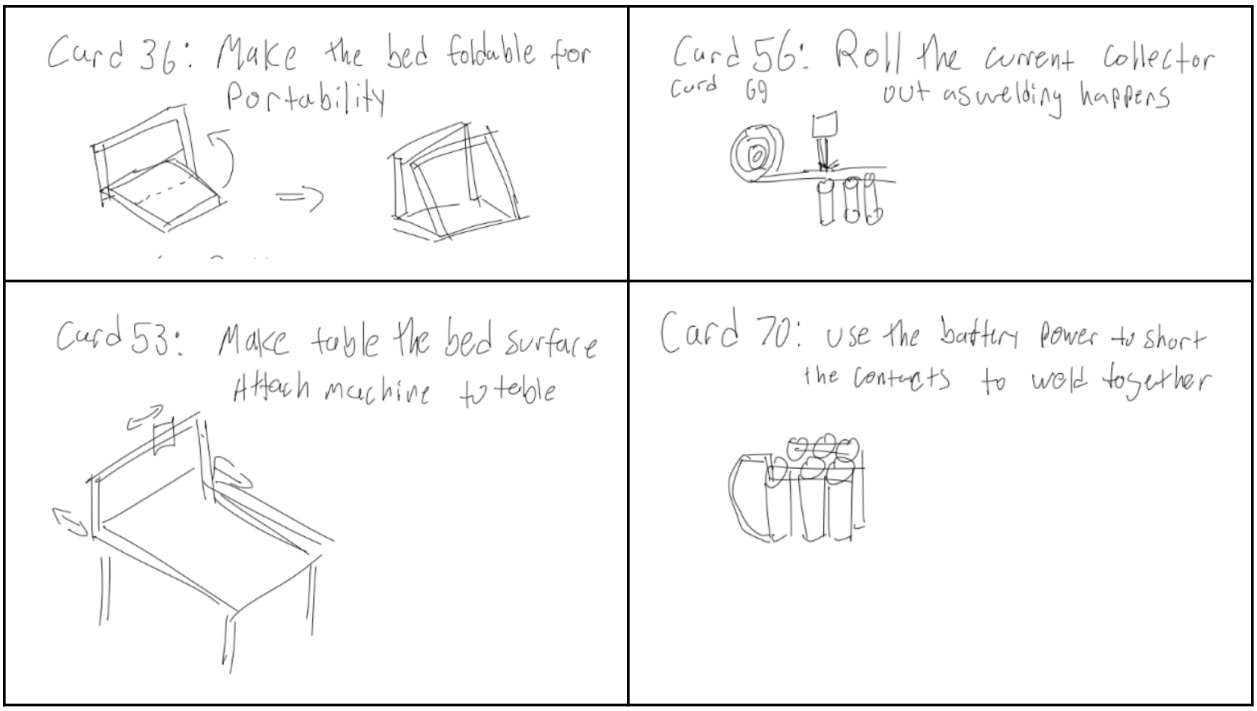
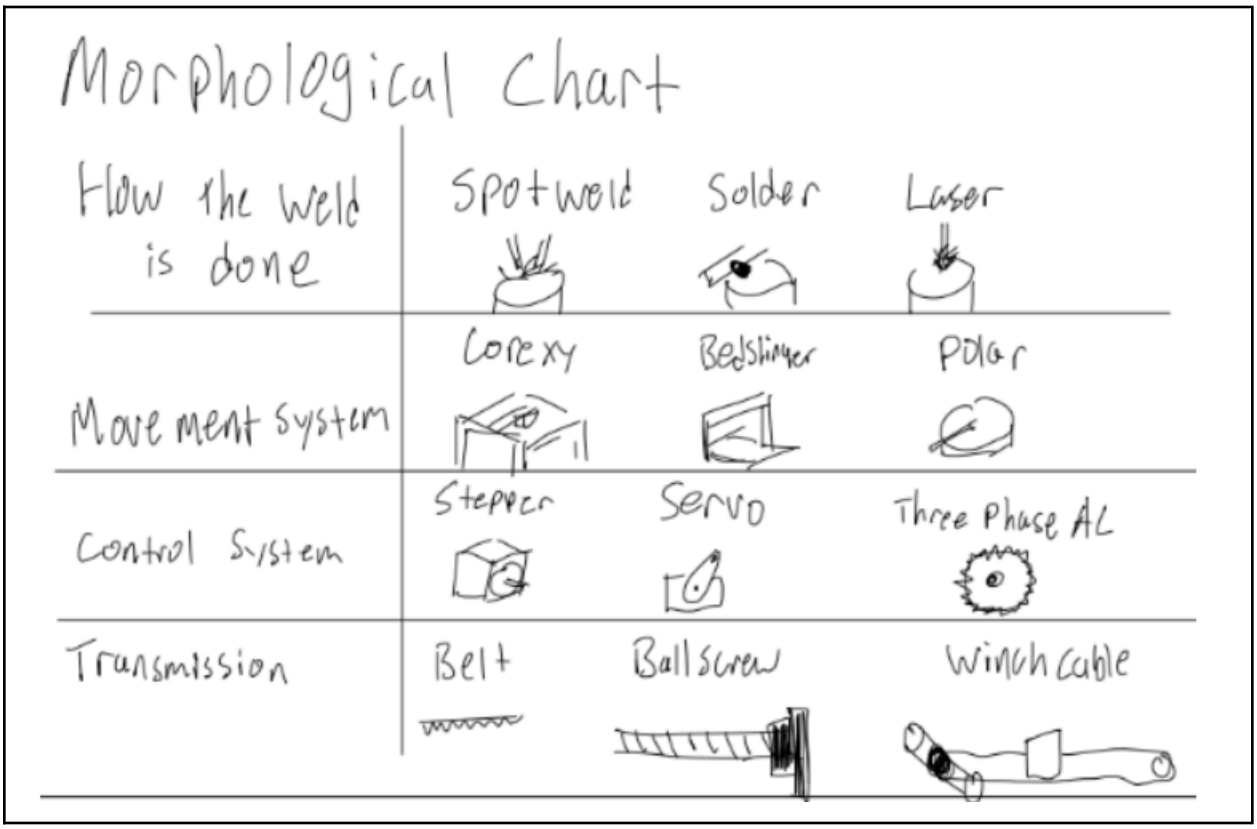
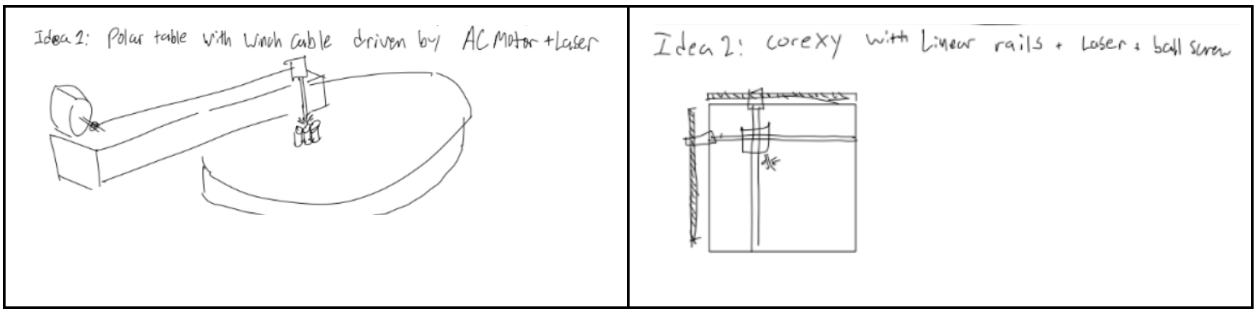


Table A.5.2 Concepts Generated using Morphological Charts





A.6 Engineering Analysis Calculations

A.6.1 Joint Stackup Angular Deviation (continued from section 7.4)

The calculations below were derived from the simplified shoulder bolt and sleeve bearing diagram expressed in **Figure 7.4.2**. The small angle approximation is valid here as angular deviations should not exceed 10 degrees if the joint is assembled correctly.

$tan(\Delta\Theta) = \frac{Bushing\ ID - \frac{Bolt\ OD}{cos(\Delta\Theta)}}{Bushing\ Length}$, $L_{bush} * sin(\Theta) = ID_{bush} * cos(\Theta) - OD_{bolt}$

Small angle approximation: $sin(x) \simeq x,\ cos(x) \simeq 1$

$L_{bush} * x = ID_{bush} - OD_{bolt} \rightarrow x = \frac{ID_{bush} - OD_{bolt}}{L_{bush}}$

x is maximized with large ID of bushing, small OD of bolt, and small length of bushing

$\Delta\Theta = 0.0055276\,rad \simeq 0.3167\,deg$

Next, to calculate the lateral deviation in the link's position, we combined this angular deviation in the XY plane with the link's maximum distance from the center of the sleeve bearing. This was done using the maximum thrust washer and roller thrust bearing thicknesses, as well as half of the sleeve bearing's minimized thickness (derived from the conditions set above for maximum angular deviation) and half of the link's thickness.

Maximum bushing thickness ($\frac{1}{16}" \pm 0.0025"$) and maximum roller thrust bearing thickness ($0.7081"$): $2 * (\frac{1}{16} + 0.0025) + 0.0781 = 0.2081"$

Half of minimum sleeve bearing length and half of link thickness:

$\frac{1}{2} * (1 - 0.005) + \frac{0.25}{2} = 0.6225"$

Total Length: $0.8306"$

Lateral deviation: $tan(0.3167\,deg) = deviation_{lateral} * 0.8306"$

$deviation_{lateral} = 0.8306 * tan(0.3167\,deg) = 0.00459"$

Finally, angular deviation in the end effector introduced by slop in the first set of joints depends on the distance between the pivots. If the top joint deviates inward by 0.00459 inches and the bottom joint deviates outward by 0.00459 inches, angular deviation in the vertically oriented plane equates to $\Delta\Theta = arctan\left(\frac{0.00459}{\frac{1}{2} * d_{J2J}}\right),\ with\ d_{J2J} = vertical\ distance\ between\ joints$

In the doubly-stacked four-bar linkage, there are four places where this angular deviation in the vertical plane can be introduced: once at the lower base pivot, twice at the central joint adapter, and once at the toolhead.

Therefore, the quantity $4 * arctan\left(\frac{0.00459}{\frac{1}{2}*d_{J2J}}\right) \leq 2\ degrees$

$\frac{0.00459}{\frac{1}{2}*d_{J2J}} \leq tan(0.5\ deg)$, $\frac{2*0.00459}{tan(0.5\ deg)} \leq d_{J2J}$, $d_{J2J} \geq 1.05\ inches$

A.6.2 Numerical Calculations for Bearing Selection

AMI Bearings UEF205-16 Specifications:
Designed for 1" Shaft diameter
Maximum RPM: 9000
Dynamic Radial Load Cap, lbs: 2800

$d = 1.05\ inches = 26.67\ mm$
$L = 22\ inches = 558.8\ mm$
$m_l = 0.394\ kg$
$j = 2\ inches = 50.8\ mm$
$m_j = 0.176\ kg$
$a = 3.5\ inches = 88.9\ mm$
$m_e = 1.269\ kg$

$M_{reaction,max} = m_l g * 2 * \left(\frac{L}{2} * cos(15deg)\right) + m_j g * \left(L * cos(15deg) + \frac{j}{2}\right) +$
$m_l g * 2 * \left(\frac{3L}{2} * cos(15deg) + j\right) + g * (2L * cos(15deg) + j + a) = 24Nm$
$F_{radial} = \frac{M_{reaction}}{d} = 933\ N = 210\ lbs < 2800\ lbs$
Safety factor ~ 13.3

Thrust Load Calculations:
$m_l = 0.394\ kg$
$m_j = 0.176\ kg$
$m_e = 1.269\ kg$
$m_{basepivot} = 0.318\ kg$
$F_{thrust,total} = m_{basepivot} + 4 * m_l + m_j + m_e = 3.339\ kg = 7.36\ lbs$
$F_{thrust\ per\ bearing} = 7.36\ lbs\ /\ 2\ bearings = 3.68\ lbs\ per\ bearing$

A.6.3 Full Dataset from Empirical Applied Force Testing

Group Member	Trial 1 Force	Trial 2 Force	Trial 3 Force	Trial 4 Force	Trial 5 Force
1	17.09	14.30	17.24	18.24	18.98
2	15.72	16.2	16.51	17.1	17.8
3	14.9	15.1	16.38	15.4	17.6

Mean force applied: 16.57 lbs
Standard deviation: 1.324 lbs
Estimated range of values ($\pm\ 3\sigma$): $[12.60, 20.54]$ lbs

A.6.4 Sensitivity Analysis of Piston Loading

$p_1 = 14.7\ psi$

$p_2 = p_1 + \frac{F_a}{2\pi * \frac{D^2}{4}}$ (pressure in each piston, F_a is total weld force applied to both electrodes)

$V_1 = s\ *\ \pi\ *\ \frac{D^2}{4}$

$V_2 = \frac{p_1 V_1}{p_2} \rightarrow final\ remaining\ stroke\ length = h_2 = \frac{V_2}{\pi * \frac{D^2}{4}}$

$\%\ compression = \frac{s - h_2}{s}$

$f(F_a) = \frac{s-h_2}{s} = 1 - \frac{\frac{V_2}{\pi * \frac{D^2}{4}}}{s} = 1 - \frac{p_1 V_1}{p_2(\pi s \frac{D^2}{4})} = 1 - \frac{14.7\ psi}{(14.7\ psi + \frac{F_a}{2 * pi * \frac{D^2}{4}})}$

$f\left(F_a = [12.60,\ 20.54]\ lbs\right) = [0.8482,\ 0.9011]$

% Compression for applied forces across the entire expected range all produce significant compression ratios, with little variation.

A.8 Verification Plans

A.8.1 Weld Location Accuracy Verification

1) Place 4 cells in each corner of the 32” x 32” work area.
2) Place 20 cells in randomized intermediate locations.
3) Approach the first cell, orient the end-effector to be properly aligned.
4) Confirm alignment falls within the 0.5 mm radius of tolerance.
5) Repeat for the other 23 locations and confirm they all meet the specification.

A.8.2 Weld Probe Orientation Verification

1) Place 4 cells in each corner of the 32” x 32” work area.
2) Place 20 cells in randomized intermediate locations.
3) Approach first cell, orient the end-effector to be properly aligned with current collector.
4) Place digital level on top of end effector and record deviation from normal to cell.
5) Repeat for the other 23 locations and confirm they all stay within the 2 degree cone of tolerance.

A.8.3 Weld Force Application Verification

1) Place 4 cells in each corner of the 32” x 32” work area.
2) Place 20 cells in randomized intermediate locations.
3) Approach first cell, orient the end-effector to be properly aligned with current collector.
4) With the load cell setup within the end-effector, apply 88N of force from the end effector onto the battery.
5) Verify that the force was reached and that the device is unaffected.
6) Repeat for the other 23 cells and confirm they all pass the test.

A.8.4 Weld Quality Verification

1) Align current collector on singular cylindrical cell.
2) Perform one spot weld onto the singular cylindrical cell.
3) Use a force gauge to pull 25N in the shear direction, do not pull to failure.
4) Use a force gauge to pull 25N in the axial direction, you can pull until failure here.
5) Ensure the weld was able to handle at least 25N in each direction.
6) Repeat for 9 additional weld nuggets and confirm they all could handle the force.

A.8.5 Spot Welding Rate Verification

1) Place a battery pack of at least 10 cells in the work area.
2) Inform the user that they will be performing welds following our standard operating procedure.
3) Do not inform them that they will be timed.
4) Have them begin and record how many welds they are able to perform within one minute.
5) Repeat with two other users and compare results.

A.8.6 Stability Verification

1) Place a battery pack of at least 10 cells in the work area.
2) Place a digital level on the cell surface plane and zero it out.
3) Move that level to the welding device frame surface plane and note the deviation.
4) Adjust the feet on the welding frame to minimize that difference and bring it within the 2 degrees of tolerance.
5) Ensure that this can be done on a variety of surfaces up to 2 cm.

A.8.7 Weld Energy Consistency Verification

1) Using standard manual welding procedure, create the confidence interval by sampling 30 welds using the circuit designed for the new device.
2) Place 12 cells randomly throughout the work area.
3) Align device to within current collector tolerance.
4) Create weld following force specification of 88N.
5) Record data for each of the twelve welds using the circuit design and confirm it falls within a 95% confidence interval.

A.8.8 Ease of Maintenance Verification

1) Have fully assembled end effectors on the playing field.
2) Provide the user with the SOP tool head maintenance section.
3) Have the user disassemble all moving parts of the tool head.
4) Confirm that they are able to do so within 10 minutes.
5) The same thing will be done for the reassembly.
6) Repeat with 2 other users and compare the time differences.

A.8.9 Easy Setup and Use Verification

1) Have a user place the entire battery module into the operating area.
2) Time them and make sure it is able to be done within 60 seconds.
3) Have the user place each necessary current collector depending on the size of the battery packs.
4) Ensure they are able to place each one within 10s.
5) Repeat with two other users.

A.8.10 Circuitry Verification

1) Gather SPICE .lib models for each IC.
2) Recreate the sketched schematics in LTSPICE

3) Generate a waveform of a pulsed square signal with magnitude 9V and width 10 ms. Vary the rise time of the signal from 1µs to 20µs.
4) Observe the output waveform from each circuit. Confirm they match the shape of the input signal with an amplitude lesser than 3.3V
5) Increase the amplitude of the input signal to 12-20V. Ensure that the protection circuits are effective by confirming that the output signal is capped at 3.3V.
6) Activate the current source circuit and verify that the output is 200mA.
7) Check the reading of the 0-50mV sensitivity voltage sensing circuit against varying contact resistance values at the weld probes.
8) Adjust op-amp gain in the 0-50mV circuit if necessary to better match output amplitude to the range of the ADC.

Appendix A.9 Bill of Materials and Manufacturing Plan

A.9.1 Bill of Materials - Purchased Items

Item	Quantity	Source	Catalog Number	Cost	Contact
AWithZ P20B 14.6 kW Battery Spot Welder Foot Pedal Trigger Spot-Welding Electrode Probes (2)	1	Amazon	P20B	$289.99	https://a.co/d/22z5Gve
Tin-Plated Copper Compression Lug	6	McMaster-Carr	6926K324	$48.66	https://www.mcmaster.com/6926K324/
Tin-Plated Copper Compression Lug	2	McMaster-Carr	6926K342	$25.76	https://www.mcmaster.com/6926K342/
Welding Cord	10 ft	McMaster-Carr	7940A81	$89.40	https://www.mcmaster.com/7940A81
T-Slotted Framing Rail	5 ft	McMaster-Carr	47065T102	$43.06	https://www.mcmaster.com/47065T102
UEF205-16 Flanged Bearing	2	AMIBearings	3710T51	$39.98	https://tinyurl.com/3w9yw6k2
M12x1.75 50mm Bolt	4	McMaster-Carr	91290A626	$3.84	mcmaster.com/91290A626
M12x1.75 Hex Nut	4	McMaster-Carr	90591A181	$0.94	mcmaster.com/90591A181
1/4-20 x 0.5in SHCS	2	McMaster-Carr	91251A537	$0.33	https://www.mcmaster.com/91251a537/
1/4-20 Nylon-Insert Locknut	8	McMaster-Carr	90630A110	$1.47	https://www.mcmaster.com/90630A110/
1/4-20 x 0.75 in SHCS	2	McMaster-Carr	91251A542	$0.49	https://www.mcmaster.com/91251a542/
1/4-20 Wing Nut	2	McMaster-Carr	99904A211	$0.20	https://www.mcmaster.com/99904A211/
1/4-20 x 2 in SHCS	2	McMaster-Carr	90044A125	$1.06	https://www.mcmaster.com/90044A125/
5/16-18 x 1.5 in Hex Head Screw	6	McMaster-Carr	92620A587	$5.35	https://www.mcmaster.com/92620a587/
5/16-18 X 2.5 in Hex Head Screw	1	McMaster-Carr	92620A593	$1.15	https://www.mcmaster.com/92620A593/
5/16-18 Thin-Profile Hex Nut	2	McMaster-Carr	94846A030	$0.15	https://www.mcmaster.com/94846A030/
5/16-18 Nylon-Insert Locknut	9	McMaster-Carr	90630A115	$1.86	https://www.mcmaster.com/90630A115/
3/8" Shoulder Screw, 1.75" Shoulder Length	9	McMaster-Carr	91259A630	$21.15	https://www.mcmaster.com/91259A630/
Oil-Embedded Bronze Thrust Bearing	40	McMaster-Carr	5906K565	$45.60	https://www.mcmaster.com/5906K565/
Needle Roller Thrust Bearings	18	McMaster-Carr	5909K25	$58.86	https://www.mcmaster.com/5909K25/

Oil-Embedded 841 Bronze Sleeve Bearing	9	McMaster-Carr	6391K178	$20.88	https://www.mcmaster.com/6391K178/
M4x0.7 18mm SHCS	23	McMaster-Carr	91290A164	$3.76	https://www.mcmaster.com/91290a164/
M4x0.7 30mm SHCS	3	McMaster-Carr	91290A180	$0.62	https://www.mcmaster.com/91290a180/
M4x0.7 Thin-Profile Hex Nut	4	McMaster-Carr	90695A035	$0.15	https://www.mcmaster.com/90695A035/
M6x1 14mm SHCS	4	McMaster-Carr	91290A319	$0.81	https://www.mcmaster.com/6131N36/
M4x0.7 Nylon-Insert Locknut	2	McMaster-Carr	94645A101	$0.27	https://www.mcmaster.com/94645A101/
1/4" Shoulder Screw, 1" Length	1	McMaster-Carr	91259A542	$1.92	https://www.mcmaster.com/91259A542/
10-24 Nylon-Insert Locknut	1	McMaster-Carr	90631A011	$0.05	https://www.mcmaster.com/90631A011/
10-32 x 0.5 in SHCS	12	McMaster-Carr	91251A342	$1.75	https://www.mcmaster.com/91251A342/
Threaded-Hole-Mount Oval Pull Handle	2	McMaster-Carr	1897A56	$11.24	https://www.mcmaster.com/1897A56/
10-32 General Purpose Washer	8	McMaster-Carr	92141A011	$0.19	https://www.mcmaster.com/92141A011/
1/4" Ground Shaft	1	McMaster-Carr	6061K415	9.16	https://www.mcmaster.com/6061K415/
6mm ID 15mm OD Shielded Ball Bearings	4	HIPICCO	696ZZ	9.99	https://a.co/d/etUih7W
High-Speed Sleeve Linear Bearing	4	McMaster-Carr	6673K11	$44.72	https://www.mcmaster.com/6673K11/
External Retaining Ring 0.5" OD	8	McMaster-Carr	9968K22	3.52	https://www.mcmaster.com/9968K22/
Load Cell	1	McMaster-Carr	61313N36	$109.59	
			Total	$897.90	

A.9.2 Bill of Materials - Manufactured Items

	Item	**Quantity**	**Material**	**Manufacturing Methods**
Manufactured Items	Base Plate	1	Aluminum	Waterjet
	Base Pivot	1	Aluminum	Mill + Lathe
	Links	4	Aluminum	Waterjet
	Joiner	1	PETG	3D Printing
	Joint Washers	8	PETG	3D Printing
	End Effector Z Pivot	1	Aluminum	Mill
	End Effector Joint and Z Host	1	Aluminum	Mill

	Z Pivot Host Plate	1	Aluminum	Waterjet
	Handle Mount Plates	2	Aluminum	Waterjet + Mill
	Load Cell Top Plate	1	Aluminum	Waterjet
	Load Cell Cage Plate	1	Aluminum	Waterjet + Mill
	Cage Side Wall 1	1	Aluminum	Waterjet + Mill
	Cage Side Wall 2	1	Aluminum	Waterjet + Mill
	Equalizer Bar Pivot	1	PETG	3D Printing
	Equalizer Bar	2	PETG	3D Printing
	Perimeter Plate	1	Aluminum	Waterjet + Mill
	Angled End Machined Copper Electrode	1	Copper	Mill
	Straight End Machined Copper Electrode	1	Copper	Mill
	Angled End Electrode Adapter	1	ABS GF	3D Printing
	Straight End Electrode Adapter	1	ABS GF	3D Printing
	Angled Adapter Bolt Washer	1	PETG	3D Printing
	Straight Adapter Bolt Washer	1	PETG	3D Printing
	Shunt Container	1	PETG	3D Printing
	Shunt Bolt Retainer	1	PETG	3D Printing
	Welding Wire Sheath	2	PETG	3D Printing

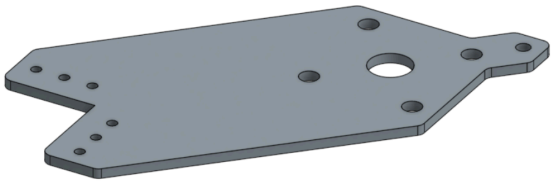
A.9.3 Bill of Materials - Electrical Items

Item	Quantity	Source	Catalog Number	Unit Cost	Cost
Solder Boards	6	Digikey	DKS-SOLDERBREAD-02-ND	$3.19	$19.14
Power Supply	1	Digikey	179-SWI10B-5-NB-P5-ND	$8.57	$8.57
DC Jack wire leads	1	Digikey	839-10-01097-ND	$2.66	$2.66
ferrite bead	1	Digikey	240-2439-1-ND	$0.23	$0.23
100 pico-farad capacitor	10	Digikey	BC2657CT-ND	$0.12	$1.20
10 nano-farad capacitor	10	Digikey	1103PHCT-ND	$0.132	$1.32
Shunt 100 micro-ohm	1	Digikey	WSBSA-.0001-ND	$16.16	$16.16
INA240	1	Digikey	296-48837-ND	$3.81	$3.81
SOIC-DIP Adapter	1	Digikey	1528-1071-ND	$2.95	$2.95
100 - ohm metal film resistor	4	Digikey	BC3564CT-ND	$0.1	$0.40
Shottky diodes	4	Digikey	497-2499-1-ND	$0.1	$0.40

1S4E	2	Digikey	3182-1S4E_0505S1.5U-ND	$1.3	$2.60
4.7 micro-farad capacitor	2	Digikey	445-FK24X7R1E475KR000-ND	$0.45	$0.90
10 micro-farad capacitor	2	Digikey	445-173132-1-ND	$0.53	$1.06
500-ohm resistor	1	Digikey	13-MFR25SFBE52-500R-ND	$0.1	$0.10
ISO224	2	Digikey	296-52315-1-ND	$15.66	$31.32
0.22 micro-farad capacitor	2	Digikey	445-181744-ND	$0.28	$0.56
OPA320	4	Digikey	296-29480-1-ND	$2.47	$9.88
SOT23-6 to DIP adapter	4	Digikey	1568-00717-ND	$1.25	$5.00
10 kilo-ohm resistors	10	Digikey	13-MFR-25FRF52-10KCT-ND	$0.039	$0.39
LT3092	1	Digikey	505-LT3092ETS8#TRMPBFCT-ND	$6.4	$6.40
SOT23-8 to DIP adapter	1	Digikey	PA0089-ND	$3.19	$3.19
10 ohm resistor	1	Digikey	A105948CT-ND	$0.1	$0.10
1 ohm resistor	1	Digikey	BC3578CT-ND	$0.1	$0.10
20 kilo-ohm resistor	2	Digikey	13-MFR-25FRF52-20KCT-ND	$0.1	$0.20
MOSFET N-CH 60V 500MA	3	Digikey	TN0606N3-G-ND	$1.06	$3.18
INA333	1	Digikey	296-23564-1-ND	$4.54	$4.54
VSSOP8 to DIP adapter	1	Digikey	PA0042-ND	$3.19	$3.19
100 kilo-ohm resistor	1	Digikey	13-MFR-25FRF52-100KCT-ND	$0.1	$0.10
3.3 kilo-ohm resistor	1	Digikey	13-MFR-25FTE52-3K3CT-ND	$0.1	$0.10
300 ohm resistor	10	Digikey	BC3491CT-ND	$0.084	$0.84
2.2 micro-farad capacitor	10	Digikey	445-173138-1-ND	$0.323	$3.23
				Total	$133.82

A.9.4 Manufacturing Plans

Base Plate



Create a DXF file of the base plate's 2D features in OMAX layout software. Obtain ¼"-inch aluminum plate and use a waterjet machine to cut out the profile of the base plate.

Base Pivot



Perform a rough cut of 1" x 1" aluminum stock to obtain a piece approximately 8.25 inches in length. Use the four-jar chuck on the lathe to turn down 4 inches of the length of the piece to a 1" final diameter. Move the workpiece to the mill, and perform two 0.5" drilling operations on the square face according to the engineering drawings, with a 3" separation between them.

Links



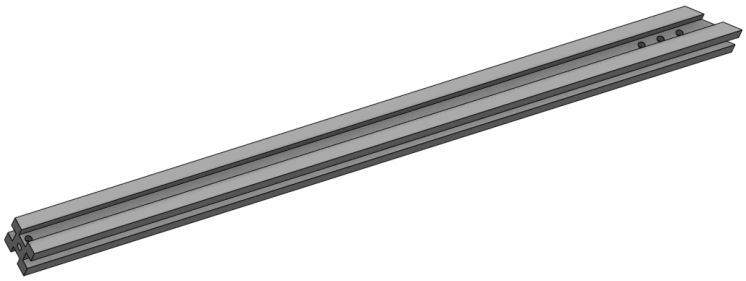
Create a DXF file of the link's 2D features in OMAX layout software, replicating it four times and organizing it so that it fits on the available stock. Obtain a piece of ¼"-inch aluminum plating that is at least 35" x 8" and use a waterjet machine to cut out the profile of links four times.

Flange Bearings



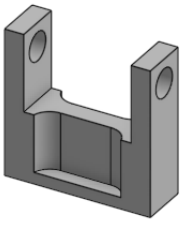
Mount the flange bearings in the mill and use a dial gauge to center the mill around each of the four holes. Once centered, load a 12mm drill bit into the mill and drill out all four holes to allow the M12 bolts to fit properly.

T-Slot Extrusion



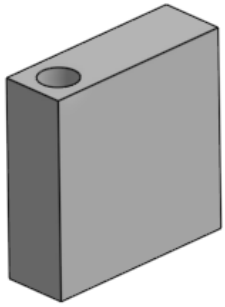
Using the horizontal band saw, cut two 28” pieces of T-slot extrusion from the available stock. Use a table saw with an adjustable cut angle to slice off material at a 45-degree angle, starting at one corner of one end of the 28” pieces.
Mount the resulting shape in the mill and zero the mill against the flat side of the extrusion. Drill out the four 0.257” diameter holes. Tap the three holes closest to the angled cut for 5/16”-18 bolt threads.

End Effector Z Pivot

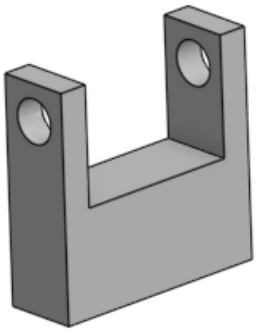


Use a horizontal band saw to cut out a piece of aluminum stock that is oversized to the Z Pivot’s final dimensions. Use a shell mill at 1000 RPM to square off all six sides of the piece, and subsequently bring it down to its outer dimensions of 1.906” x 1.913” x 0.625”, consistently measuring with a micrometer to ensure dimensional compliance. Flip the mounting position in the mill such that the 1.913” side dimension is horizontal, and the side of the prism with the largest surface area is facing you. Zero the mill off the back right corner of the prism, and use a

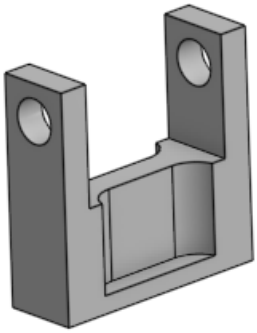
⅜” drill bit to drill all the way through the part from top to bottom. The workpiece should look like this:



Next, rotate the workpiece 90-degrees clockwise such that the hole runs horizontally. Zero the mill against the back right corner again, and begin making passes with a 4-flute ½” end mill to remove the material between the two ends of the pivot component. The workpiece should look like this:



Use the same end mill to create the link clearance cutouts in the sides of the bulk body of the pivot. Now the workpiece should look like this:

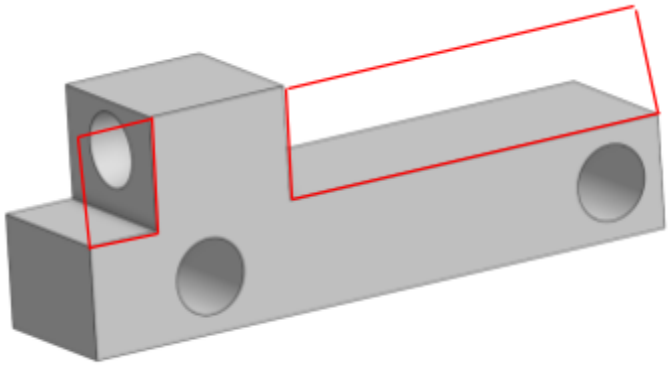


Flip the workpiece upside down from this position, zero against the back right corner once more, and drill four #30 20mm deep holes for the M4 bolts. Tap all of them to full depth for M4x0.7mm threads.

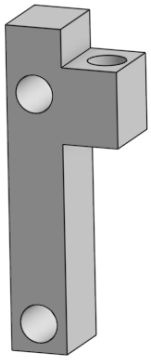
End Effector Joint and Z Host

Use a horizontal band saw to cut out a piece of aluminum stock that is oversized to the joint’s final dimensions. Use a shell mill at 1000 RPM to square off all six sides of the piece, and

subsequently bring it down to its outer dimensions of 1.000” x 4.250” x 1.500”, measuring with a micrometer after each pass to ensure dimensional compliance. With the workpiece mounted such that the 4.25” dimension lays from left to right and the 1.5” dimension from front to back, zero the mill against the back right corner and drill out the two joint holes using a 0.5” drill bit. Rotate the workpiece towards the user such that the 4.250” dimension still lays left to right, but the 1.5” dimension now runs from bottom to top, with the drill holes closer to the vice. Zero the mill’s X-axis off of the piece’s right surface. With a 4-flute 0.5” end mill, make passes to remove the material colored in the image below. The critical dimension here is the length of the remaining section that will eventually contain the hole.



Rotate the workpiece 90 degrees clockwise so it now sits like this:



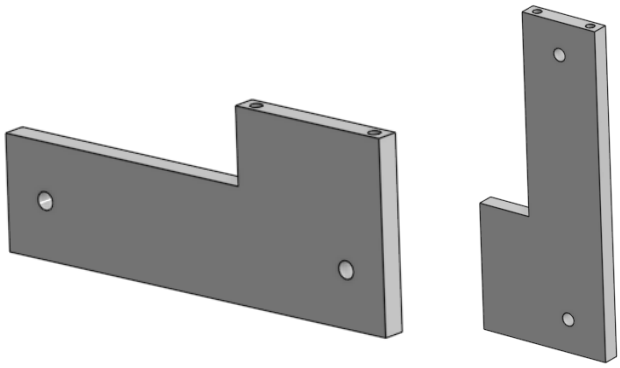
Zero the mill off the back left corner, and use a 0.5” end mill to drill the hole through the remaining stock on the right side of the workpiece.

Z Pivot Host Plate

Create a DXF file of the host plate’s 2D features in OMAX layout software. Obtain ¼” aluminum plate that can fit the part’s dimensions, and use a waterjet to cut the plate’s profile.

Handle Mount Plates

Create a DXF file of the handle mount plate’s 2D features in OMAX layout software. Obtain ¼” aluminum plate that can fit the combined dimensions of two parts, and use a waterjet to cut the profile of two plates. Mount each plate in the mill afterwards, in the following two orientations (order does not matter):



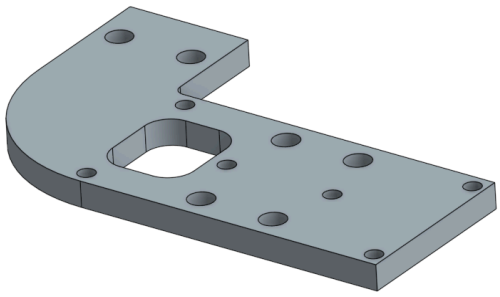
After re-orienting, ensure that the mill is still zeroed to the back right corner of the plate's upward-facing face. On each face, use a #30 drill bit to drill the two holes for the M4 bolts. Tap these holes to full depth for M4x0.7mm threading.

Load Cell Top Plate

Create a DXF file of the top plate's 2D features in OMAX layout software. Obtain ¼" aluminum plate that can fit the dimensions of the part, and use a waterjet to cut the profile of the plate.

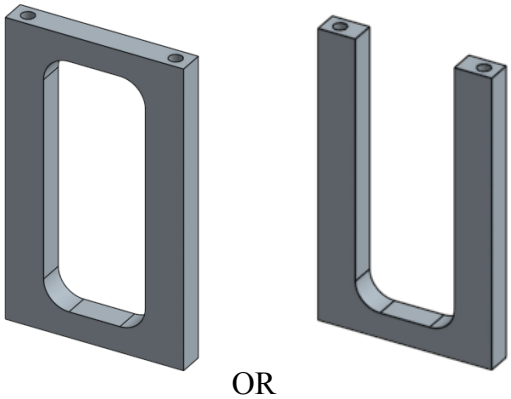
Load Cell Cage Plate

Create a DXF file of the cage plate's 2D features in OMAX layout software. Obtain ¼" aluminum plate that can fit the dimensions of the part, and use a waterjet to cut the profile of the plate. Mount the plate in the mill as shown below, zero it off on the back right corner, and use a 0.257" reamer at 100 RPM to increase the size of the 0.250" holes that were waterjetted.



Cage Side Walls 1 and 2

Create a DXF file of the side wall plates' 2D features in OMAX layout software. Obtain ¼" aluminum plate that can fit the combined dimensions of both parts, and use a waterjet to cut the profile of the two different plates. Mount the first plate in the mill in the orientation shown below, and use a jaw stop to mark the corner whereby each successive re-placement of the plates can be done without losing the zeroed-out position of the mill.

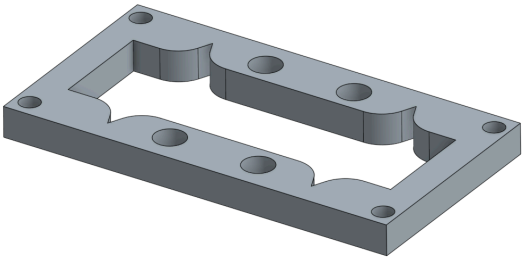


OR

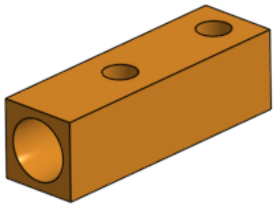
Use a #30 drill bit to drill two 20mm deep holes in the top side according to the dimensions marked in the drawings. Flip the part 180 degrees around the mill's y-axis and repeat the process, ensuring that the part is still pressed against the jaw stop's marked location. Tap all holes created to full depth for M4x0.7mm thread.

Perimeter Plate

Create a DXF file of the perimeter plate's 2D features in OMAX layout software. Obtain ¼" aluminum plate that can fit the dimensions of the part, and use a waterjet to cut the profile of the plate. Mount the plate in the mill as shown below, zero it off on the back right corner, and use a 0.257" reamer at 100 RPM to increase the size of the 0.250" holes that were waterjetted.



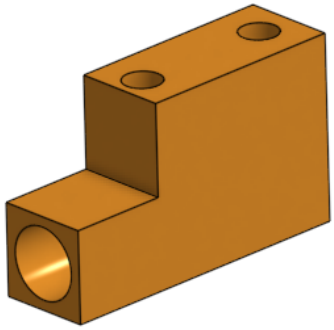
Angled End Machined Copper Electrode



Use a horizontal band saw to cut out a piece of aluminum stock that is oversized to the copper electrode's final dimensions. Use a shell mill at 1200 RPM with very small pass depths (0.030" max) to square off all six sides of the piece, and subsequently bring it down to its outer dimensions of 0.400" x 0.400" x 1.349", measuring with a micrometer after each pass to ensure dimensional compliance. Mount the long face of the piece against the jaws in the horizontal

orientation shown above, zero the mill against the back right corner, and use a #19 drill bit to create the two holes for the M4 bolts that will be traveling through this piece. Rotate the stock 90 degrees around the mill's y axis, and zero the mill off the back right corner of the workpiece. Use a 5/16" drill bit to drill a 10mm deep hole in the small face on the top of the workpiece, careful not to cut into the cylindrical surface of the M4 clearance holes that had just been drilled.

Straight End Machined Copper Electrode



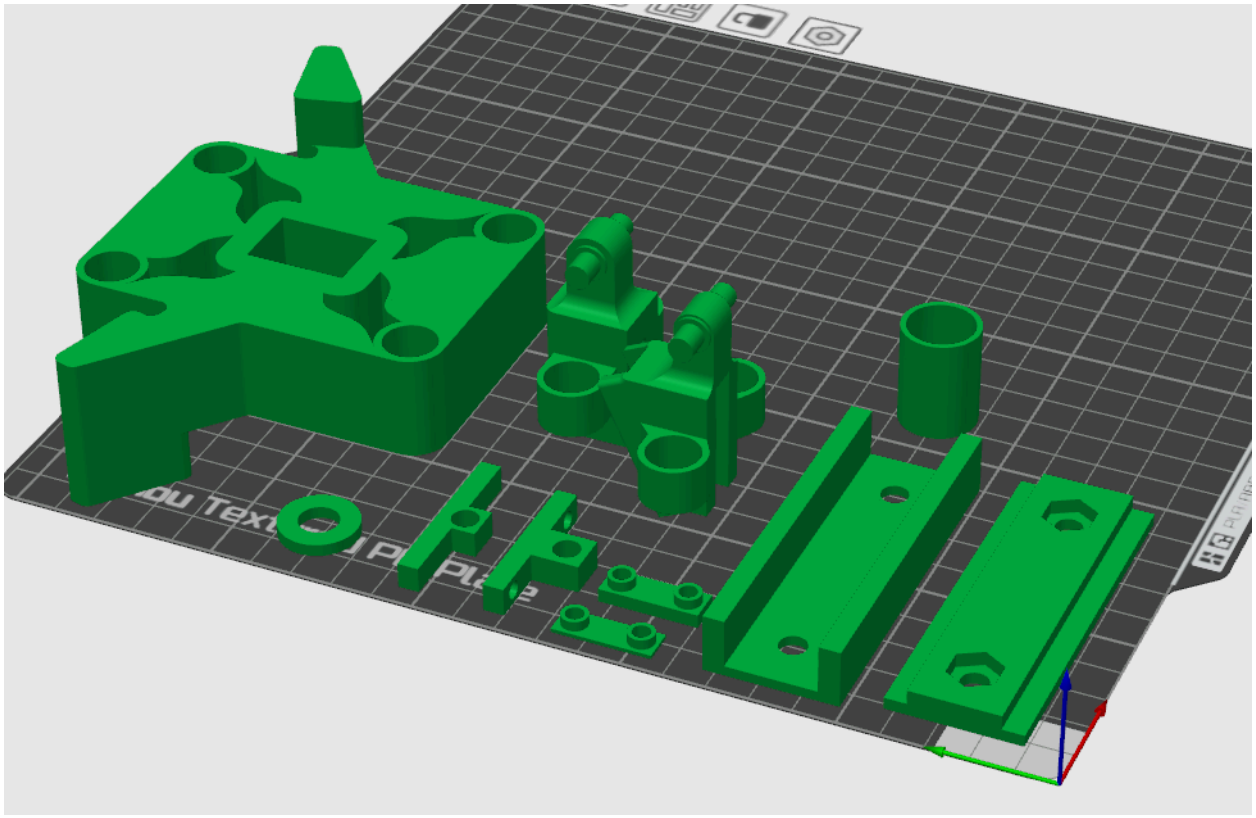
Use a horizontal band saw to cut out a piece of aluminum stock that is oversized to the copper electrode's final dimensions. Use a shell mill at 1200 RPM with very small pass depths (0.030") to square off all six sides of the piece, and subsequently bring it down to its outer dimensions of 0.800" x 0.400" x 1.349", measuring with a micrometer after each pass to ensure dimensional compliance. Mount the long face of the piece against the jaws in the orientation shown above, zero the mill against the back right corner, and use a #19 drill bit to create the two holes for the M4 bolts that will be traveling through the piece. Switch the cutting tool to a 0.5" 4-flute end mill, and increase the speed to 1200 RPM. Utilizing very low chip load, remove the material above the future large hole location until a depth of 0.400" has been reached. The critical dimension of this feature is the resulting length of the "box" encasing the circular feature, which should be within 0.005" tolerance of 0.400".

¼" Ground Shafts



Mount the ground shaft in the four-jar lathe chuck with a protective cloth wrapped on the surface. Use a dial gauge to accurately adjust the chuck until the shaft is spinning in a centered fashion. Use a #21 drill bit to drill out a hole approximately 0.75" deep. Tap this hole using the lathe's drill chuck for 10-32 threads. Repeat this process across 4 shafts, once per side for a total of 8 repetitions.

3D-Printed Components (Print Orientation on a Bambu P1S):

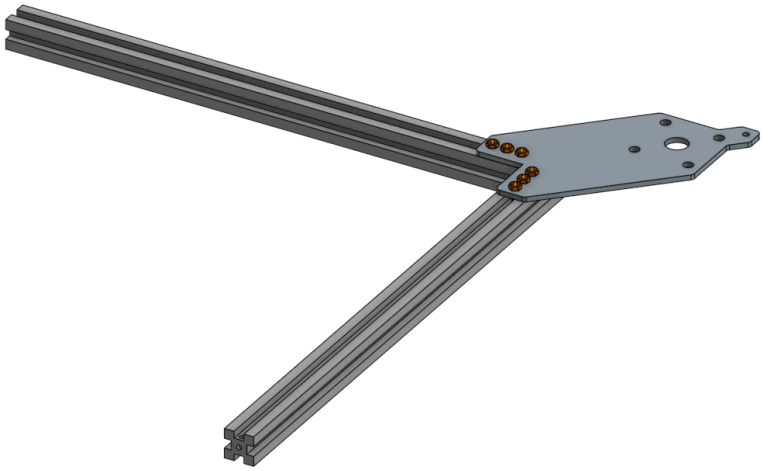


It is recommended to print the Joiner component with 4 wall layers and with at least 50% infill. The equalizer bars and the equalizer bar pivots should be printed with 4 wall layers and 100% infill. The angled end and straight end electrode adapters should be printed with 3 wall layers and 50% infill. All other components are non structural and should be printed with default settings. Enable tree supports to enable printing of the overhangs in the joiner and the two electrode adapters.

A.9.5 Assembly Plans

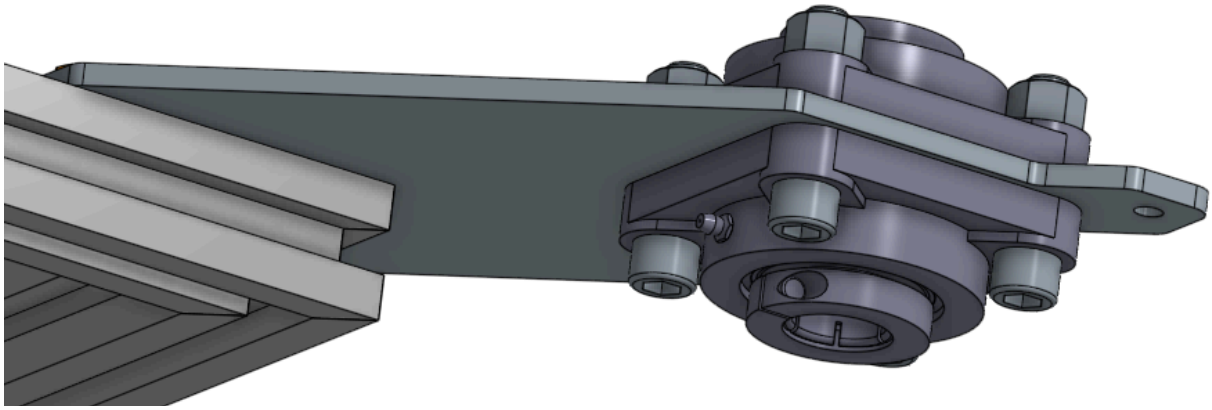
Step 1: Assemble Rigid Base Subassembly

1. Use the six 5/16”-18 x 1.5” screws to join the base plate and the two t-slotted aluminum extrusions.

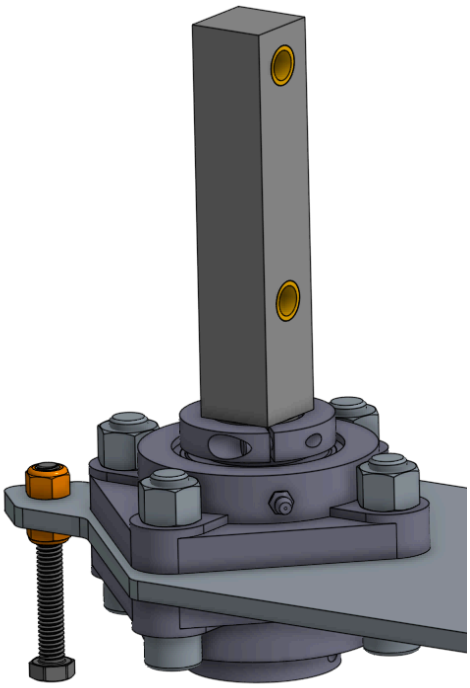


\

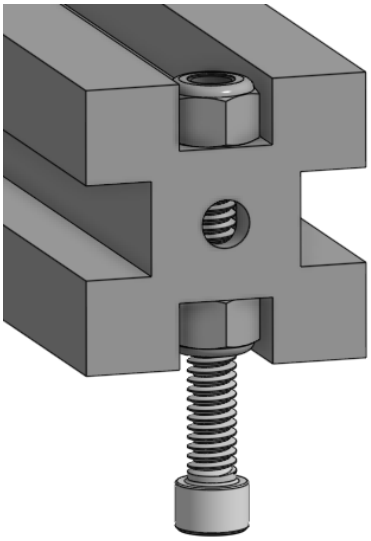
2. Mount the two flanged spherical bearings using the four M12 bolts and M12 nuts.



3. Use an arbor-press to press-fit two 1” oil-embedded sleeve bearings for ⅜” shaft diameters into the two holes drilled through the base pivot part. Insert the base pivot through both spherical bearings and use an allen key to lock the concentric lock collars. Insert a 5/16”-18 x 2.5” screw through the height adjustment hole at the tip of the base plate and secure it with two nuts.

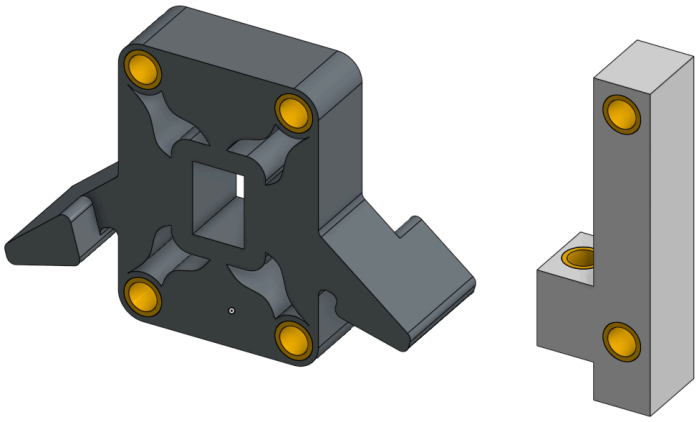


4. On each end of the aluminum extrusion, affix one of the ¼”-20 x 2” screws using two ¼”-20 lock nuts, one on each side of the central rail.

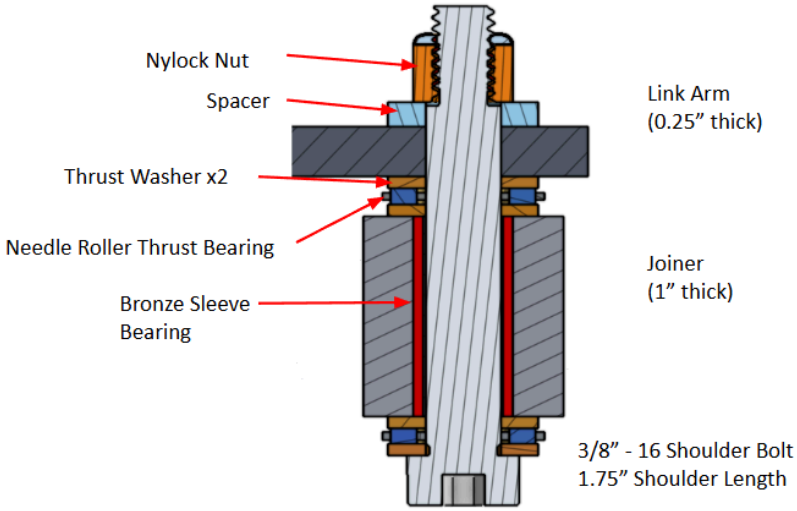


Step 2: Assemble Link Arms and Joints

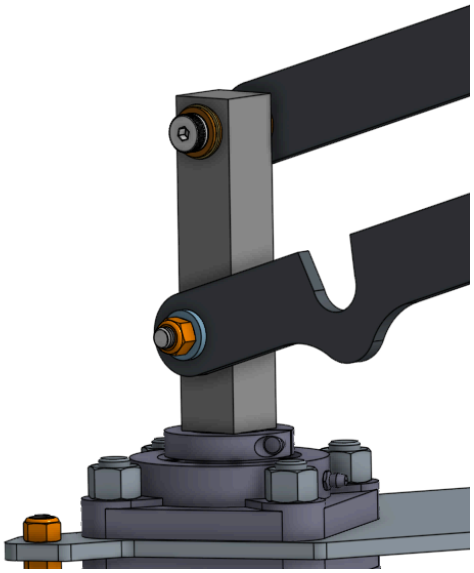
1. Use the arbor press again to press-fit the 1” oil-embedded sleeve bearings into all four bearing holes on the Joiner and End Effector Joint and Z Host components, as seen below.



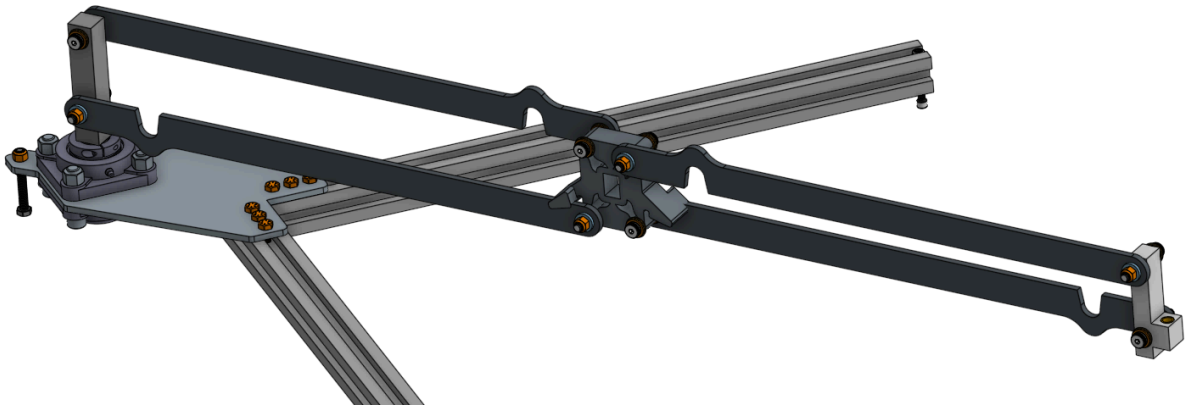
2. Follow the pictured joint stackup to assemble the 8 joints that comprise the four-bar linkage. Orient the links such that the links alternate which side of the joining components they are mounted on, and such that when the linkage is raised nearly fully vertical, the machined gaps encase the screw head of the other link that is attached to the same base component.



For example, on the base pivot joints, assemble them like so. When the lower arm rotates upwards, the machined gap will encase the screwhead of the upper joint instead of causing interference.



3. Depending on the position your linkage is in, it should look something like this when fully extended.



Step 3: Modification of Stock Electrode Probes

Repeat this process for each of the two spot-weld electrode cables that come with the AWithZ P20B spot welding kit.

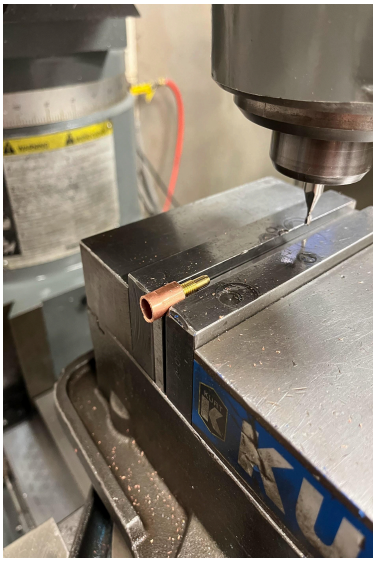
1. Use a razor blade to cut into the grips of the electrodes on the probe side of each welding wire that comes with the AWithZ P20B spot welder.



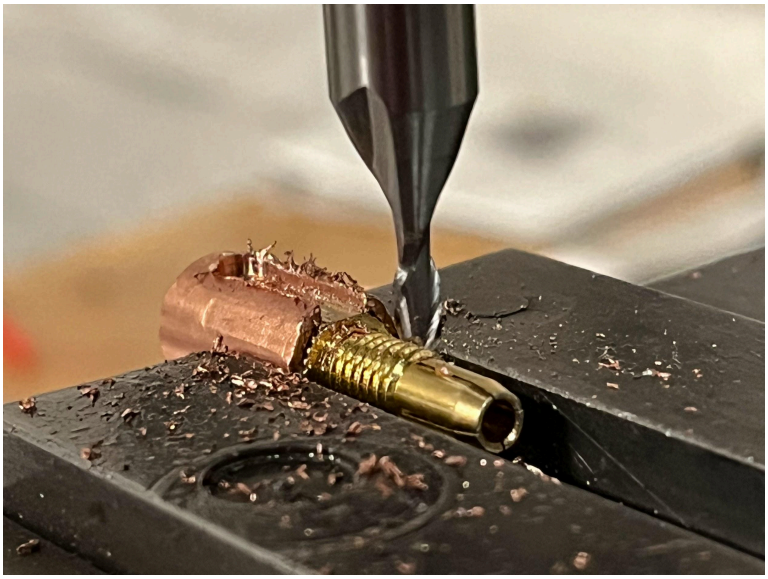
2. Pry out the copper tube that lies inside. Bring it to a band saw or other machine capable of cutting through copper and make a cut at least 20 mm from the beginning of the copper on the probe-side of the welding wire.



3. Mount the small end in the mill like so, and utilize a 0.25” end mill at high speeds (>1500 RPM) to chip away carefully at the material holding the copper tube to the bronze threaded electrode holder. Once the copper is broken through and the bronze is visible, stop milling and remove the electrode tip from the vice. Use a pair of needle nose pliers or a similar tool to pry away the copper tube from the bronze piece. Discard the copper.







4. You should now have the bronze piece free from the copper tubing and wire, as shown below. Gather the hydraulic crimpers and your machined copper blocks, and insert the bronze piece into the machined copper block of your choice. Use the hydraulic crimper, with a 2/0 AWG die installed, to crimp the copper surrounding the 5/16” diameter hole that was drilled previously around the bronze tip, locking it in place. The process is illustrated below.

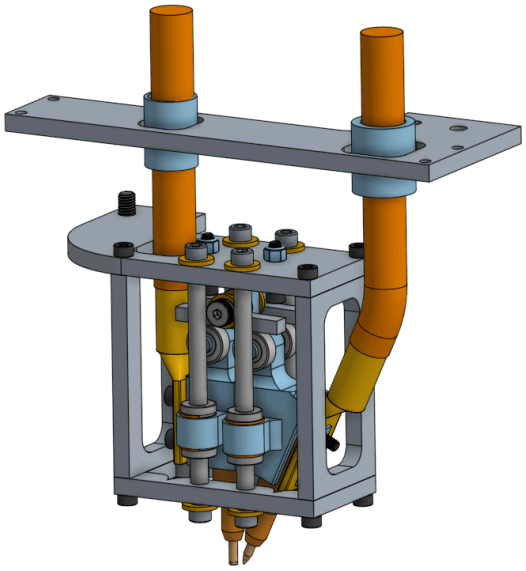




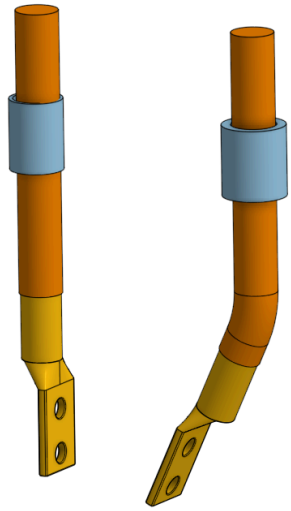


5. Insert the copper probe and the retaining nut, then tighten. Repeat this process for the other electrode, then move onto the end effector assembly. Be sure to save the welding cables, they will be needed later.

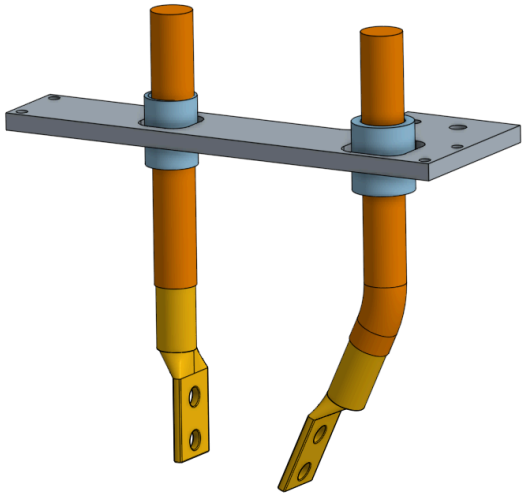
Step 4: Assemble End Effector Cage



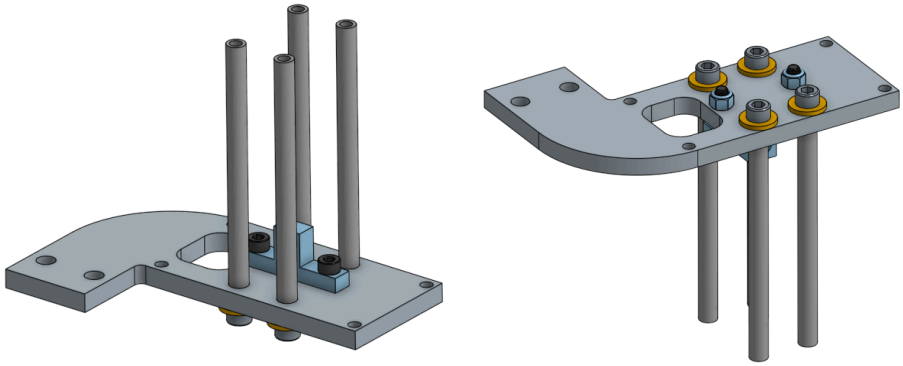
1. Splice compression lugs onto welding wires. Cut the 10-ft welding wire into two 5-ft segments using a high-strength cable cutter. Use a razor blade to remove the insulation on both ends of both segments. Slide a welding wire sheath onto one end of each wire segment, letting it sit 3-4 inches from the tip. For each segment, take the bare copper end closest to the wire sheath and insert it into the 2-hole compression lug. Use a hydraulic crimper with a 2/0 AWG die to compress them together. You should end up with two components that look like this. The wires would continue after the truncated ends in the photo below.



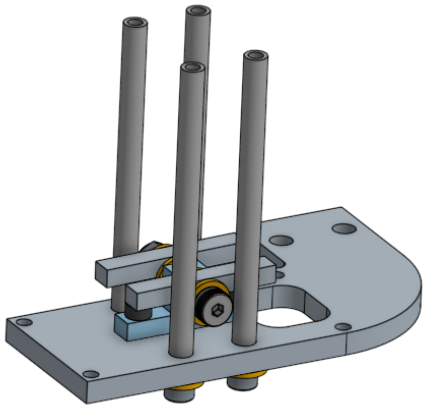
2. Slide these two long wires through the gaps in the load cell top plate.



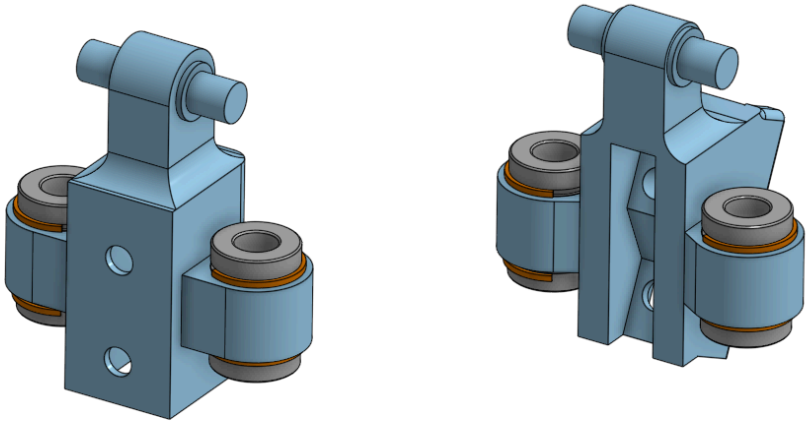
3. Begin to assemble the cage by mounting the equalizer bar pivot onto the load cell cage plate as shown, using two M4x18mm screws and two M4 nylon locknuts. Take the four ground shafts and thread a 10-32 screw through a #10 washer and into the shaft on one end.



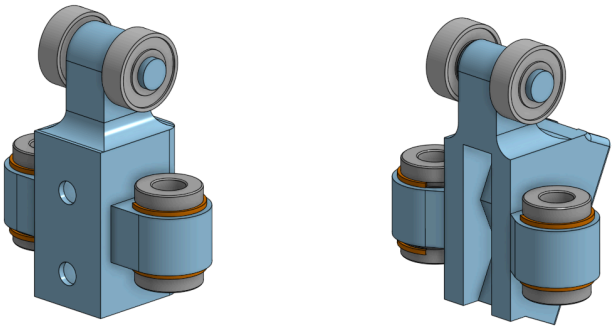
4. Add the ¼” shoulder screw by passing it through a thrust washer, one equalizer bar, a second thrust washer, the equivalizer bar pivot, a third thrust washer, the second equalizer bar, and a fourth thrust washer, before screwing it into a 10-24 nylon locknut.



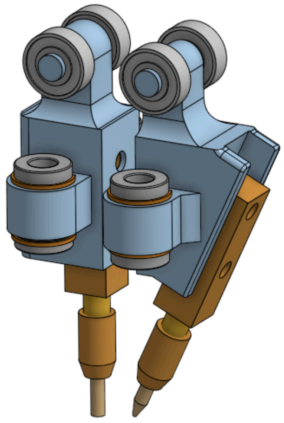
5. Begin a second assembly on the side for both the angled electrode adapter and the straight electrode adapter. Bring together the following components in the manner shown below:
    a. Straight end electrode adapter
    b. Angled end electrode adapter
    c. Straight end machined copper electrode
    d. Angled end machined copper electrode
    e. 2x Compression lugs from welding wire segments
    f. Straight end adapter bolt washer
    g. Angled end adapter bolt washer
    h. 3x M4x30mm bolts
    i. 1x M4x18mm bolt
    j. 4x M4x0.7mm Thin-Profile hex nuts
    k. 4x High-Speed Linear Slide Bearings
    l. 8x Retaining Rings
    m. 4x Ball Bearings
6. First, use the arbor press to insert the linear slide bearings into the straight end electrode adapter and angled end electrode adapter. Use a careful amount of force to avoid breaking the plastic. Place the retaining rings in the outermost slots on the bearings, as shown.



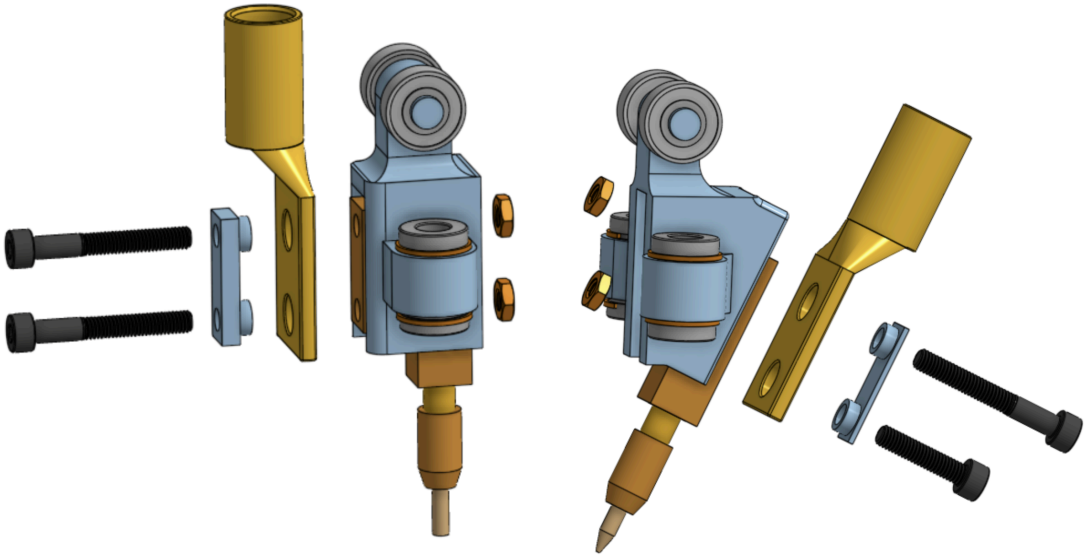
7. Press the ball bearings onto the cylinders on the upper sections of the electrode adapters, as shown. Be sure that they can spin freely.



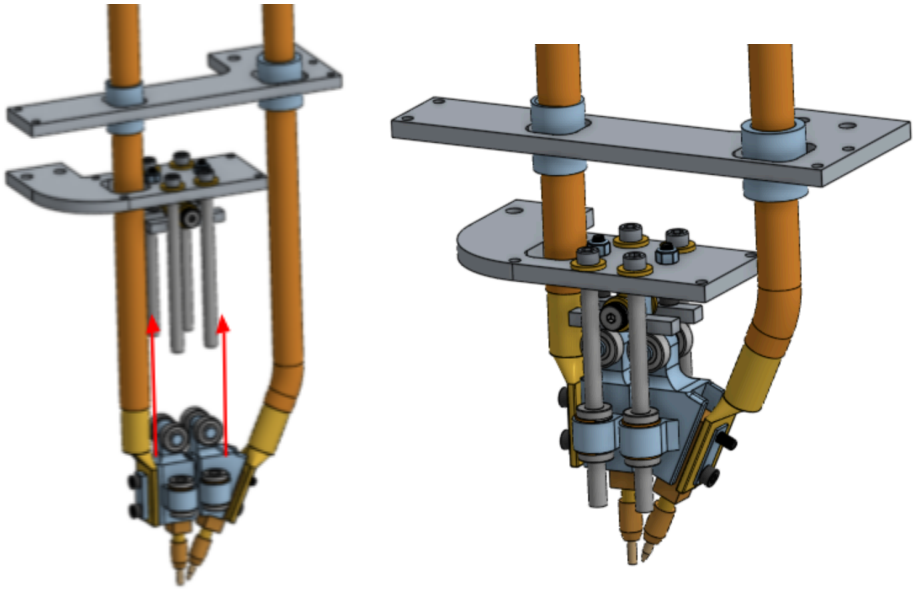
8. Insert the machined copper ends with the crimped bronze threaded electrode holders.



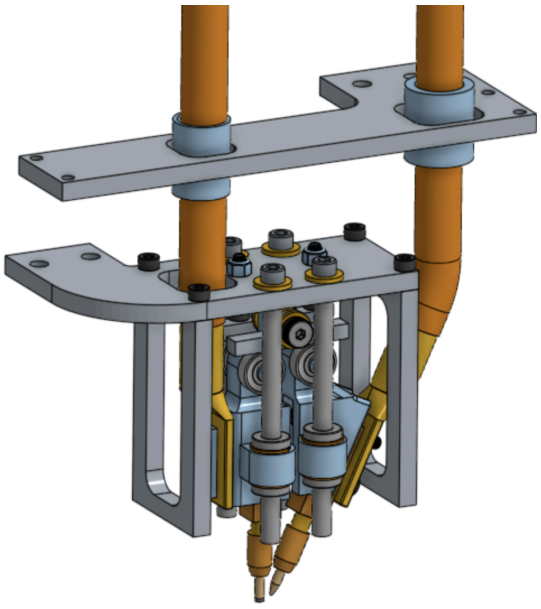
9. Draw the straight end welding wire through the load cell cage plate's wire clearance hole. Bring the two electrode adapter assemblies towards the rest of the end effector parts, and use the M4 bolts and the adapter washers for each type of electrode adapter to join the copper electrode adapters with the 2-hole compression lugs. The welding wire that has gone through two plates by the time it reaches the copper electrodes should be mated to the straight end electrode adapter, while the other welding wire segment should be mated to the angled electrode adapter components.



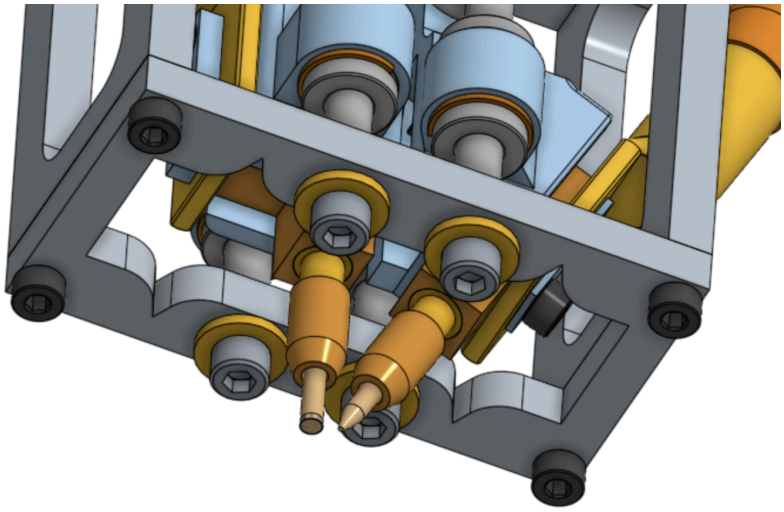
10. Once the M4 screws are tightened down, slide each electrode assembly onto the ground shafts until they make contact with the equalizer bars. Test the assembly for smoothness of linear motion. It should not take more than approximately 2 pounds of force to move the electrode assembly along the shafts. By this point, the entire assembly should look similar to the picture below.



11. Attach end effector side walls 1 and 2 to the load cell cage plate using four M4x18mm screws.

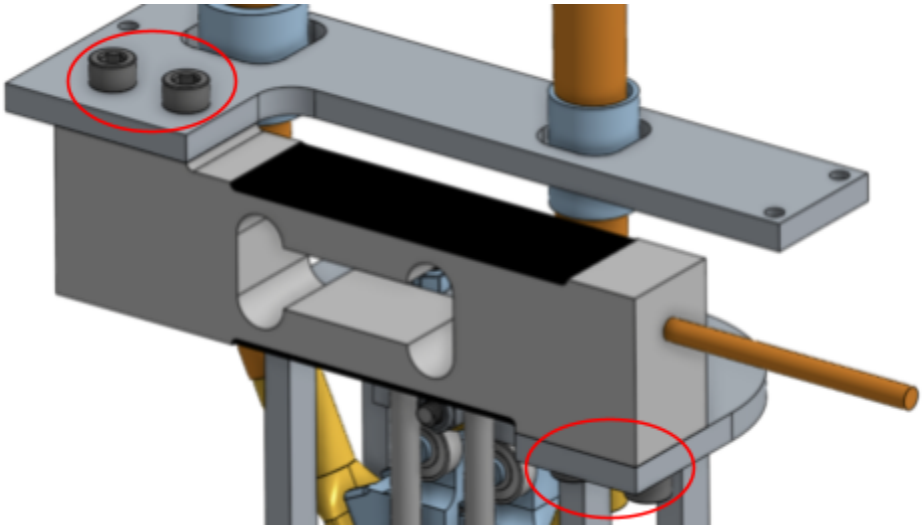


12. Slide the perimeter plate onto the ground shafts and secure it using four M4x18mm screws. Also secure the ground shafts using four 10-32 screws and 4 #10 washers.

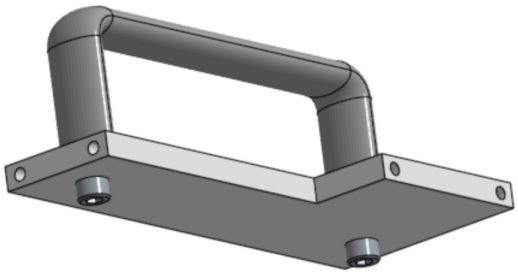


Step 5: Assemble End Effector Overarching Structure

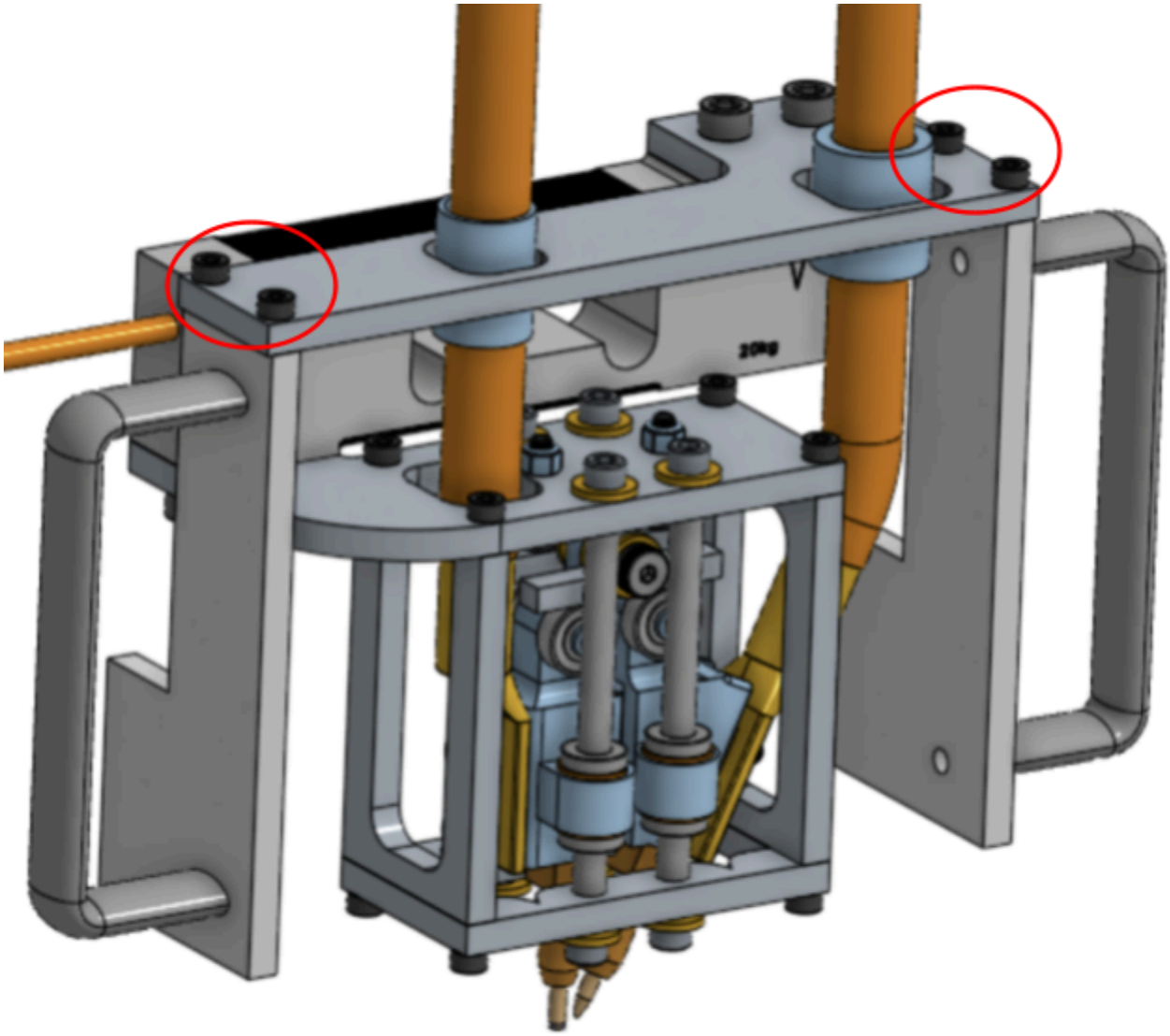
1. Join the load cell cage plate to the load cell using two M6 x 14mm screws. Join the load cell top plate to the load cell using two M6 x 14mm screws.



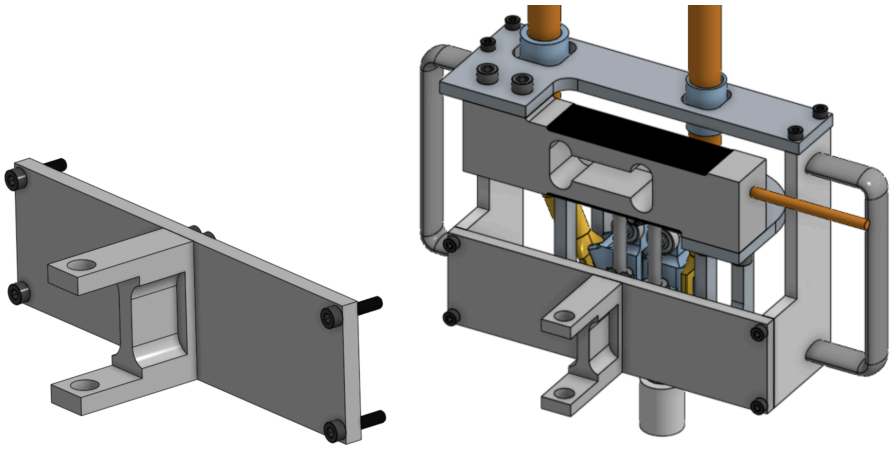
2. Attach the handles to the handle point plates using two 10-32 screws per handle.



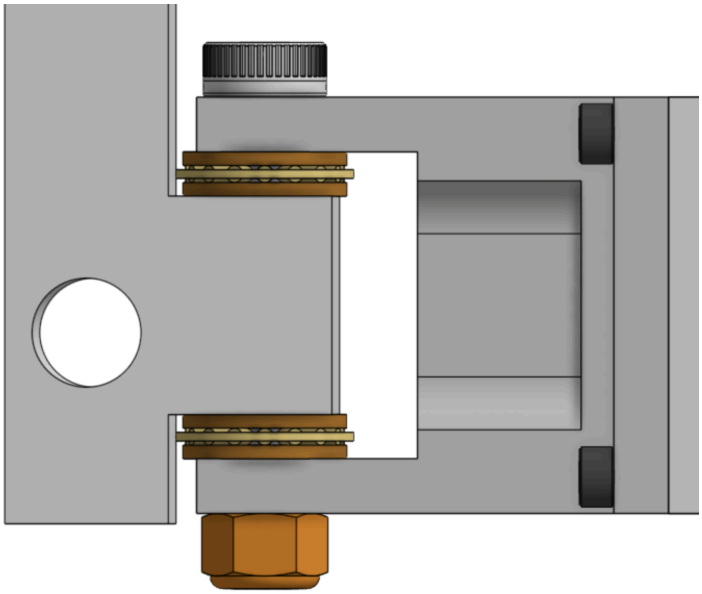
3. Attach the handle plates to the load cell top plate using four M4x18mm screws total.



4. Attach the end effector Z pivot to the Z pivot host plate, and attach it to the rest of the end effector assembly.

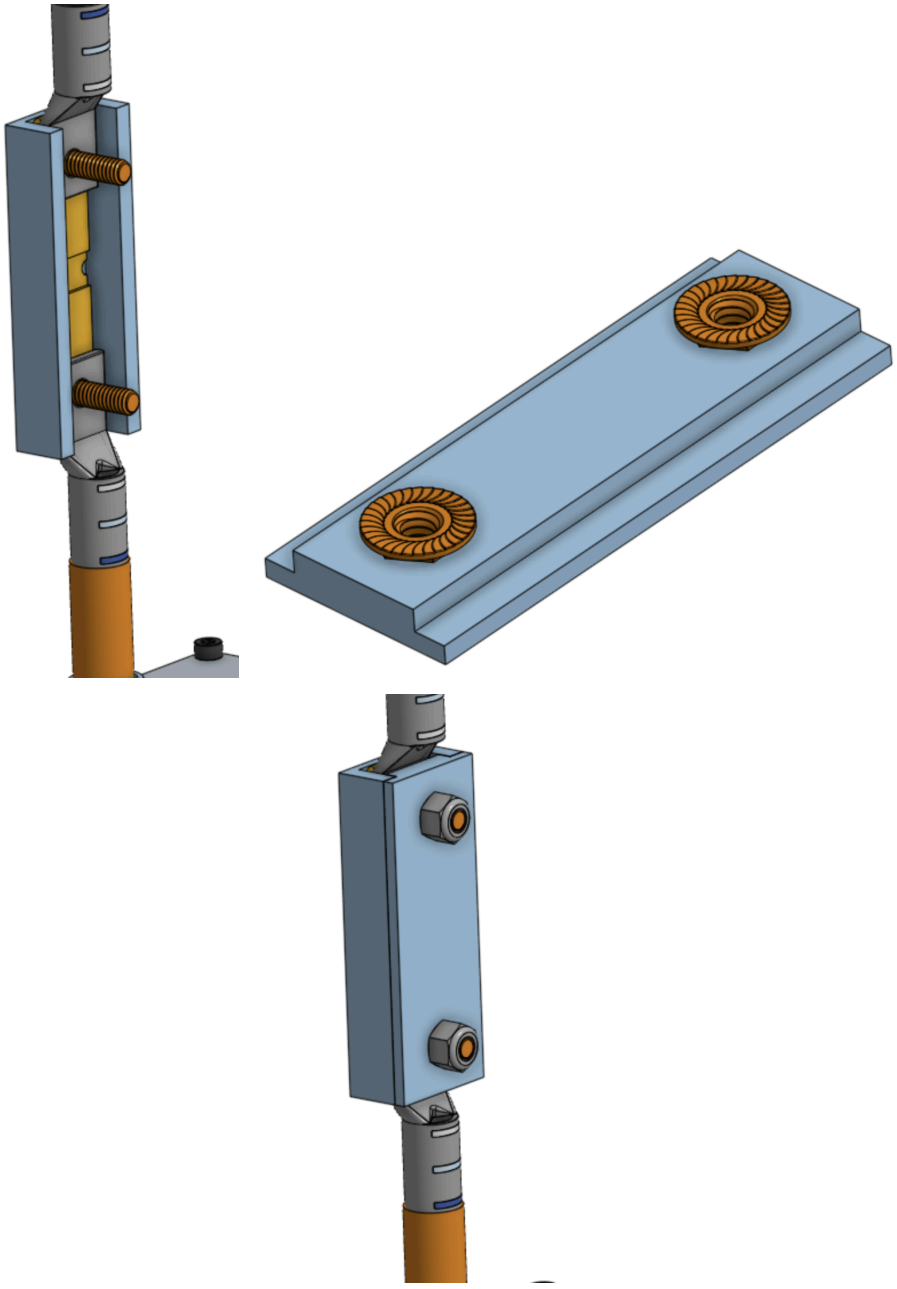


5. Assemble the Z pivot joint using the following stackup, also pictured below:
    a. ⅜”shoulder screw
    b. End Effector Z Pivot
    c. Oil-Embedded Thrust Washer
    d. Needle Roller Thrust Bearing
    e. Oil-Embedded Thrust Washer
    f. End Effector Joint and Z Host
    g. Oil-Embedded Thrust Washer
    h. Needle Roller Thrust Bearing
    i. Oil-Embedded Thrust Washer
    j. End Effector Z Pivot
    k. 5/16”-18 Nylon Locknut



Step 6: Assembly of Current Sensing Hardware

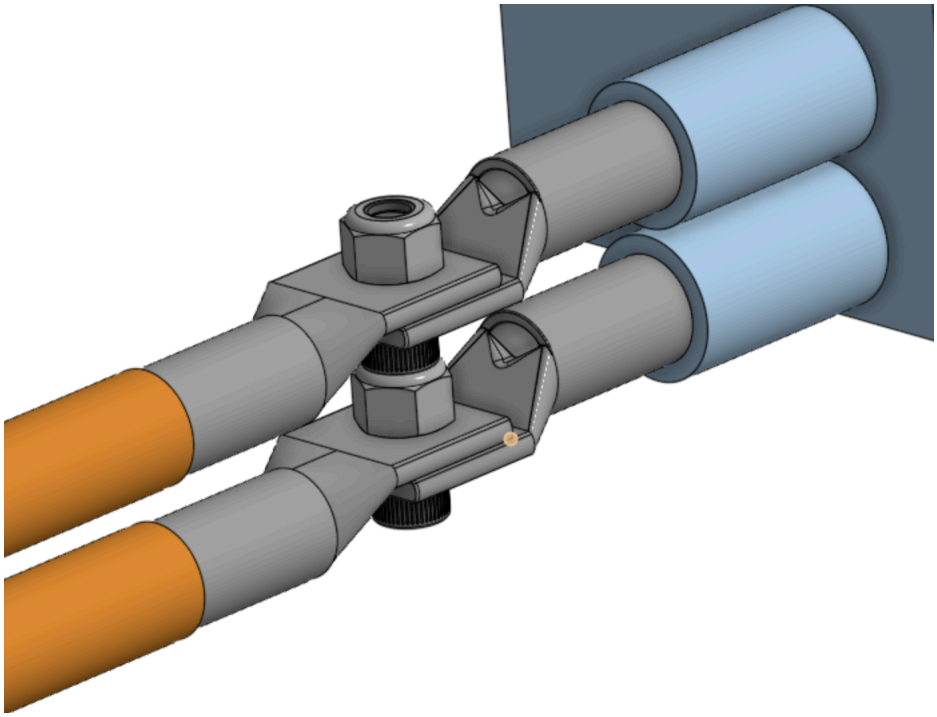
1. Use a sharpie to mark a location on the straight end welding wire that is approximately 4 inches above the surface of the load cell top plate. Cut the welding wire here, and use a cutting instrument to strip the insulation on both sides of the cut. Use the hydraulic crimper to attach a single-hold compression lug to the wire on both sides of the cut. Place the 100 micro-Ohm shunt into Shunt Casing 1, and slide two ¼”-20 x 0.75” screws into place. Then, place two ¼”-20 wing nuts in the Shunt Casing 2’s hexagonal recesses, slide it into place on the two ¼”-20 screws, and tighten the screws hard. Further secure the shunt by tightening two ¼”-20 nylon locknuts onto the Shunt Casing 2, as shown below.



Step 7: Assembly of Spot Welder Connections

1. Take the stock welding cables (the ones whose probes were deconstructed earlier) and cut them at a location a few centimeters along the cable from the spot welder interface plugs. Use the hydraulic crimper to attach a single-hole compression lug to each cable stub.
2. Do the same for the custom welding wire segments, stripping away the insulation at the tips and crimping a single-hole compression lug onto each end.
3. Attach the two sets of lugs together using two ¼”-20 x 0.5” bolts and two ¼”-20 nylon locknuts so that a continuous welding wire connection is formed between each

spot-welder plug port and either the straight end electrode or the angled end electrode. Coming out of the welder, the setup should look something like this:



Step 8: Circuit Assembly

As outlined above in our verification section, we were unable to translate the performance seen in the SPICE simulations of our circuit designs into the real world. The source of the errors in the behavior of our constructed circuits remains under investigation. Therefore, we cannot provide a correct assembly or manufacturing plan for the circuits we designed. The simulation-verified diagrams are included above, however. Despite this, the mechanically assistive features of the spot welder, ensuring probe orientation and improving ergonomics, are still entirely functional.

Final Assembly:

Spot welder not shown, but the ends of the welding cables that have electrical tape are meant to connect directly to the welder.

